Molecular Structures and Conformations of Some Diisopropyl Compounds Investigated by Gas Electron Diffraction Combined with Vibrational Spectroscopy, Molecular Mechanics and Ab Initio Calculations

A Doctoral Thesis

Presented by

Hiroshi Takeuchi

to

Faculty of Science

Hokkaido University

Acknowledgments

The author would like to thank Professor Shigehiro Konaka for his advice and encouragement on both experimental and theoretical aspects, and Emeritus Professor Masao Kimura for his encouragement.

The author is greatly indebted to Professor Kimio Ohno, Professor Yoshio Matsunaga and Professor Masahiro Kawasaki for their valuable suggestions and critical reading of the manuscript.

The author wishes to acknowledge Professor Lother Schäfer for allowing him to use some results of ab initio calculations prior to publication, Professor James E. Boggs for his permission to use the ab initio program TEXAS, Dr. Kouichi Takeshita for his assistance in the ab initio calculations, Dr. Kohji Fukushi for his technical assistance in recording the Raman and infrared spectra, Professor Shun-ichi Ikawa and Dr. Tetsuhiko Ohba for measuring the far infrared spectra, and Professor Eiji Ōsawa for his advice on molecular mechanics calculations.

The members of Professor Konaka's laboratory, especially Messrs. Hiroyuki Kondo, Mikio Fujii, Teruhisa Sakurai, Atsuhiko Suwa and Masami Sugino, are also thanked for their help.

Finally the author is grateful to his parents for their support and encouragement.

CONTENTS

Chapter 1

Introduction

The substitution of bulky groups for atoms or less bulky groups generally gives rise to steric strain in molecules. Thus the molecular structures with bulky substituents are different from the structures of unstrained reference molecules and such difference gives information on intramolecular interactions, especially, on non-bonded interactions. During the last two decades, a number of structural investigations by gas electron diffraction (GED) have been performed for the molecules with more than one t-butyl [1-7] or trimethylsilyl [8-15] groups bonded to a common atom, and have clarified structural features showing very large steric hindrance between bulky groups.

An isopropyl group is less bulky than a t-butyl group but low symmetry of the isopropyl group introduces considerable complexity about the conformation. No experimental study has ever been reported on the structures of gaseous molecules with more than one isopropyl groups. The purpose of the present thesis is to determine structures and conformations of some molecules with two geminal isopropyl groups and to examine how the geometries are understood in terms of the steric hindrance between the isopropyl groups. Selected molecules are diisopropyl ether ($(i\text{-}Pr)_2O$), diisopropylamine ($(i\text{-}Pr)_2NH$), diisopropyl sulfide ($(i\text{-}Pr)_2S$), and diisopropyl ketone ($(i\text{-}Pr)_2C{=}O$). It is quite difficult to investigate the structures of these diisopropyl molecules by microwave spectroscopy, because the

large degrees of freedom of internal rotation produce quite complicated spectra and, even if they were to be tractable, many isotopically substituted molecules would be required for the determination of the structures. Therefore GED is the most suitable method at present for determining the molecular structures of these diisopropyl compounds in the vapour phase. However, it is difficult to determine the structures precisely by GED alone. Therefore, appropriate assumptions must be made to decrease the number of the adjustable structural parameters. Such assumptions are usually made on an empirical or intuitive basis and sometimes give errors to resulting data. Hence, additional information is needed for reliable structural investigations. It is recognized that the combination of GED data with ab initio SCF and molecular mechanics calculations is useful in the structural investigations of relatively large molecules [16-20]. In the present study, ab initio SCF calculations at the 4-21G level [21] and molecular mechanics calculations using the MM2 force field [22] have been performed to obtain the information necessary for the data analysis of GED.

As shown in Chapter 5, the most stable conformers of $(i\text{-}Pr)_2O$ and $(i\text{-}Pr)_2S$ have C_2 symmetry and the conformer with nearly C_2 symmetry is predominant in $(i\text{-}Pr)_2NH$. Recently, the molecular structure of 2,4-dimethylpentane ($(i\text{-}Pr)_2CH_2$) has been determined by GED in our laboratory [23]. This

investigation has confirmed the conformer with C_2 symmetry as a major constituent of $(i\text{-}Pr)_2CH_2$. On the other hand, the C_1 conformer of $(i\text{-}Pr)_2C{=}O$ has the largest population. In order to examine whether the difference in the conformational behaviour of $(i\text{-}Pr)_2C{=}O$ and $(i\text{-}Pr)_2X$ (X = O, NH, CH_2, S) is related with the existence of the double bond, the molecular structure of 2-isopropyl-3-methyl-1-butene ($(i\text{-}Pr)_2C{=}CH_2$) has been investigated by ab initio calculations using the 3-21G [24] basis set in this thesis.

The molecular structures and conformations of the above diisopropyl compounds were studied by several authors. The conformation of $(i\text{-}Pr)_2O$ was investigated by means of vibrational spectroscopy [25,26]. By comparing the vibrational frequencies observed in the liquid and solid phases with the calculated ones, Snyder and Zerbi [25] identified only one conformer with C_2 symmetry in both the phases. Clague and Danti [26] measured low-frequency vibrational bands in the liquid and vapour phases and reported the presence of a single conformer in which two isopropyl groups rotate in opposite directions to minimize steric hindrance. These investigations showed that the molecule has C_2 or nearly C_2 symmetry. No experimental study has been reported on the structure in the vapour phase prior to the present study. Recently Schäfer [27] has calculated the structure of the C_2 conformer using the 4-21G basis set [21], and Pulay's gradient method and computer

program TEXAS [28-30], but he has not calculated the energies and geometries of other conformers.

In the case of $(i\text{-}Pr)_2NH$, no experimental structural investigation has been reported before the present study. Recently the structure of a conformer with nearly C_2 skeletal symmetry similar to the C_2 conformer of $(i\text{-}Pr)_2O$ was calculated by Schäfer [27] by using the same basis set and method as those applied to $(i\text{-}Pr)_2O$.

The conformation of $(i\text{-}Pr)_2S$ was studied by vibrational spectroscopy [31-33], normal coordinate analysis [34] and CNDO/2 calculations [35]. In these investigations, staggered conformations about the S-C axes were assumed and as a result, possible stable conformers were restricted to four conformers with C_1, C_s, C_2, and C_{2v} symmetry. According to the spectroscopic investigations, the conformer with the C_2 symmetry is the most stable in the liquid phase and the molecule takes only the C_2 symmetry in the crystalline state. Scott and El-Sabban [34] carried out normal coordinate analysis and showed that the conformer with the C_s symmetry is the next stable in the vapour and liquid phases. Ohsaku et al. [32] and Sakakibara et al. [33] measured the vibrational spectra in the liquid and solid phases and suggested the presence of the other stable conformers with the C_s and C_1 symmetry in the liquid phase. Ohsaku [35] calculated energies of the four conformers by the CNDO/2 method and concluded that the stability is in the

following order: $C_2 > C_1 > C_s > C_{2v}$. Recently Schäfer [27] has investigated the conformation by the ab initio SCF calculation with the 4-21G basis set [21] for carbon and hydrogen atoms and the 3-3-21G basis set [36] for a sulfur atom. Energies of several conformers have been calculated by rotating two isopropyl groups at the interval of 60° . The result shows that the C_2, C_s, and C_{2v} conformers are stable but that the C_1 conformer is unstable. The resulting C_2 and C_{2v} conformers are essentially equal to those assumed in the vibrational spectroscopic studies and CNDO/2 calculations. However, the C_s conformer predicted by the ab initio calculation is different from that considered before. According to the ab initio calculation, one of the C-H_{i-Pr}* bonds of the C_s conformer is eclipsed with the S-C bond but the other is anti to the S-C bond, while in previous investigations [32-35] both C-H_{i-Pr} bonds were assumed to be gauche to the S-C bonds and to be on the same side of the plane including the S-C bonds.

The conformations of $(i\text{-Pr})_2C{=}O$ suggested by several authors [37-39] are different from each other. Aroney et al. [37] measured the molar Kerr constant of $(i\text{-Pr})_2C{=}O$ in the CCl_4 solution. They assumed the existence of two conformers; the C_{2v} conformer in which both H_{i-Pr} atoms are

---

* H_{i-Pr} denotes the hydrogen atom bonded to the central carbon atom in an isopropyl group.

anti to the oxygen atom and the C_s conformer in which one H_{i-Pr} atom is anti to the oxygen atom and the other is syn to the oxygen atom. By comparing the observed molar Kerr constant with the calculated ones, they inferred that the C_{2v} and C_s conformers exist with the ratio of 1 : 2. Hirota et al. [38] measured the infrared spectra of this molecule in the CCl_4 solution and concluded from the carbonyl stretching frequencies that the two H_{i-Pr} atoms of the predominant conformer are eclipsed with the oxygen atom. Suter [39] constructed the molecular mechanics force field for ketones. According to his calculation, the most stable conformer of $(i\text{-}Pr)_2C{=}O$ has the C_2 symmetry and its energy is 1.2 kcal/mol lower than that of the next stable conformer with the C_s symmetry. The results obtained with the CCl_4 solution [37,38] contradict each other and both are inconsistent with the molecular mechanics calculation [39].

Vibrational mean amplitudes are important quantities in the data analysis of GED and they can be calculated by using the harmonic force constants which should be consistent with the observed vibrational frequencies. Therefore, the reliable data analysis necessitates the observation of vibrational spectra. The vibrational spectra were reported in the literature for $(i\text{-}Pr)_2O$ and $(i\text{-}Pr)_2S$ [25,26,31-33]. No spectroscopic data are available for $(i\text{-}Pr)_2NH$. As for $(i\text{-}Pr)_2C{=}O$, some investigations on the carbonyl stretching band were reported in the literature [38,40] and the

vibrational frequencies of other bands were measured by Karabatsos [41], and by Katon and Bentley [42]. Karabatsos [41] recorded the infrared spectra in the CS_2 solution but he did not report the numerical data except some vibrational frequencies. The infrared spectrum in the region of 700 cm^{-1} to 350 cm^{-1} was reported in ref. 42. The far-infrared spectrum of the liquid of $(i\text{-}Pr)_2C{=}O$ was measured by Ohba et al. [43] using a far-infrared interferometer installed at the Beam-Line 6A at UVSOR at the Institute for Molecular Science. Thus, these investigations gave an incomplete set of the vibrational spectra for the latter two diisopropyl compounds. In the present study, infrared and Raman spectra have been measured for $(i\text{-}Pr)_2NH$ and $(i\text{-}Pr)_2C{=}O$.

In Chapter 2, experimental conditions on recording the GED intensities and vibrational spectra, and the observed vibrational frequencies are presented. Theoretical calculations by ab initio and molecular mechanics methods are described in Chapter 3. Chapter 4 describes the normal coordinate analysis of the vibrational frequencies for each compound by using the geometry determined by GED. In Chapter 5, the analyses of GED data are performed with the help of the vibrational spectra and the theoretical calculations. In Chapter 6, the results are discussed together with the result of $(i\text{-}Pr)_2CH_2$ [23].

Chapter 2

Experimental

2-1 Gas Electron Diffraction

The samples were purchased from Tokyo Chemical Industry Co., Ltd. and purity is at least 99% for $(i\text{-}Pr)_2X$ with X= O, NH, and C=O and 98% for $(i\text{-}Pr)_2S$. The samples were used after distillation in vacuum. The electron diffraction experiment was performed by the use of an apparatus equipped with an r^3-sector [44]. Incident electrons with an accelerating voltage of about 38 kV were focussed on a photographic plate with an electromagnetic lens. Sample gas was introduced into the diffraction chamber through the nozzle and a cold trap was used to prevent the delocalization of the sample gas into the diffraction chamber. Incident electrons were scattered by sample gas and the diffraction patterns were recorded on Kodak electron image plates at room temperature with the camera distances of 109.3 mm and 244.3 mm. The camera distance is the distance between the scattering center and the photographic plate. An r^3-sector [44] was used because the intensity of the scattered electrons is approximately proportional to s^{-3}. Here s represents $(4\pi/\lambda)\sin(\theta/2)$ where λ is the electron wavelength and θ is the scattering angle. The sector was rotated rapidly above photographic plates. The undiffracted electrons were trapped by a beam stopper. The wavelength of incident electrons was determined from the diffraction patterns of carbon disulfide (r_a(C-S) = 1.5570

Å) [45] taken after those of the samples. The uncertainties in the scale factor were estimated from the limits of error of the determined r_a(C-S) values. The other experimental conditions and information on the photographic plates used for data analysis are listed in Table 1. Optical densities were measured at an interval of 1/3 mm by microphotometry and converted to total intensities [46]. They were leveled by using the theoretical background* which were calculated from the elastic scattering factors $f_i(s)$ and inelastic scattering factors $S_i(s)$ given in refs. 47 and 48, respectively. Leveled intensities were averaged at each camera distance after they were confirmed to be consistent with each other by preliminary data analyses. The molecular scattering intensities, sM(s), defined by

$$sM(s)^{obs.} = s(I_T/I_B-1), \qquad (2\text{-}1)$$

---

* The theoretical background is proportional to [49]

$$\sum_i [|f_i(s)|^2 + \left(\frac{2}{as^2}\right)^2 S_i(s)]$$

where a is the relativistic Bohr radius, f_i is the complex atomic scattering factor for elastic electron scattering, S_i is the atomic scattering factor for inelastic X-ray scattering and the suffix i denotes the i-th atom in the molecule.

were obtained by drawing smooth backgrounds, I_B, through the leveled intensities, I_T**.

** The theoretical expression for sM(s) is given in Section 5-1.

TABLE 1

Experimental conditions and photographic plate data

Sample	$(i\text{-}Pr)_2O$		$(i\text{-}Pr)_2NH$		$(i\text{-}Pr)_2S$		$(i\text{-}Pr)_2C{=}O$	
Camera distance(mm)	109.3	244.3	109.3	244.3	109.3	244.3	109.3	244.3
Room temperature(℃)	19	19	20	20	20	20	24	24
Electron wavelength(Å)	0.06283	0.06298	0.06276	0.06298	0.06287	0.06271	0.06274	0.06275
Uncertainties in the scale factor(%)	0.05	0.06	0.06	0.07	0.07	0.06	0.06	0.08
Sample pressure(Torr)	30-32	30-32	30	30	9-11	8-11	9-11	10-12
Background pressure during the exposure(Torr)	1×10^{-4}	7×10^{-5}	5×10^{-5}	3×10^{-5}	3×10^{-5}	2×10^{-5}	3×10^{-5}	3×10^{-5}
Beam current(μA)	0.15-0.16	0.07-0.09	0.13-0.16	0.09-0.12	0.13-0.16	0.10-0.12	0.14-0.15	0.11-0.12
Exposure time(s)	45-60	21-29	55-63	19-27	100-130	48-55	160-170	43-52
Number of plates	4	6	3	4	2	3	3	3
Range of s values($Å^{-1}$)	10.0-32.2	2.9-17.4	9.4-36.8	2.6-17.4	7.6-30.6	3.1-17.4	9.4-37.1	2.6-16.9

2-2 Vibrational Spectroscopy

— Measurement of Vibrational Spectra —

Infrared and Raman spectra were recorded for $(i\text{-Pr})_2NH$ and $(i\text{-Pr})_2C{=}O$. The infrared spectrum of $(i\text{-Pr})_2NH$ in the vapour phase was measured on a DIGILAB FTS-14A Fourier transform spectrometer with a resolution of 4 cm^{-1} by using a cell with the path length of 10 cm and KRS-5 windows. The infrared spectrum of the liquid was recorded by using NaCl windows. The infrared spectrum of $(i\text{-Pr})_2C{=}O$ in the gas phase was measured with a resolution of 2 cm^{-1} by using KBr windows. The Raman spectra of $(i\text{-Pr})_2NH$ and $(i\text{-Pr})_2C{=}O$ in the liquid phase were measured with a JASCO R300S laser Raman spectrophotometer using the 632.8 nm line of a He-Ne laser. The observed vibrational frequencies for $(i\text{-Pr})_2NH$ and $(i\text{-Pr})_2C{=}O$ are listed in Tables 2 and 3, respectively. For $(i\text{-Pr})_2C{=}O$ the frequencies reported in the literature [41-43] are also listed in Table 3.

TABLE 2

Infrared and Raman vibrational frequencies (cm^{-1}) observed for diisopropylamine[a]

Raman liquid	IR liquid	IR vapour
3313w	~3300w	~3300w
	~3190w	~3190w
2968s	~2964v	~2968vs
2935s	2940w	2937s
2918vs	2925sh	2924sh
2902sh		
2875s	2872sh	2885s
2865s		
2840sh	2840m	2849m
2790vw	2795sh	2800sh
2755w		
2720w	2720vw	2735w
2620vw	2620w	2625w
2600sh	2600sh	
1457m	1468m	1476m
~1440sh	~1450sh	~1450sh
1383vw	1381s	1385s
1372w	1372m	
1343w	1339m	1342m
~1325sh	1330sh	

~1310sh		
1196w		
1179w	1179s	1182s
1139w	1138m	1135m
1116w	1117w	
1093w	1091w	1095w
1020vw	1018w	1022w
951w	950vw	950sh
940m		
931m	~935sh	928vw
922m	918vw	
849s	848w	~850sh
829s	828w	830vw
706w	701m	693m
	504w	
487s		
445w		
406vw		
393vw		
317m		
256vw		
193w		

[a] Abbreviations used: vs, very strong; s, strong; m, medium; w, weak; vw, very weak; sh, shoulder.

TABLE 3

Infrared and Raman vibrational frequencies (cm^{-1}) observed for diisopropyl ketone[a]

Raman liquid	IR vapour	IR liquid[b]
2970s	2979vs	
2935s	2945s	
2910vs	2910s	
2870vs	2887s	
2755vw		
2714vw		
1712w	1730vs	1712[c]
	1480sh	
1464m	1470s	
1449m		
	1394m	
	1389m	
	1384m	
	1370m	
1326vw		
1280vw	1298vw	
	1264vw	
	1207sh	1203[c]
	1188sh	
	1183w	

1174w	1178sh	
1129vw	1127w	1129[c]
1115m		
1085vw		
	1080m	
1070vw		
	1027s	1024[c]
	986w	983[c]
964w	960sh	
	930vw	
895vs		
860w	860vw	858[c]
	~800vw	
740s	740vw	
716m		
609vw	610w	610s
568vw		565m
		553w-m
525vw		525m
		488w
471s		468w
395vw		391s
330w		332s
290m		
240sh		
206w		
		45[d]

[a] Abbreviations are the same as shown in Table 2. [b] Ref. 42. [c] In CS_2 solution. Ref. 41. [d] Ref. 43.

Chapter 3

Theoretical Calculation

3-1 Ab Initio SCF MO Calculations

The ground-state electronic energy of a molecule is given by [50]

$$E = \langle \Psi | H | \Psi \rangle, \tag{3-1}$$

where Ψ is a normalized molecular wave function and H is the Hamiltonian operator. In the SCF MO calculations for a molecule with 2n electrons, Ψ can be expressed as

$$\Psi = 1/(2n!)^{1/2} |\psi_1 \overline{\psi}_1 \cdots \psi_n \overline{\psi}_n|, \tag{3-2}$$

where the bar indicates that the orbital ψ_i includes a β-spin function. Then the total electronic energy is given by

$$E = 2\Sigma H_{ii} + \Sigma\Sigma(2J_{ij}-K_{ij}) \tag{3-3}$$

Here H_{ii}, J_{ij}, and K_{ij} are one electron, Coulomb, and exchange integrals, respectively. In the LCAO MO approximation, ψ_i is expressed as a linear combination of atomic orbitals.

$$\psi_i = \Sigma c_{\mu i} x_\mu \tag{3-4}$$

The coefficients $c_{\mu i}$ are determined by the variational principle. The results of the variational calculations are written in the following matrix form.

$$FC = SCE \tag{3-5}$$

Here the element, S_{ij}, of the S matrix is the overlap integral for atomic orbitals, x_i and x_j, C is the matrix whose element is C_{ij}, E is the diagonal matrix consisting of the orbital energies and F is the Fock matrix [50]. The matrix C is obtained by an iterative method since the Fock matrix is dependent on the atomic orbitals.

The gradient method developed by Pulay [28-30] is very effective to optimize molecular geometries. In this method the force acting along a nuclear coordinate r is calculated as

$$f = -\frac{dE}{dr} = -\left\langle \psi \left| \frac{\partial H}{\partial r} \right| \psi \right\rangle - 2\left\langle \frac{\partial \psi}{\partial r} \middle| H \middle| \psi \right\rangle \qquad (3\text{-}6)$$

The above two integrals are expressed in analytical forms as shown in ref. 30.

The 4-21G basis set [21] was mainly employed in the present study. A large number of ab initio calculations with this basis set have been published and the evaluation of the 4-21G calculation on molecular geometries has already been established [51,52].

The symmetry of $(i\text{-}Pr)_2NH$ is lower than that of $(i\text{-}Pr)_2O$ because of the existence of the hydrogen atom attached to the nitrogen atom. Thus the ab initio calculation of the potential energy surface against dihedral angles, $\phi_1(C_5NC_2H)$ and $\phi_2(C_2NC_5H)$, requires more computational time than in the case of $(i\text{-}Pr)_2O$. The molecule of $(i\text{-}Pr)_2S$ has a sulfur atom which requires large computational time for ab initio

calculations. The 4-21G calculations could not be performed for $(i\text{-}Pr)_2NH$ and $(i\text{-}Pr)_2S$ in the present study because of the limit of the expenditure for computations.

Ab initio calculations with geometry optimization yield r_e structures, i.e., equiliblium structures. Such r_e structures are different from the true r_e structures because of the approximation used in the calculations. The structures determined by GED are usually the r_g and/or r_α structures for bond lengths and the r_α structures for bond and torsional angles, respectively. Here the symbols, r_g and r_α, denote the thermal average values of interatomic distances and the distances between average nuclear positions, respectively [53]. Therefore, the difference in the physical meaning must be taken into consideration in comparison of the calculated structures with the r_g and/or r_α structures obtained by GED.

Diisopropyl Ether. Calculations were performed using the 4-21G basis set [21] and Pulay's program TEXAS [29]. The numbering of atoms is shown in Fig. 1. For the 4-21G basis set, the set of empirical corrections is available to convert the r_e bond lengths into the r_g ones [51,52]. In order to search for stable conformers, the total energies for several conformations were calculated varying the values of the dihedral angles, $\phi_1(C_5OC_2H)$ and $\phi_2(C_2OC_5H)$, at the interval of 20° . Here, ϕ_1 and ϕ_2 are defined to be zero when the C-O bond eclipses the C-H bond and are defined to

be positive when the C-H bond rotates clockwise looking along the direction of the O-C axis. The conformers around $\phi_1 = \phi_2 = 180°$ were excluded in the calculations since they are considered to be unstable because of the strong CH_3 - CH_3 interactions between isopropyl groups. The resulting potential energy surface shows two energy minima at $\phi_1 = \phi_2 = 40°$ (C_2 symmetry), and $\phi_1 = 0°$ and $\phi_2 = 180°$ (C_s symmetry). The optimization of the C_2 conformer has already been carried out by Schäfer [27]. Therefore, the geometry of the conformer with the C_s symmetry was optimized in the present study until the residual Cartesian forces became less than 0.001 a. u. which is one-order larger than the value in the calculation by Schäfer [27]. It is expected that the bond lengths and angles obtained at the level of 0.001 a. u. are usually within 0.001 Å and a few tenths of 1° of the best optimized values, respectively [52]. The geometries and energies of the two conformers are shown in Table 4. The conformer with the C_2 symmetry is more stable than the C_s conformer by 2.18 kcal/mol. From this energy difference, the mixture ratio, C_2/C_s, at 20°C is calculated to be 97.7/2.3 by assuming the Boltzmann distribution. The largest differences of the structural parameters of the same type between the two conformers are 0.007 Å and 6.4° on the bond lengths and angles, respectively. The dihedral angles, $\phi(OC_5C_{6,7}H)$, in the C_s conformer deviate by about 9° from the staggered configurations. Here the dihedral angle,

$\phi(OC_5C_{6,7}H)$, is defined similarly to ϕ_1 and ϕ_2.

Diisopropyl Ketone. The numbering of the atoms in $(i\text{-}Pr)_2C{=}O$ is shown in Fig. 2. The potential energy surface against the dihedral angles, $\phi_1(C_4C_2C_3H)$ and $\phi_2(C_3C_2C_4H)$, was calculated by the same manner as described for $(i\text{-}Pr)_2O$. No conformers around $\phi_1 = \phi_2 = 180°$ are included in the calculations. The resulting potential energy surface shows three energy minima at $\phi_1 = 20°$ and $\phi_2 = -60°$ (C_1 symmetry), $\phi_1 = \phi_2 = 60°$ (C_2 symmetry), and $\phi_1 = 0°$ and $\phi_2 = 180°$ (C_s symmetry). The geometries of the two conformers with the C_2 and C_s symmetry were optimized until the largest residual Cartesian forces were below 0.001 a. u. The optimization procedure for the C_1 conformer was terminated when the largest residual Cartesian force was 0.0013 a. u., since much more iterations were needed for achieving the same level of the optimization as made for the C_2 and C_s conformers. The geometries and energies of these conformers are shown in Table 5. The most stable conformer has the C_1 symmetry and the conformers with the C_2 and C_s symmetry are less stable than the most stable conformer by 0.09 and 1.17 kcal/mol, respectively. From these energy differences, the populations of the C_1 , C_2 and C_s conformers at 24°C were calculated to be 66%, 29% and 5%, respectively. The calculated r_e bond lengths can be converted to the r_g bond lengths by using the empirical $r_g - r_e$ corrections [52]. For the (O=)C-C and C-C (aliphatic) bond lengths, the

correction values are 0.002(2) and -0.008(2) Å, respectively. Therefore, the differences between r_g((O=)C-C) and r_g(C-C) are smaller than those in the corresponding r_e distances. The variations of the CCC bond angles are within 3.3° , 1.4° and 2.1° for the C_1, C_2, and C_s conformers, respectively, except for ∠CC(=O)C.

2-isopropyl-3-methyl-1-butene. Calculations were performed by using the 3-21G basis set [24]. The calculation procedure is almost similar to that for $(i\text{-Pr})_2O$ and $(i\text{-Pr})_2CO$ except for the optimization level. The optimization of geometries was terminated at the level of about 0.002 a. u. The results are listed in Table 6. Two stable conformers with $\phi_1 = \phi_2 = 30°$ (C_2 symmetry), and $\phi_1 = 0°$ and $\phi_2 = 180°$ (C_s symmetry) were obtained. The detailed information about the geometries of the two conformers is not presented in the table, since it is not important in the present thesis. The energy difference, 0.1 kcal/mol, between the two conformers indicates that they have nearly equal populations.

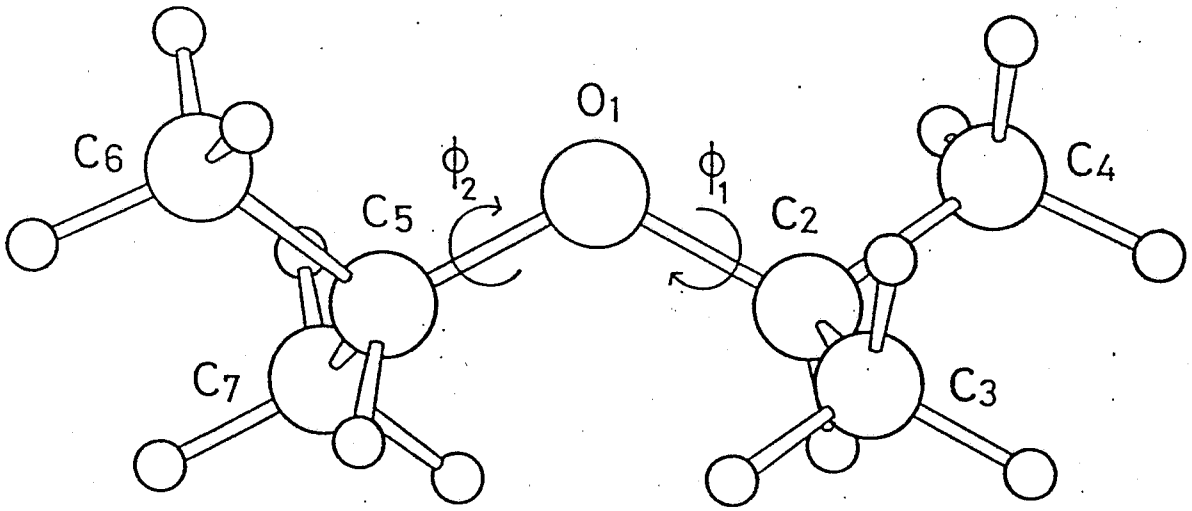

Figure 1 The numbering of atoms in diisopropyl ether with C_2 symmetry

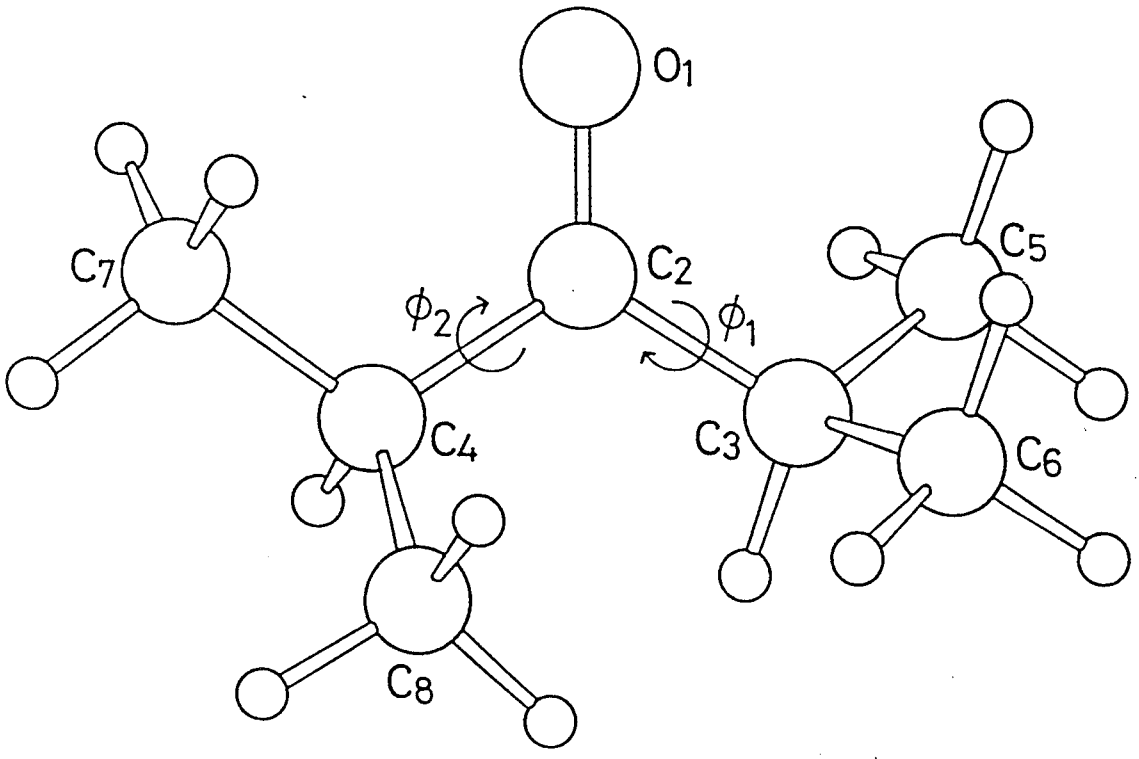

Figure 2 The numbering of atoms in diisopropyl ketone

TABLE 4

Structures and energies of diisopropyl ether obtained by the 4-21G and MM2 calculations[a]

	4-21G		MM2
Symmetry	C_2[b]	C_s[c]	C_2[c]
$r(O_1-C_2)$	1.453	1.457	1.426
$r(O_1-C_5)$	1.453	1.452	1.426
$r(C_2-C_3)$	1.533	1.531	1.540
$r(C_2-C_4)$	1.529	1.531	1.539
$r(C_5-C_6)$	1.529	1.536	1.539
$r(C_5-C_7)$	1.533	1.536	1.540
r(C-H)	1.082[d]	1.082[d]	1.115[d]
$\angle C_2O_1C_5$	117.4	119.1	114.2
$\angle O_1C_2C_3$	109.7	107.7	110.9
$\angle O_1C_2C_4$	105.7	107.7	108.2
$\angle O_1C_5C_6$	105.7	112.1	108.2
$\angle O_1C_5C_7$	109.7	112.1	110.9
$\angle C_3C_2C_4$	112.3	112.2	109.9
$\angle C_6C_5C_7$	112.3	112.4	109.9
$\angle C_{3,4}C_2H_{i\text{-}Pr}$	109.7[d]	109.4	108.9[d]
$\angle C_{6,7}C_5H_{i\text{-}Pr}$	109.7[d]	108.4	108.9[d]
$\angle CCH_{Me}$[e]	110.2[d]	110.3[d]	110.9[d]
$\phi(C_5O_1C_2C_3)$	-85.8	-119.4	-81.6
$\phi(C_5O_1C_2C_4)$	153.0	119.4	157.8

$\phi(C_5O_1C_2H_{i\text{-}Pr})$	34.8	0.0	40.0
$\phi(C_2O_1C_5C_6)$	153.0	-63.7	157.8
$\phi(C_2O_1C_5C_7)$	-85.8	63.7	-81.6
$\phi(C_2O_1C_5H_{i\text{-}Pr})$	34.8	180.0	40.0
$\phi(O_1C_2C_3H)$ [f]	1.8	0.7	3.3
$\phi(O_1C_2C_4H)$ [f]	-0.2	-0.7	0.7
$\phi(O_1C_5C_6H)$ [f]	-0.2	9.1	0.7
$\phi(O_1C_5C_7H)$ [f]	1.8	-9.1	3.3
E [g]	-309.55580	-309.55232	
ΔE [h]	0.0	2.18	

[a] Bond length in Å and angles in degrees. [b] Calculated by Schäfer [27]. [c] This work. [d] Average value. [e] H_{Me} denotes the hydrogen atom in methyl groups. [f] Average value of the deviation of dihedral angles, OCCH, from the staggered form (±60° or 180°). [g] Energies in hartrees. [h] Relative energies in kcal/mol.

TABLE 5

Structures and energies of diisopropyl ketone obtained by the 4-21G and MM2 calculations[a]

	4-21G			MM2
Symmetry	C_1	C_2	C_s	C_1
r(C=O)	1.216	1.216	1.217	1.211
$r(C_2-C_3)$	1.531	1.531	1.530	1.527
$r(C_2-C_4)$	1.528	1.531	1.525	1.527
$r(C_3-C_5)$	1.540	1.537	1.545	1.538
$r(C_3-C_6)$	1.550	1.549	1.545	1.537
$r(C_4-C_7)$	1.536	1.549	1.545	1.538
$r(C_4-C_8)$	1.547	1.537	1.545	1.537
r(C-H)	1.082[b]	1.082[b]	1.082[b]	1.114[b]
$\angle C_3C_2C_4$	118.5	118.6	119.4	118.5
$\angle O_1C_2C_3$	120.1	120.7	119.7	120.1
$\angle O_1C_2C_4$	121.5	120.7	120.9	121.4
$\angle C_2C_3C_5$	110.0	110.4	109.0	110.9
$\angle C_2C_3C_6$	108.4	111.5	109.0	110.4
$\angle C_2C_4C_7$	110.3	111.5	111.1	112.2
$\angle C_2C_4C_8$	111.6	110.4	111.1	111.3
$\angle C_5C_3C_6$	109.8	110.1	110.1	110.3
$\angle C_7C_4C_8$	110.9	110.1	111.1	110.0
$\angle C_{5,6}C_3H_{i\text{-}Pr}$	109.6[b]	108.6[b]	109.4	108.5[b]
$\angle C_{7,8}C_4H_{i\text{-}Pr}$	108.7[b]	108.6[b]	109.0	108.4[b]

$\angle CCH_{Me}$	110.5[b]	110.5[b]	110.5[b]	111.3[b]
$\phi(C_4C_2C_3C_5)$	136.7	178.2	119.9	128.1
$\phi(C_4C_2C_3C_6)$	-103.3	-59.0	-119.9	-109.4
$\phi(C_4C_2C_3H_{i\text{-}Pr})$	16.0	59.4	0.0	9.9
$\phi(C_3C_2C_4C_7)$	179.7	-59.0	62.1	-170.4
$\phi(C_3C_2C_4C_8)$	55.9	178.2	-62.1	65.8
$\phi(C_3C_2C_4H_{i\text{-}Pr})$	-61.6	59.4	180.0	-52.9
$\phi(C_2C_3C_5H)$[c]	-2.2	-0.6	-3.3	3.4
$\phi(C_2C_3C_6H)$[c]	4.1	0.2	3.3	-2.3
$\phi(C_2C_4C_7H)$[c]	0.1	0.2	-3.1	-3.6
$\phi(C_2C_4C_8H)$[c]	0.3	-0.6	3.1	-0.6
E[d]	-347.35010	-347.34995	-347.34823	
ΔE[e]	0.0	0.09	1.17	

[a] Bond lengths in Å and angles in degrees. [b] Average value. [c] Average value of the deviation of the dihedral angles, C_2CCH, from the staggered form (±60° or 180°). [d] In hartrees. [e] In kcal/mol.

TABLE 6

Conformational energies of 2-isopropyl-3-methyl-1-butene obtained by the 3-21G calculations

ϕ_1[a]	ϕ_2[a]	E[b]	ΔE[c]	Population[d]
180	0	-310.52058	0.0	53
30	30	-310.52047	0.1	47

[a] The dihedral angles in degrees. [b] In hartrees. [c] In kcal/mol. [d] Percentage calculated at 20°C.

3-2 Molecular Mechanics Calculations

In molecular mechanics calculations, the relative energy of a molecule is expressed in terms of such an empirical force field as

$$E = \Sigma E_r + \Sigma E_\theta + \Sigma E_\phi + \sum_{ij}\Sigma E_{vw}$$

$$= \Sigma k(r-r_0)^2 + \Sigma h(\theta-\theta_0)^2 + \Sigma \sum_n V_n/2\{1-\cos(n\phi)\} +$$

$$\sum_{ij}\Sigma\{A\exp(-B/r_{ij}) - C/r_{ij}^6\} \qquad (3\text{-}7)$$

where E_r, E_θ, E_ϕ, and E_{vw} are stretching, bending, torsional and non-bonded-interaction terms, respectively*. Force fields parameters, k, h, V_n, A, B, C, r_0, and θ_0, are determined to reproduce appropriate experimental results or the results of ab initio calculations if experimental data are not available.

In the present study, molecular mechanics calculations were performed by using Allinger's force field, MM2 [22]. This force field was calibrated to fit the geometries mainly determined by GED. Therefore, the MM2 geometries are directly comparable with the geometries obtained by GED.

Diisopropyl Ether. According to the results of the

---

* The force field used in the present study includes anharmonic terms and dipole-dipole or Coulomb interactions in addition to E_r, E_θ, E_ϕ and E_{vw}.

present calculations, the most stable conformer has C_2 symmetry with $\phi_1 = \phi_2 = 40°$ and it is more stable than the next stable conformer with $\phi_1 = 12°$ and $\phi_2 = 177°$ by 2.6 kcal/mol. The third conformer has the dihedral angles of $\phi_1 = \phi_2 = 165°$ and is less stable than the most stable conformer by 7.4 kcal/mol. The population of the next stable conformer is calculated to be 2%. This result is similar to the 4-21G result. The relative abundance of the third conformer is calculated to be 0.0%. Thus the neglect of the conformers around $\phi_1 = \phi_2 = 180°$ in the 4-21G calculations was justified by the MM2 calculations. The geometry of the most stable conformer obtained by MM2 is listed in Table 4, column 4.

Diisopropylamine. The conformation of $(i\text{-Pr})_2NH$ with the skeletal geometry of C_2 symmetry is shown in Fig. 3 with atomic numbering. Conformational energies obtained by the MM2 calculations are listed in Table 7. The result shows that the conformer with $\phi_1 = 62.6°$ and $\phi_2 = 61.9°$ is the most stable, being more stable than the next stable conformer by 2.5 kcal/mol. This suggests that the amount of other conformers present is a few percent at room temperature. The calculated structures of three stable conformers are given in Table 8 together with the 4-21G geometry of the most stable conformer calculated by Schäfer [27].

Diisopropyl Sulfide. The atomic numbering of $(i\text{-Pr})_2S$

is shown in Fig. 4. Five stable conformers were found and the resulting structures and the conformational energies of three conformers with relatively large populations are listed in Table 9. The C_2 conformer is the most stable and it is considered that other conformers with C_1 symmetry exist in large concentrations.

Diisopropyl ketone. The parameter set for ketones and aldehydes in the MM2 force field was recently revised by Bowen et al. [54]. The modification is related with only the torsional parameters. The MM2 calculations were performed by using both the new and original parameter sets and the conformational energy differences calculated by using the new parameter set are listed in Table 10. The considerable difference between the two results appears in the most stable conformation. The MM2 calculations with the new parameter set show that the most stable conformer has C_1 symmetry with $\phi_1 = 10°$ and $\phi_2 = -53°$ and the population of 65% (the geometry is listed in Table 5, column 5). On the other hand, the original parameter set gives the result that the C_2 conformer with $\phi_1 = \phi_2 = 61°$ is the most stable, having the relative abundance of 65%.

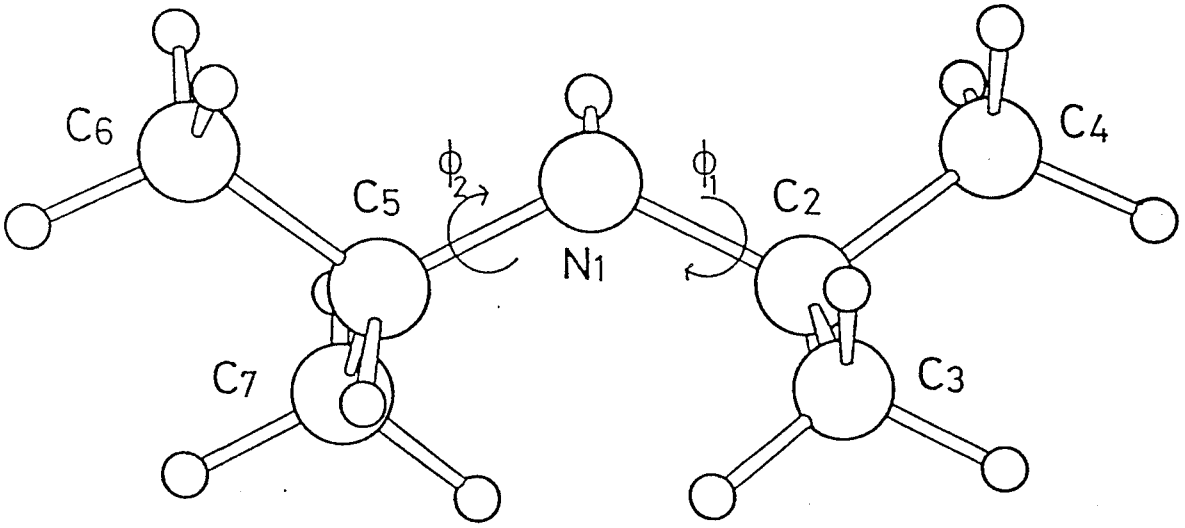

Figure 3 The numbering of atoms in diisopropylamine

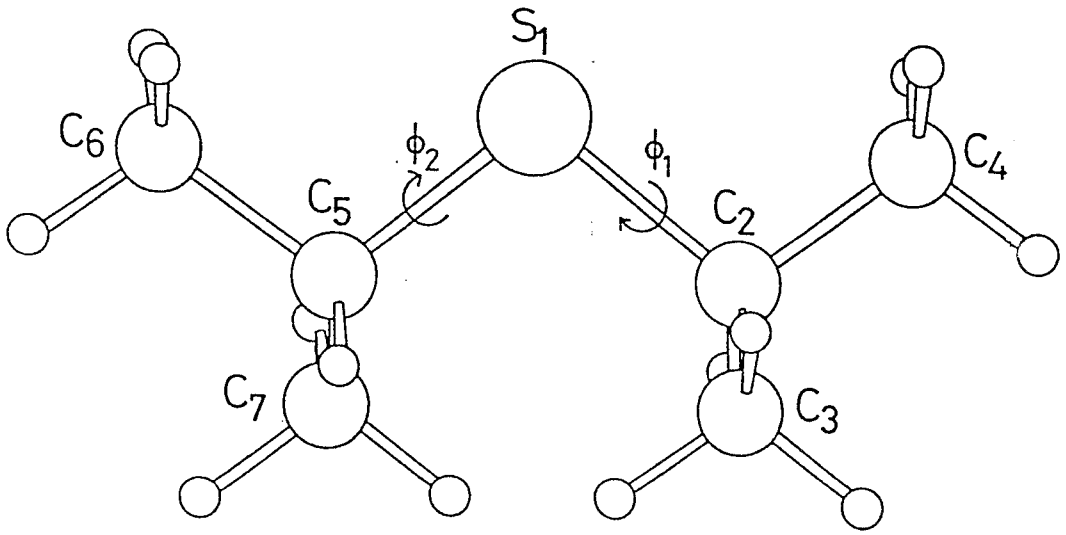

Figure 4 The numbering of atoms in diisopropyl sulfide with C_2 symmetry

TABLE 7

Conformational energies of diisopropylamine obtained by the MM2 calculations

ϕ_1[a]	ϕ_2[a]	ΔE[b]	Population[c]
62.6	61.9	0.0	96.0
-28.3	59.8	2.49	1.3
60.8	-26.6	2.50	1.3
-60.0	160.3	3.12	0.5
161.5	-61.0	3.23	0.3
177.8	32.7	3.43	0.3
33.0	178.8	3.44	0.3
167.5	166.3	5.90	0.0

[a] The dihedral angles in degrees. [b] In kcal/mol.

[c] Percentage calculated at 20°C.

TABLE 8

Structural parameters of diisopropylamine given by the 4-21G and MM2 calculations[a]

	4-21G[b]	MM2[c]		
	(47,49)[d]	(63,62)[d]	(-28,60)[d]	(61,-27)[d]
$r(N_1-C_2)$	1.479	1.467	1.467	1.468
$r(N_1-C_5)$	1.478	1.467	1.467	1.468
$r(C_2-C_3)$	1.538	1.539	1.541	1.537
$r(C_2-C_4)$	1.538	1.540	1.540	1.541
$r(C_5-C_6)$	1.538	1.540	1.540	1.540
$r(C_5-C_7)$	1.544	1.538	1.537	1.542
$r(N_1-H_{22})$	1.004	1.016	1.016	1.017
$r(C-H)^e$	1.083	1.114	1.114	1.114
$\angle C_2N_1C_5$	118.7	116.1	115.6	115.5
$\angle N_1C_2C_3$	109.8	112.9	108.4	114.4
$\angle N_1C_2C_4$	107.9	108.8	112.7	108.7
$\angle N_1C_5C_6$	108.0	108.7	108.5	111.5
$\angle N_1C_5C_7$	113.5	113.0	114.4	109.8
$\angle C_3C_2C_4$	110.2	109.7	108.6	109.5
$\angle C_6C_5C_7$	110.8	109.8	109.6	108.4
$\angle C_{3,4}C_2H_{i\text{-}Pr}{}^e$	108.5	107.9	108.5	107.7
$\angle C_{6,7}C_5H_{i\text{-}Pr}{}^e$	108.5	107.8	107.8	108.5
$\angle CCH_{Me}{}^e$	110.4	110.0	111.0	111.0
$\angle C_{2,5}N_1H^e$	111.2	108.7	109.7	108.5

$\phi(C_5N_1C_2C_3)$	-73.5	-59.0	-145.5	-60.1
$\phi(C_5N_1C_2C_4)$	166.3	179.0	94.4	177.1
$\phi(C_5N_1C_2H_{i\text{-}Pr})$	47.3	62.6	-28.3	60.8
$\phi(C_2N_1C_5C_6)$	165.9	178.2	176.0	95.3
$\phi(C_2N_1C_5C_7)$	-70.8	-59.7	-61.3	-144.5
$\phi(C_2N_1C_5H_{i\text{-}Pr})$	49.4	61.9	59.8	-26.6
$\phi(N_1C_2C_3H)$ [f]	3.3	6.1	-1.4	6.6
$\phi(N_1C_2C_4H)$ [f]	-2.1	1.9	-1.8	2.8
$\phi(N_1C_5C_6H)$ [f]	4.0	3.1	4.1	-1.9
$\phi(N_1C_5C_7H)$ [f]	-1.0	5.6	7.4	0.2
$\phi(HN_1C_2H_{i\text{-}Pr})$	-83.3	-60.3	-152.9	-61.5
$\phi(HN_1C_5H_{i\text{-}Pr})$	-179.6	-175.2	-175.6	94.9

[a] Bond lengths in Å and angles in degrees. [b] Calculated by Schäfer [27]. [c] This work. [d] Values in parentheses indicate the dihedral angles, $C_5N_1C_2H_8$ and $C_2N_1C_5H_{21}$. [e] Average value. [f] Average value of the deviation of dihedral angles, NCCH, from the staggered form (±60° or 180°).

TABLE 9

Structures and relative energies of three stable conformers of diisopropyl sulfide obtained by the MM2 calculations[a]

	C_2 (44,44)[b]	C_1 (12,-52)[b]	C_1 (17,175)[b]
$r(S_1-C_2)$	1.825	1.825	1.824
$r(S_1-C_5)$	1.825	1.826	1.824
$r(C_2-C_3)$	1.537	1.536	1.537
$r(C_2-C_4)$	1.537	1.537	1.537
$r(C_5-C_6)$	1.537	1.536	1.536
$r(C_5-C_7)$	1.537	1.537	1.535
$r(C-H)$[c]	1.114	1.114	1.114
$\angle C_2S_1C_5$	100.7	100.3	102.9
$\angle S_1C_2C_3$	109.8	108.8	108.9
$\angle S_1C_2C_4$	107.9	108.2	108.0
$\angle S_1C_5C_6$	107.9	110.4	110.5
$\angle S_1C_5C_7$	109.8	107.9	111.7
$\angle C_3C_2C_4$	110.6	110.9	110.8
$\angle C_6C_5C_7$	110.6	110.7	112.2
$\angle C_{3,4}C_2H_{i\text{-}Pr}$[c]	108.4	108.5	108.2
$\angle C_{6,7}C_5H_{i\text{-}Pr}$[c]	108.4	108.6	107.2
$\angle CCH_{Me}$[c]	111.5	111.1	111.1
$\phi(C_5S_1C_2C_3)$	-76.9	-108.3	-104.0
$\phi(C_5S_1C_2C_4)$	162.5	131.1	135.6
$\phi(C_5S_1C_2H_{i\text{-}Pr})$	44.2	12.3	16.9

$\phi(C_2S_1C_5C_6)$	162.5	69.5	-68.2
$\phi(C_2S_1C_5C_7)$	-76.9	-169.5	57.5
$\phi(C_2S_1C_5H_{i\text{-}Pr})$	44.2	-51.5	175.0
$\phi(S_1C_2C_3H)$[d]	2.6	0.5	1.1
$\phi(S_1C_2C_4H)$[d]	0.0	-0.4	-0.8
$\phi(S_1C_5C_6H)$[d]	0.0	-4.0	4.6
$\phi(S_1C_5C_7H)$[d]	2.6	0.0	-5.9
ΔE[e]	0.0	0.56	1.00
X[f]	45.8	35.0	16.5

[a] Bond lengths in Å and angles in degrees. Calculated results on three stable conformers are listed. The calculation gives other stable conformers with ϕ_1 = -51.6° and ϕ_2 = 152.2° , and $\phi_1 = \phi_2$ = 164.5° which have the energy differences (and populations) of 2.06 kcal/mol (2.7%) and 4.43 kcal/mol (0.0%), respectively. [b] Values in parentheses indicate the dihedral angles, $C_2S_1C_2H$ and $C_2S_1C_5H$. [c] Average value. [d] Average value of the deviation of the dihedral angles, SCCH, from the staggered form (±60° or 180°). [e] Relative energy in kcal/mol. [f] Populations calculated from ΔE values. Summation of them is not 100%, since other two stable conformers contribute to the population.

TABLE 10

Conformational energies of diisopropyl ketone obtained by the MM2 calculations

ϕ_1[a]	ϕ_2[a]	ΔE[b]	Population[c]
9.9	-52.9	0.0	65.3
63.0	63.0	0.14	25.8
7.6	178.7	1.45	5.6
140.5	-44.3	1.77	3.3
162.5	162.5	4.69	0.0

[a] The dihedral angles in degrees. [b] In kcal/mol.

[c] Calculated at 20°C.

3-3 Discussion on the Results of Calculations

The 4-21G and MM2 calculations on the conformations of $(i\text{-}Pr)_2O$ and $(i\text{-}Pr)_2C{=}O$ are compared in Table 11. The 4-21G and MM2 calculations have been performed for $(i\text{-}Pr)_2CH_2$ [23] and the results are also listed in this table. An apparent discrepancy is seen in the number of the stable conformers of $(i\text{-}Pr)_2CH_2$ and $(i\text{-}Pr)_2C{=}O$. The MM2 calculations for $(i\text{-}Pr)_2CH_2$ and $(i\text{-}Pr)_2C{=}O$ yield the conformers with $\phi_1 \simeq -50°$ and $\phi_2 \simeq 150°$ in addition to the conformers corresponding to those obtained by the 4-21G calculations. The differences between the ϕ_1 and ϕ_2 values of $(i\text{-}Pr)_2X$ (X = O, CH_2, C=O) calculated by the two methods are less than 12° . The relative abundance of the most stable conformer of $(i\text{-}Pr)_2X$ estimated by the MM2 calculations is in agreement with that by the 4-21G calculations. Thus we confirm a general agreement between the results of the MM2 calculations and the 4-21G calculations on the dihedral angles and the conformational compositions of $(i\text{-}Pr)_2X$ (X = O, CH_2, C=O), except for the number of stable conformers.

Recently Schäfer [27] has calculated the potential energy surface for $(i\text{-}Pr)_2S$ against $\phi_1(C_5SC_2H)$ and $\phi_2(C_2SC_5H)$ at the interval of 60° by the ab initio SCF calculations. A C_2 conformer with $\phi_1 = \phi = 60°$, a C_s conformer with $\phi_1 = 0°$, $\phi_2 = 180°$, and a C_{2v} conformer with $\phi_1 = \phi_2 = 180°$ are considered to be present at energy minima

(the energy differences between these conformers are ambiguous since no geometry optimization was performed). The most, third, and fifth stable conformers calculated by the MM2 method correspond to the above three conformers, respectively. It is noted that the second and fourth conformers obtained by the MM2 calculations have not been included in the ab initio calculations. Therefore, the MM2 calculations does not necessarily contradict the ab initio calculations.

The C-H bond lengths in the 4-21G geometries of $(i\text{-}Pr)_2O$, $(i\text{-}Pr)_2NH$ and $(i\text{-}Pr)_2C{=}O$ are about 0.03 Å smaller than those in the MM2 geometries. This is mainly attributed to the difference in the physical meaning of the obtained bond lengths. The differences between the 4-21G and MM2 geometries are more striking for $(i\text{-}Pr)_2O$ than for the other diisopropyl molecules. The C-O bond length of the C_2 conformer of $(i\text{-}Pr)_2O$ is calculated to be 1.453 and 1.426 Å by the 4-21G and MM2 methods, respectively. The empirical correction, $r_g - r_e$, for the C-O bond length is -0.023 Å for the 4-21G geometry [52]. The corrected r_g(C-O) value, 1.430 Å, is close to the value of the MM2 geometry. The COC and CCC bond angles in the 4-21G geometry are 3° and 2° larger than the corresponding values in the MM2 geometry. The value of $\angle OCC_4$ is 105.7° in the 4-21G geometry and is 4° smaller than that in the MM2 geometry. The differences in the bond angles of $(i\text{-}Pr)_2NH$ by these two calculations are

smaller than 1° except for the CNC and NCC_3 bond angles. The 4-21G values of ∠CNC is 3° larger than the MM2 value, while the 4-21G value of $\angle NCC_3$ is 3° smaller than the MM2 value. For the bond angles in $(i\text{-}Pr)_2C{=}O$, the values by these two calculations agree within 2° .

TABLE 11

Conformations and relative abundance of diisopropyl ether, 2,4-dimethylpentane and diisopropyl ketone by the 4-21G and MM2 calculations[a]

	4-21G[b]			MM2		
	ϕ_1	ϕ_2	Population	ϕ_1	ϕ_2	Population
$(i\text{-}Pr)_2O$						
	35	35	98	40	40	98
	0	180	2	12	177	2
				165	165	0
$(i\text{-}Pr)_2CH_2$[c]						
	58	58	95	62	62	88
	25	-59	4	25	-59	8
				-58	161	2
	20	180	1	25	175	2
				168	168	0
$(i\text{-}Pr)_2CO$						
	16	-62	66	10	-53	65
	59	59	29	63	63	26
	0	180	5	8	179	6
				-44	141	3
				163	163	0

[a] The values of ϕ_1 and ϕ_2 in degrees. [b] The conformers around $\phi_1 = \phi_2 = 180°$ are not included in the calculations.

[c] Ref. 23.

Chapter 4

Normal Coordinate Analysis

4-1 General Description

Normal Coordinate Analysis. Normal coordinate analysis was performed by the GF matrix method [55]. In this treatment, the harmonic vibrations with small amplitudes are assumed. The kinetic and potential energies are given by

$$T = \frac{1}{2}\tilde{\dot{\mathbb{X}}}\mathbb{M}\dot{\mathbb{X}} \tag{4-1}$$

$$V = \frac{1}{2}\tilde{\mathbb{R}}\mathbb{F}\mathbb{R} \tag{4-2}$$

where $\mathbb{X}$ and $\mathbb{R}$ are the Cartesian and internal coordinate column vectors, respectively, and F and M denote the potential energy and mass diagonal matrices, respectively. The transformation matrix from $\mathbb{X}$ to $\mathbb{R}$ is denoted as B

$$\mathbb{R} = \mathrm{B}\mathbb{X} \tag{4-3}$$

The matrix elements of B are obtained by using the procedure in ref. 55, but the elements of the B matrix about the torsional coordinates are incorrect in ref. 55. The correct expression was given by Hilderbrandt [56].

The momentum associated with the internal coordinate is given by

$$P_i = \partial T / \partial \dot{R}_i \tag{4-4}$$

Then the kinetic energy is expressed in terms of the internal momentum column vector as

$$T = \frac{1}{2}\tilde{\mathbb{P}}G\mathbb{P} \qquad (4\text{-}5)$$

where the kinetic energy matrix G is given by $BM^{-1}\tilde{B}$. Using the above kinetic and potential energies ((4-2) and (4-4)), and solving Lagrange's equation of motion, we can obtain

$$GFL = L\Lambda \qquad (4\text{-}6)$$

$$| GF - E\lambda | = 0 \qquad (4\text{-}7)$$

The relation between the eigen value, λ, and the vibrational frequency, ν, is given by

$$\nu = \frac{1}{2\pi C}\sqrt{\lambda} \qquad (4\text{-}8)$$

The normal coordinate column vector, $\mathbb{Q}$, is related to $\mathbb{R}$ by

$$\mathbb{R} = L\mathbb{Q} \qquad (4\text{-}9)$$

Calculations of Mean Amplitudes and Shrinkage Corrections. In general polyatomic molecules, the Z axis of local Cartesian coordinates is taken in the direction from the position of one nucleus, i, to that of another nucleus, j. Then the mean amplitude l_{ij}^2 is equal to $\langle \Delta z_{ij}^2 \rangle$ in a good approximation, and the terms, $\langle \Delta x_{ij}^2 \rangle$ and $\langle \Delta y_{ij}^2 \rangle$, are related with the shrinkage correction. Here Δx_{ij}, Δy_{ij} and Δz_{ij} represent $x_j - x_i$, $y_j - y_i$ and $z_j - z_i$, respectively and $\langle\ \rangle$ denotes the vibrational average at a

given temperature. From the result of normal coordinate analysis, Cartesian coordinate shift Δz_i can be related with normal coordinates by a linear transformation

$$\Delta z_i = \sum_{\alpha} a_{i\alpha} Q_{\alpha} \qquad (4\text{-}10)$$

Therefore $\langle \Delta z_{ij}^2 \rangle$ is easily calculated:

$$\langle \Delta z_{ij}^2 \rangle = \sum_{\alpha} (a_{i\alpha} - a_{j\alpha})^2 \langle Q_{\alpha}^2 \rangle \qquad (4\text{-}11)$$

where

$$\langle Q_{\alpha}^2 \rangle = \frac{h}{8\pi^2 c\nu} \coth \frac{hc\nu}{2kT} \qquad (4\text{-}12)$$

The other quantities, $\langle \Delta x_{ij}^2 \rangle$ and $\langle \Delta y_{ij}^2 \rangle$, are obtained similarly.

Shrinkage effects are observed in the r_g structures [53]. For example, in a linear triatomic molecule, X-Y-Z, $r_g(X \cdots Z)$ is generally less than the sum of $r_g(X\text{-}Y)$ and $r_g(Y\text{-}Z)$ because of bending vibrations, but the symmetry of the equiliblium molecular structure is retained in the r_{α} structure. Therefore, it is necessary that the GED analysis is based on the r_{α} structure.

The instantaneous internuclear distance is given by

$$r_{ij} = \{(r_e + \Delta z_{ij})^2 + \Delta x_{ij}^2 + \Delta y_{ij}^2\}^{1/2} + \delta r \qquad (4\text{-}13)$$

where δr denotes the centrifugal stretching due to molecular rotation. Under the assumption of the the small amplitude vibrations, Eq. 4-13 can be replaced by Eq. 4-14 in a good

approximation,

$$r_{ij} = r_e + \Delta z_{ij} + \frac{\Delta x_{ij}^2 + \Delta y_{ij}^2}{2r_e} + \delta r \qquad (4\text{-}14)$$

Since the r_g and r_α distances are equal to $\langle r_{ij} \rangle$ and $r_e + \langle \Delta z_{ij} \rangle$, respectively, we have

$$r_g = r_\alpha + \frac{\langle \Delta x_{ij}^2 \rangle + \langle \Delta y_{ij}^2 \rangle}{2r_e} + \delta r \qquad (4\text{-}15)$$

Then the shrinkage corrections defined by $\delta_g = r_g - r_\alpha$ can be expressed as

$$\delta_g = \frac{\langle \Delta x_{ij}^2 \rangle + \langle \Delta y_{ij}^2 \rangle}{2r_e} + \delta r \qquad (4\text{-}16)$$

The values of δr are calculated on condition that the restoring force obeying Hooke's law is equal to the centrifugal force [57]. Therefore, the values of $\langle \Delta x_{ij}^2 \rangle$, $\langle \Delta y_{ij}^2 \rangle$, $\langle \Delta z_{ij}^2 \rangle$ and δr can be computed if harmonic force constants are known.

In usual investigations by GED, the r_g and/or r_α values are reported for bond lengths, while the values defined in the r_α structures are reported for bond angles.

4-2 Diisopropyl Ether

In the present study, the geometry of the C_2 conformer determined by GED was used in normal coordinate analysis, whereas Snyder and Zerbi [25] made the assignment using the assumed geometry. The force constants used for the calculations were initially taken from ref. 25 except for the torsional ones [56]. The observed fundamental frequencies were taken from refs. 25 and 26. Some of the force constants were modified so as to decrease differences between the frequencies calculated for the most stable conformer and the observed frequencies. The modified force constants are as follows: K_s = 5.340, K_R = 4.511, K_r = 4.700, F_r = 0.003, F_β = -0.042, H_β = 0.570, H_π = 0.961, and H_ψ = 0.668. The notations and units are the same as those in ref. 25. The averaged frequency error is about 9 cm^{-1}, which is nearly equal to that reported in ref. 25.

Snyder and Zerbi [25] did not measure the spectrum in the frequency range lower than 300 cm^{-1}. Clague and Danti [26] measured the low-frequency bands for various ethers, but did not mention the assignment for $(i\text{-}Pr)_2O$. Durig et al. [58] observed bands at 258 and 236 cm^{-1} for isopropylamine and assigned them to the methyl torsional modes. By referring to these results, a band at 255 cm^{-1} observed in the liquid phase was assigned to the torsional mode of methyl groups of the most stable conformer and the

force constant for the quadratic term of the torsional angle was determined to be 0.115 mdyn Å rad^{-2}.

The COC deformation frequency calculated for the most stable conformer was 192 cm^{-1}. This value was almost the same as the frequency of 194 cm^{-1} observed in the vapour phase [26]. Our calculated value of 192 cm^{-1} is different from a value of 160 cm^{-1} calculated by Snyder and Zerbi [25]. This is owing mainly to the difference in dihedral angles, $\phi_1(C_5OC_2H)$ and $\phi_2(C_2OC_5H)$, used in the two calculations. Snyder and Zerbi assumed that ϕ_1 and ϕ_2 are 60° , whereas we used the value of 38° for ϕ_1 and ϕ_2 which was determined finally by GED.

A band around 90 cm^{-1} observed in the liquid phase [26] was assigned to the torsional mode about the C-O axis after Clague and Danti [26], who assigned a band at 98 cm^{-1} observed for isopropyl methyl ether in the vapour phase to the torsional mode about the O-C(isopropyl) axis. However, the value of 90 cm^{-1} is not definite enough to specify the peak frequency of the torsional mode in the vapour phase, since the center of a very broad, weak low-frequency band is difficult to be identified accurately and moreover, the torsional frequencies in the liquid phase are known to be appreciably higher than those in the vapour phase [59]. Therefore, the force constant for the torsional motion about the C-O axis was estimated by using GED data (see Chapter 5 for details). As a result, the torsional force constant was

determined to be 0.070 mdyn Å rad^{-2}. From this value the torsional frequencies were calculated to be 77 and 50 cm^{-1}. The value of 0.070 mdyn Å rad^{-2} is reasonable compared with the values of 0.0682 and 0.0769 mdyn Å rad^{-2} reported by Kitagawa et al. [59] for ethyl methyl ether. The observed frequencies of 140 and 118 cm^{-1} are considered to be a combination tone and an overtone, respectively. The assignment of the bands and calculated frequencies below 300 cm^{-1} are summarized in Table 12

The normal coordinate analysis was carried out for the second conformer with ϕ_1 of 0° and ϕ_2 of 180° (C_s symmetry). The force constants dependent on ϕ_2, i.e., $f_{\mu\theta}{}^{t}$, $f_{\mu\theta}{}^{g}$, $f_{\theta X}{}^{t}$, and $f_{\theta X}{}^{g}$, were taken from ref. 25, while the force constants dependent on ϕ_1 were assumed to be either the same as those dependent on ϕ_2 or zero since they were not given in ref. 25. Other force constants were taken to be the same as those used for the most stable conformer. The above two assumptions on the force constants brought about no significant difference in the calculated frequencies. The calculated frequencies for the two conformers were significantly different from each other in the region from 300 to 600 cm^{-1}. The frequencies calculated for the second conformer in this region were as follows: 580 (532), 548 (503), 439 (448), 398 (408), 362 (400), and 338 (305) cm^{-1}, where the values in parentheses are the calculated frequencies for the most stable conformer. No bands were

observed near 580, 362, and 338 cm^{-1} in the liquid and vapour phases [26]. This finding suggests that the molar fraction of the second conformer is not large enough to be detected by vibrational spectroscopy.

The mean amplitudes and shrinkage corrections calculated by using the harmonic force constants were used in the data analysis of GED. The normal coordinate analysis and the diffraction data analysis were repeated until the calculated frequencies, the calculated mean amplitudes, and the determined geometry were little different from those obtained in the preceding step. This procedure is common to the data analyses of $(i\text{-}Pr)_2NH$, $(i\text{-}Pr)_2S$, and $(i\text{-}Pr)_2C{=}O$.

TABLE 12

Observed and calculated frequencies of diisopropyl ether lower than 300 cm^{-1} (in cm^{-1})

Obs.[a]		Calc.[b]	Assignment
IR	Raman		
		262	C-C torsion
	255[c]	262	C-C torsion
		262	C-C torsion
		262	C-C torsion
194[d]	200[c]	192	COC deformation
140[d,e]			combination tone ($77 + 50\ cm^{-1}$)
118[c,e]			overtone ($50 \times 2\ cm^{-1}$)
90[c,e]		77	C-O torsion
		50	C-O torsion

[a] Ref. 26. [b] The present study. [c] Spectra of the liquid. [d] Spectra of the vapour. [e] Very weak band.

4-3 Diisopropylamine

The assignments of observed bands were carried out by referring to assignments for secondary aliphatic amines by Gamer and Wolff [60] and for aliphatic ethers by Snyder and Zerbi [25]. Two bands around 3300 cm^{-1} were assigned to N-H stretching modes. A weak band observed at 3190 cm^{-1} was relatively broad and was about 100 cm^{-1} lower than the N-H stretching frequency. Therefore, the band at 3190 cm^{-1} may be regarded as a band of the hydrogen-bonded N-H stretching mode. Bands ranging from 3000 to 2900 cm^{-1} and those ranging from 2900 to 2800 cm^{-1} can be ascribed to the asymmetric and symmetric CH_3 stretching vibrations, respectively. Some overtones and/or combination bands of CH_3 deformation vibrations and other skeletal ones may appear in the region, 3000 - 2600 cm^{-1}. A shoulder around 2902 cm^{-1} and a band at 2847 cm^{-1} are probably overtones or combination bands. A few weak bands observed in the range 2800 to 2600 cm^{-1} are also considered to be overtones or combination bands.

Gamer and Wolff [60] made the assignment for the CNH bending modes of three secondary amines. According to these authors, the frequencies of the CNH bending modes are about 1480 cm^{-1} (a value which is higher than the methyl deformation frequencies) and about 720 cm^{-1}. Thus, the bands observed at 1476 and 693 cm^{-1} for the present molecule

in the vapour phase were assigned to the CNH bending modes. Bands observed around 1450 and 1380 cm^{-1} were assigned to the asymmetric and symmetric CH_3 deformation modes, respectively. Remaining bands around 1340 cm^{-1} were assigned to the $C-H_{i-Pr}$ bending mode after Snyder and Zerbi [25]. A band observed at 256 cm^{-1} was assigned to the methyl torsion as the bands observed at 258 and 236 cm^{-1}, for isopropylamine had been assigned to the methyl torsion by Durig et al. [58]. Bands to be assigned to the C-N torsion could not be observed. These bands will appear at much lower frequencies than the frequency of the methyl torsion.

Other bands observed below 1200 cm^{-1} are associated with the CH_3 rocking and skeletal vibrations. Assignments of these bands were made by means of a normal coordinate analysis with a general valence force field including interactions between neighboring internal coordinates. The force constants except those for the methyl and isopropyl torsions were transferred initially from those for diisopropyl ether [25] and dimethylamine [61] and then modified by a tial-and-error method until the calculated frequencies well reproduce the observed ones. The force constant for the methyl torsion was determined so as to reproduce the observed frequency, 256 cm^{-1}. The value of the force constant for the isopropyl torsion was estimated at the stage of the analysis of GED data (see Chapter 5).

Determination of force constants was carried out in every least-squares analysis of the GED data by employing the structure determined by the last GED analysis. The force constants finally employed are shown in Table 13. Table 14 shows the calculated frequencies and the assignments with the potential energy distributions for the final molecular structure. The present normal coordinate analysis indicates that all the observed bands can be interpreted as the bands originating from only one conformer.

Since the potential field involved no interactions between non-neighboring internal coordinates, the calculated frequencies, especially for the bands associated with hydrogen atoms, were split less than the observed values. However, uncertainties in calculated mean amplitudes and shrinkage corrections do not influence significantly the final result for the molecular structure since contributions from interatomic distances associated with hydrogen atoms to the total scattering intensities are relatively small.

TABLE 13

Quadratic force constants for diisopropylamine[a]

Force constant	Atoms common to interacting coordinates	Value
Stretch		
K(N-C)		5.071
K(C-C)		4.467
K(N-H)		6.065
$K(C\text{-}H_{Me})$		4.687
$K(C\text{-}H_{i\text{-}Pr})$		4.663
Bend		
H(∠CNC)		1.500
H(∠CCC)		1.086
H(∠NCC)		1.290
H(∠NCH)		0.735
H(∠CNH)		0.620
$H(\angle CCH_{Me})$		0.607
$H(\angle CCH_{i\text{-}Pr})$		0.735
H(∠HCH)		0.530
Torsion		
H_{τ}(C-C)		0.115
H_{τ}(N-C)		0.055[b]
Stretch-stretch		
F(N-C,N-C)	N	0.350

F(N-C,C-C)	C	0.300
F(C-C,C-C)	C	0.300
F(C-H,C-H)	C	0.033
Stretch-bend		
F(N-C,∠CNC)	N-C	0.490
F(N-C,∠NCC)	N-C	0.610
F(N-C,∠CNH)	N-C	0.161
F(N-C,∠NCH)	N	0.043
F(N-C,∠NCH)	N-C	0.362
F(C-C,∠NCC)	C-C	0.410
F(C-C,∠CCC)	C-C	0.517
$F(C\text{-}C,\angle CCH_{Me})$	C-C	0.328
$F(C\text{-}C,\angle CCH_{i\text{-}Pr})$	C	0.079
$F(C\text{-}C,\angle CCH_{i\text{-}Pr})$	C-C	0.450
Bend-bend		
F(∠NCC,∠NCC)	N-C	0.110
F(∠NCC,∠CCC)	C-C	0.110
F(∠CNC,∠CNH)	N-C	-0.200
F(∠NCC,∠NCH)	N-C	-0.030
$F(\angle NCC,\angle CCH_{i\text{-}Pr})$	C-C	-0.030
$F(\angle CCC,\angle CCH_{i\text{-}Pr})$	C-C	-0.030
F(∠CNH,∠CNH)	N-H	-0.033
$F(\angle NCH,\angle CCH_{i\text{-}Pr})$	C-H	0.030
$F(\angle CCH_{Me},\angle CCH_{Me})$	C-C	-0.023
$F(\angle CCH_{i\text{-}Pr},\angle CCH_{i\text{-}Pr})$	C-H	0.030
$f^{t}(\angle CNC,\angle NCC)$	$(C)N\overset{trans}{\text{———}}C(C)$	-0.011

$f^{g}(\angle CNC,\angle NCC)$	(C)N$\underline{\text{gauche}}$C(C)	0.011
$f^{t}(\angle NCC,\angle CCH_{Me})$	(N)C$\underline{\text{trans}}$C(H)	0.030
$f^{g}(\angle NCC,\angle CCH_{Me})$	(N)C$\underline{\text{gauche}}$C(H)	-0.110
$f^{t}(\angle CCC,\angle CCH_{Me})$	(C)C$\underline{\text{trans}}$C(H)	0.049
$f^{g}(\angle CCC,\angle CCH_{Me})$	(C)C$\underline{\text{gauche}}$C(H)	-0.052
$f^{t}(\angle CCH_{Me},\angle CCH_{i\text{-}Pr})$	(H)C$\underline{\text{trans}}$C(H)	0.127
$f^{g}(\angle CCH_{Me},\angle CCH_{i\text{-}Pr})$	(H)C$\underline{\text{gauche}}$C(H)	-0.005

[a] Units of stretch, bend and torsion constants are mdyn $Å^{-1}$, mdyn Å rad^{-2} and mdyn Å rad^{-2}, respectively. Units of stretch-stretch, stretch-bend and bend-bend interaction constants are mdyn $Å^{-1}$, mdyn rad^{-1} and mdyn Å rad^{-2}, respectively. [b] Force constant determined from GED data.

TABLE 14

Observed and calculated frequencies (cm^{-1}), and assignments with potential energy distributions for diisopropylamine

Obs.[a]	Calc.[b]	Assignment (PED%)[c]
~3300	3314	νNH(100)
~2968,2937	2958-2955(8)	$\nu_a CH_3$(98-100)
2924	2928,2927	νCH_{i-Pr}(95)
2885	2882-2881(4)	$\nu_s CH_3$(97-98)
1476	1478	δCNH(60)
~1450	1455-1440(80)	$\delta_a CH_3$(74-91)
1385	1394-1386(4)	$\delta_s CH_3$(96-101)
1342	1351,1344	δCH_{i-Pr}(87); δCH_{i-Pr}(80)
1330[d]	1322	δCH_{i-Pr}(82)
~1310[e]	1310	δCH_{i-Pr}(83)
1196[e]	1192	νCN(39), rCH_3(23)
1182	1188,1183	rCH_3(31), νCC(31); νCC(43), rCH_3(25)
1135	1131	νCC(51), rCH_3(29)
1117[d]	1105	rCH_3(40), νCC(29)
1095	1100	νCC(38), rCH_3(33)
1022	1000	rCH_3(46), νCN(36)
950	960	rCH_3(69), νCC(22)
940[e]	952	rCH_3(66), νCC(24)
928	914,908	rCH_3(80); rCH_3(78)
918[d]	900	rCC(55), rCH_3(35)

~850	861	rCC(68)
830	830	rCN(32), rCH_3(28)
693	679	δCNH(57), νCN(22)
504[d]	518	δNCC(32)
487[e]	479	δNCC(29), δCNC(23)
445[e]	440	δNCC(50), $\delta CH_{i\text{-}Pr}$(20)
406[e]	402	δNCC(89)
393[e]	385	δCCC(80)
317[e]	296	δNCC(52), δCCC(43)
256[e]	258-254(4)	tCH_3(89-99)
193[e]	190	δCNC(44), δNCC(35)
	70	tCN(81)
	43	tCN(99)

[a] Fundamental frequencies are listed. [b] Values in parentheses indicate the numbers of bands calculated in this range. [c] Contributions less than 20% were omitted. ν, stretching; δ, bending; r, rocking; a, asymmetric; s, symmetric; t, torsion. [d] Taken from infrared spectrum in the liquid phase. [e] Taken from Raman spectrum in the liquid phase.

4-4 Diisopropyl Sulfide

Scott and El-Sabban derived a valence force field [34] for aliphatic sulfide from the observed frequencies of several sulfides in which the present molecule was not included. They applied the valence force field to $(i\text{-}Pr)_2S$ and calculated frequencies of the C_2 and C_s conformers assuming appropriate geometries. Some force constants in the above force field were modified in the present study to decrease the differences between the observed frequencies [31] and the frequencies calculated for the C_2 conformer whose geometry was determined by GED. The modified force constants are as follows: F_{C-C} = 4.700, $F_{C-H,C-H}$ = 0.006, H_{CCH} = 0.636, and $H'_{CCH,CCH}$ = -0.057. The notations and units are the same as those in ref. 34. An interaction force constant between C-S stretchings (0.250 mdyn Å rad^{-2}) was added to improve the agreement between the observed and calculated frequencies attributed to the C-S stretching modes.

The value of the force constant for methyl torsion was transferred from that determined for 2-propanethiol and 2-methyl-2-propanethiol (0.1035 mdyn Å rad^{-2}) by Scott and Crowder [62], since the band to be assigned to the methyl torsion was not observed [31]. Scott and Crowder [31] determined the barrier governing the internal rotation of isopropyl groups, V_3, to be 2.80 kcal/mol. From this value,

the force constant for the torsional motion about the C-S axis was estimated to be 0.09 mdyn Å rad^{-2}. The normal coordinate calculation using this constant did not reproduce the torsional frequency of 74 cm^{-1} [31] observed in the vapour phase. Therefore, the interaction force constant for two isopropyl torsions was introduced into the calculation and its value was determined to be -0.015 mdyn Å rad^{-2}. The average discrepancy between the observed and calculated frequencies for the C_2 conformer was about 7 cm^{-1}. The above force constants were used to calculate the mean amplitudes and shrinkage corrections of all the conformers included in the data analysis of GED.

The next stable conformers inferred in previous investigations [32-35] were based on the empirical consideration and on the assumption of the staggered configuration for the isopropyl groups. Scott and El-Sabban [34] suggested that the C_s conformer is the next stable. Ohsaku et al. [32,35] and Sakakibara et al. [33] reported that possible conformers except the C_2 conformer are the C_1 and C_s conformers but they could not clarify the order of the stability of the two conformers. According to the ab initio calculations by Schäfer [27], the C_1 and C_s conformers described in the literature [32-35] are unstable. Therefore, the stable conformers given by the MM2 calculations were taken into account in the following analysis. Normal coordinate analyses were carried out for

the two C_1 conformers with ϕ_1 = 12° and ϕ_2 = -52° , and ϕ_1 = 17° and ϕ_2 = 175° . Calculated frequency differences among the C_2 and two C_1 conformers were small except for the frequency at about 450 cm^{-1}: the frequencies calculated for the C_2, C_1(ϕ_1 = 12° and ϕ_2 = -52°), and C_1(ϕ_1 = 17° and ϕ_2 = 175°) conformers are 437, 453, and 477 cm^{-1}, respectively. Scott and Crowder observed bands at 432 and 476 cm^{-1} [31]. The former band was ascribed to the C_2 conformer in the previous investigations [32-34]. The C_1 conformer with ϕ_1 = 17° and ϕ_2 = 175° is considered to be the next stable, since the observed frequency of 476 cm^{-1} is attributed to this conformer.

4-5 Diisopropyl Ketone

The assignments of the vibrational spectra were carried out by referring to the assignments for diisopropyl ether and amine. The methyl stretching and deformation modes and the $C\text{-}H_{i\text{-}Pr}$ stretching and bending modes were assigned by following the assignments for the above diisopropyl compounds. The carbonyl stretching vibration is located at 1730 cm^{-1} [37,38]. The bands at 240 cm^{-1} and 45 cm^{-1} [43] were considered to be due to the methyl and isopropyl torsional modes, respectively.

The other bands were not easy to be assigned. Therefore, they were assigned by carrying out normal coordinate analyses. The valence force constants were initially transferred from those for acetone [63], diethyl ketone [64] and hydrocarbons [65]. Some force constants with small values were ignored and some force constants were assumed to be the same in order to simplify the force field. The resulting force field consists of 27 independent force constants. The geometry of the C_1 conformer determined by GED was used in the normal coordinate analysis. Some observed frequencies could not be assigned to the fundamental modes of the conformer by using the normal values of the force constants. They are considered to be combination tones, overtones or the frequencies attributable to other conformers. Therefore, they were excluded in the

initial normal coordinate analysis and the force constants were modified so that the calculated frequencies might reproduce the observed ones. Vibrational frequencies of the C_2 and C_s conformers were then calculated by employing the force constants determined for the C_1 conformer. The final values of the force constants and the calculated frequencies are shown in Tables 15 and 16, respectively. The comparison between the observed and calculated frequencies shows that most of the observed bands are assigned to the vibrational modes of the C_1 conformer and that some bands are due to the C_2 and/or C_s conformers.

TABLE 15

Valence force field for diisopropyl ketone

Force constant[a]	Atoms common to interacting coordinates	Value[b]
Stretch		
K(C=O)		9.168
K((O=)C-C)		3.736
K(C-C)		4.019
$K(C\text{-}H_{i\text{-}Pr})$		4.606
$K(C\text{-}H_{Me})$		4.705
Bend		
H(CC(=O)C)		1.820
H(OCC)		1.220
H((O=)CCC)		1.021
H(CCC)		1.095
$H((O=)CCH_{i\text{-}Pr})$		0.718
$H(CCH_{i\text{-}Pr})$		0.648
$H(CCH_{Me})$		0.687
H(HCH)		0.503
H(C=O out of plane)		0.215
Torsion		
H_{τ}((O=)C-C)		0.026
H_{τ}(C-C)		0.100
Stretch-Stretch		

F((O=)C-C,C-C)	C	0.192[c]
F(C-C,C-C)	C	
$F(C\text{-}H_{Me},C\text{-}H_{Me})$	C	0.030
Stretch-Bend		
F((O=)C-C,(O=)CCC)	C-C	0.255[c]
F(C-C,CCC)	C-C	
$F(C\text{-}C,CCH_{Me})$	C-C	0.289
$F((O=)C\text{-}C,(O=)CCH_{i\text{-}Pr})$	C-C	0.395[c]
$F(C\text{-}C,CCH_{i\text{-}Pr})$	C-C	
$F((O=)C\text{-}C,CCH_{i\text{-}Pr})$	C	0.018[c]
$F(C\text{-}C,CCH_{i\text{-}Pr})$	C	
$F(C\text{-}C,(O=)CCH_{i\text{-}Pr})$	C	
Bend-Bend		
$F(CCH_{Me},CCH_{Me})$	C-C	-0.073
F((O=)CCC,(O=)CCC)	C-C	-0.075[c]
F((O=)CCC,CCC)	C-C	
$F(CCH_{i\text{-}Pr},(O=)CCH_{i\text{-}Pr})$	C-H	0.025[c]
$F(CCH_{i\text{-}Pr},CCH_{i\text{-}Pr})$	C-H	
$F((O=)CCC,(O=)CCH_{i\text{-}Pr})$	C-C	0.081[c]
$F((O=)CCC,CCH_{i\text{-}Pr})$	C-C	
$F(CCC,CCH_{i\text{-}Pr})$	C-C	
$f^{t}(CCH_{Me},CCH_{i\text{-}Pr})$	$(H)C\overset{trans}{=\!=}C(H)$	0.161

[a] $H_{i\text{-}Pr}$ and H_{Me} denote a hydrogen atom attached to the tertiary carbon atom and a hydrogen atom in methyl groups, respectively. [b] In units of mdyn $Å^{-1}$ (stretch constants),

mdyn rad^{-1} (stretch-bend interaction constants), and mdyn Å rad^{-2} (bend and torsion constants). [c] These values are refined as groups.

TABLE 16

Observed and calculated frequencies (in cm^{-1}), and assignments with potential energy distributions for diisopropyl ketone

Obs.[a]	Calc.[b]			PED[c]
	C_1	C_2	C_s	C_1
2979,2945	2965-2963(8)	2965-2963(8)	2965-2963(8)	$\nu_a CH_3$(98-99)
2910	2912,2908	2909,2908	2913,2909	$\nu CH_{i\text{-}Pr}$(97,98)
2887	2883(4)	2883(4)	2883(4)	$\nu_s CH_3$(99)
1730	1736	1742	1713	νC=O(64)
1480	1481	1486		$\delta_a CH_3$(54)
1470	1474-1473(3)	1479-1476(3)	1476-1470(4)	$\delta_a CH_3$(58-63)
1449[d]	1461-1453(4)	1465-1459(4)	1459-1451(4)	$\delta_a CH_3$(77-84)
1394	1390	1395		$\delta_s CH_3$(58)
1389	1388	1391	1387,1386	$\delta_s CH_3$(73)
1384	1380(2)	1386,1385	1381,1378	$\delta_s CH_3$(96,94)
1370	1366	1370	1355	$\delta_s CH_3$(25)
1326[d]	1340-1328(3)	1346-1333(3)	1335-1324(3)	$\delta CH_{i\text{-}Pr}$(46-47)

1298			1291	
1264	1272	1278		$\delta CH_{i-Pr}(25)$
1207	1208	1203	1205	$rCH_3(45)$
1188		1185	1192	
1183	1180	1174	1172	$rCH_3(43)$
1178	1162	1150	1157	$rCH_3(36), \nu CC(34)$
1127	1146			$rCH_3(43)$
1115[d]	1114	1113	1111	$rCH_3(48), \delta CH_{i-Pr}(30)$
1085[d]	1090	1092		$rCH_3(58)$
1070[d]			1054	
1027	1019,1010	1024,1010	1014,1010	$rCH_3(54,49), \nu CC(32,36)$
986	980	982	981	$rCH_3(74), \delta CH_{i-Pr}(31)$
960	973	976	973	$rCH_3(69), \delta CH_{i-Pr}(27)$
930			906	
895[d]	903	899	886	$\nu CC(66)$
860	859	863		$\nu CC(79)$
740	734			$\nu (O=)CC(46)$
716[d]		713	708	
610	612	623	608	$\delta CCC(40), \omega CO(27)$
568[d]	559		576	$\delta CCC(39)$

525[d]			524	
488[d]		499,489		
471[d]	483			δCCC(36)
395[d]	408	403	398	δCCC(79)
		373	371	
330[d]	337			δCCC(77)
290[d]	292,285	297,277	312,274	δCCC(70,64)
240[d]	252-238(4)	247-239(4)	242-236(4)	tCH$_3$(72-99)
206[d]	200			δCCC(46)
		195	181	
	179	184	176	ξCO(40), δCCC(39)
45[d]	34,30	36,29	36,28	t(O=)CC(97,99)

[a] Fundamental frequencies are listed. [b] Values in parentheses indicate the numbers of bands calculated in this range. [c] Potential energy distributions of the C_1 conformer. Contributions less than 25% were omitted. Abbreviations used in this table are the same as in Table 14 except ω and ξ. ω; in-plane bending, ξ; out-of-plane bending. [d] Taken from infrared spectra in the liquid phase.

Chapter 5

Analysis of Gas Electron Diffraction Data

5-1 General Procedure of Data Analysis

Molecular scattering intensities are obtained by the experimental total intensities and empirical backgrounds (see Chapter 2). The theoretical expression for molecular scattering intensities derived from the modified first Born approximation and the small amplitude approximation for vibrations is as follows [49]:

$$sM(s)^{theor.} = \Sigma\Sigma A_{ij}\mu_{ij}\cos\Delta\eta_{ij}\sin[s(r_{aij}-\kappa_{ij}s^2)]\exp(-\frac{l_{ij}^2}{2}s^2) \quad (5\text{-}1)$$

$$A_{ij} = \frac{2Z_iZ_j}{r_{aij}\sum_k\{Z_k(Z_k+1)\}} \quad (5\text{-}2)$$

$$\mu_{ij} = \frac{\sum_k\{Z_k(Z_k+1)\}}{Z_iZ_j}\ \frac{|f_i(s)|\ |f_j(s)|}{\sum_k\{|f_k(s)|^2+\left(\frac{2}{as^2}\right)^2 S_k(s)\}} \quad (5\text{-}3)$$

where r_{aij} is the apparent distance between atoms, i and j, κ_{ij} is the asymmetry parameter due to the anharmonicity of the vibration and l_{ij} is the mean amplitude.

The r_a distances directly observed by GED have no definite physical meaning but they can be easily converted to the r_g values:

$$r_g = r_a + \frac{l^2}{r_a} \quad (5\text{-}4)$$

In the present study, asymmetry parameters κ_{ij} for bonding atom pairs were calculated in a diatomic approximation by using the relation

$$\kappa_{ij} = \frac{a}{6} l_{ij}^{4} \qquad (5\text{-}5)$$

where a is the Morse parameter [66]. By assuming a to be 2 $\mathring{A}^{-1}$, the asymmetry parameters for bonding atom pairs were calculated. Asymmetry parameters for nonbonded atom pairs were assumed to be zero. Bond lengths, valence and torsional angles, conformational composition, asymmetry parameters, mean amplitudes and index of resolution can be selected as adjustable parameters and they can be determined by the least-squares calculation on sM(s). The index of resolution, k, is defined as

$$sM(s)^{obs.} = ksM(s)^{theor.} \qquad (5\text{-}6)$$

The index of resolution must be equal to unity if both experiment and theory are correct. Since it is quite difficult to eliminate the extraneous scattering completely, k often takes a value smaller than unity and indicates the quality of experiment. Goodness of the least-squares fitting is evaluated by the R-factor. The R-factor is defined by

$$\{\Sigma W_i(\Delta sM(s)_i)^2/\Sigma W_i(sM(s)^{obs.})^2\}^{1/2}, \qquad (5\text{-}7)$$

where

$$\Delta sM(s) = sM(s)_i^{obs.} - ksM(s)_i^{theor.} \qquad (5\text{-}8)$$

and W_i is a diagonal element of the weight matrix.

Radial distribution curves are calculated by the application of the Fourier sine transformation:

$$f(r) = \int_0^{s_{max}} sM(s)\exp(-bs^2)\sin(sr)ds \qquad (5\text{-}9)$$

where an artificial damping factor $\exp(-bs^2)$ is introduced to reduce the truncation effect because the experiment gives the molecular scattering intensities only for the limited s-range. In the present study, the b value was chosen so as to satisfy a condition,

$$\exp(-bs_{max}^2) = 0.1 \qquad (5\text{-}10)$$

Experimental backgrounds are corrected by the non-negativity criterion on the RD curves.

5-2 Treatment common to the GED analysis of $(i\text{-}Pr)_2O$, $(i\text{-}Pr)_2NH$, and $(i\text{-}Pr)_2S$

According to the theoretical calculations described in Chapter 3, the most stable conformers of $(i\text{-}Pr)_2O$, $(i\text{-}Pr)_2NH$, and $(i\text{-}Pr)_2S$ have C_2 or nearly C_2 symmetry. On the other hand, the most stable conformer of $(i\text{-}Pr)_2C{=}O$ has C_1 molecular symmetry. In the case of $(i\text{-}Pr)_2O$, $(i\text{-}Pr)_2NH$ and $(i\text{-}Pr)_2S$, we reached the same conclusion in the GED data analyses carried out prior to the theoretical calculations although the abundance and molecular symmetry of the next stable conformers were ambiguous [67-69]. On the other hand, the GED data analysis for $(i\text{-}Pr)_2C{=}O$ showed that the C_2 conformer was not predominant. Since the conformation of $(i\text{-}Pr)_2C{=}O$ is different from the conformations of other three diisopropyl compounds, its data analysis will be described separately.

In the preliminary data analyses of $(i\text{-}Pr)_2O$, $(i\text{-}Pr)_2NH$, and $(i\text{-}Pr)_2S$, the following assumptions were made to reduce the number of independent parameters: (1) two isopropyl groups have the same local geometry with C_s symmetry; (2) four methyl groups have the same local geometry with C_{3v} symmetry; (3) each methyl group takes the staggered position against the C-X bond and has no tilt, where X is O, N, and S; (4) all the C-H bond lengths are equal; (5) two C-X bond lengths are equal. An additional assumption was made for

$(i\text{-}Pr)_2NH$: two CNH bond angles are equal. Then the following independent structural parameters were selected: r(C-X), r(C-C), r(C-H), ∠CXC, $\angle XCC_3$, $\angle XCC_4$, $\angle XCC_6$, $\angle XCC_7$, ∠CCC, $\angle CCH_{Me}$, $\angle CCH_{i\text{-}Pr}$, $\phi_1(C_5XC_2H)$, and $\phi_2(C_2XC_5H)$. Two independent structural parameters ,r(N-H) and ∠CNH, were added in the analysis of $(i\text{-}Pr)_2NH$.

In every least-squares calculation, some mean amplitudes of bonding atom pairs were treated as least-squares parameters, but other mean amplitudes and shrinkage corrections were fixed at values calculated from the force constants and the structural parameter values obtained in the preceding step. The details of the force constants except those of the isopropyl torsion in $(i\text{-}Pr)_2O$ and $(i\text{-}Pr)_2NH$ were described in Chapter 4. For the above two compounds, the value of the force constant of the isopropyl torsion could not be determined in the normal coordinate analysis, since the corresponding torsional frequency in the vapour phase was not measured. Therefore, the force constant was estimated in the following manner. The mean amplitudes and shrinkage corrections were calculated from various values of the torsional force constant. The least-squares analysis on the molecular scattering intensities, sM(s), was repeated until we found a value of the force constant minimizing the R-factor. As a result, the torsional force constants about the C-O and C-N axes were determined to be 0.070 and 0.055 mdyn Å rad^{-2}, respectively.

The limits of error of the adjustable parameters were evaluated from the squared sums of the estimated random and systematic errors by following the law of propagation of errors. The limits of random error were estimated to be 2.6 times the standard errors in the least-squares calculation. The systematic errors were estimated from the uncertainties of the scale factor. Other systematic errors except those due to the small amplitude approximation about the isopropyl torsion were estimated to be negligible.

The torsional vibration of the isopropyl group was treated as a small amplitude motion. The torsional force constant, f, of $(i\text{-}Pr)_2NH$ is 0.055 mdyn Å rad^{-2}, which is the lowest among the three molecules. If the potential energy for internal rotation is expressed by a function,

$$V = (V_3/2)(1-\cos 3\phi) \qquad (5\text{-}1)$$

then the value of V_3 is calculated to be 2f/9. Thus the V_3 value of the isopropyl torsion of $(i\text{-}Pr)_2NH$ was approximately estimated to be 1.76 kcal/mol from the f value. The root mean squares amplitude of the C-N torsional angles of $(i\text{-}Pr)_2NH$ was estimated to be 16° by using the same value of f. These values of the potential barrier and the mean amplitude are not so small. Therefore, it is desirable to treat the torsion as a large-amplitude motion [70].

As for the above three molecules, precise potential

functions have not been determined by experimental methods. In the usual treatment of the large-amplitude motion, bond lengths and bond angles are assumed to be independent of the torsional motion [71]. However, these molecules have at least two kinds of XCC bond angles and these bond angles cannot be regarded as independent of the torsion. Therefore, it is necessary to treat pseudo-conformers with C_1 symmetry in which four XCC bond angles have different values. This makes the treatment of the large-amplitude motion too difficult to be performed in the present study. The examination of the systematic errors introduced by the small amplitude approximation has been left for future investigations.

5-3 Diisopropyl Ether

Table 17 shows the mean amplitudes for relatively important atom pairs calculated by using the final structural parameter values. Mean amplitudes, l(C-O) and l(C-H), were treated as adjustable parameters. At first the data analysis was carried out by assuming the existence of a single conformer. The number of the structural parameters related with the OCC bond angles was reduced by consideration of symmetry. For example, $\angle OCC_3$ and $\angle OCC_4$ are equal to $\angle OCC_7$ and $\angle OCC_6$, respectively, for conformers with C_2 symmetry. On the other hand, the four OCC angles are different from each other for conformers with C_1 symmetry. However, they were assumed to be the same in the present study since they could not be determined separately. Because the $CCH_{i\text{-}Pr}$ angle could not be determined by GED, it was fixed at a mean value obtained from the 4-21G geometry [27].

A C_2 conformer with $\phi_1 = \phi_2 = 38°$ reproduced the observed molecular intensities best. This result is consistent with the prediction by the 4-21G and MM2 calculations. The molecular scattering intensities and radial distribution (RD) curves for the C_2 conformer are shown in Figs. 5 and 6, respectively. Determined structural parameters are listed in Table 18, column 2. The difference between $r(C_2\text{-}C_3)$ and $r(C_2\text{-}C_4)$ in the 4-21G geometry [27] is

0.004 Å. The R-factor of 0.0583 was obtained by the analysis using the calculated difference and it almost coincided with the R-factor of 0.0582 listed in Table 18. Thus the difference in the C-C bond lengths was not detected by GED.

In the next step of data analysis, the C_s conformer with ϕ_1 of 0° and ϕ_2 of 180° was included as the second conformer referring to the results of the ab initio calculations. It is apparent from the RD curves shown in Fig. 5 that the concentration of the C_s conformer is small. This implied that the geometry of the C_s conformer can not be determined by GED alone. The structural parameters of the C_2 and C_s conformers can not be the same. According to the 4-21G geometries, the differences in the OCC bond angles and the C-C bond lengths between the C_2 and C_s conformers are 2° - 6° and 0.002 - 0.007 Å, respectively. Thus, the dependence of the structural parameters on conformations must be taken into account in the data analysis.

In the present study, the differences among similar structural parameters of the C_2 and C_s conformers were fixed at the values given by the 4-21G calculations [27]. The corresponding differences obtained by the molecular mechanics calculations seem less reliable than the 4-21G calculations [72,73]. The detail of the procedure is shown in Table 19. It was assumed that the mean amplitudes for bonding atom pairs are independent of the conformations.

According to the results of the 4-21G calculations, the C_3 and C_4 methyl groups of the C_s conformer rotate by about 9° from the staggered configuration. This rotational displacement of the methyl groups was incorporated in the data analysis but no appreciable change was observed for the converged values of the other structural parameters. The population of the C_2 conformer was refined as an independent parameter in the least-squares analysis and the relative abundance of the second conformer was determined to be 27(8)%. The observed values for the structural parameters of the most stable conformer are listed in Table 18 together with the estimated limits of error.

The inclusion of the second conformer in data analysis little altered the structural parameter values of the C_2 conformer except for $\angle COC$, $\angle OCC_3$, and ϕ_1. The population of the second conformer, 27(8)%, is so large that the existence of this conformer may be detected by vibrational spectroscopy. However, no band attributable to the second conformer was detected in the vibrational spectra. Moreover, the conformational composition of the C_s conformer, 27(8)%, indicates that the energy difference between the C_2 and C_s conformers is $550 \begin{smallmatrix} + 300 \\ - 190 \end{smallmatrix}$ cal/mol, which is much smaller than 2.2 and 2.6 kcal/mol, estimated by the 4-21G and MM2 calculations. Therefore, the population of the second conformer determined by GED seems to contradict the results of both vibrational spectroscopy and theoretical

calculations. This discrepancy was suspected to be apparent due to the deficiency in the data analysis. Thus a different data analysis was attempted by restricting the structural parameter values of the C_2 conformer to be consistent with the results of the model 1. A solution consistent with the vibrational spectra and the theoretical investigations was obtained by fixing the ϕ_1-value to be 38° , and varying the values of the OC_2C_3 and C_2OC_5 bond angles by 1.5 times the standard error, i.e., 0.4° and 0.9° , respectively. Then, the population of the C_s conformer became $3\ ^{+6}_{-3}$%. This suggests that the relative abundance of the second conformer is overestimated in the conformational mixture model described above. Thus the relative abundance of the second conformer was estimated to be less than 15% on the basis of the vibrational spectra and the theoretical calculations. The structural parameter values listed in the second column in Table 18 seem to be more reasonable than those in the third column and they were taken as the final result in the present study.

TABLE 17

Calculated mean amplitudes (l_{ij}) for the C_2 conformer of diisopropyl ether (in Å)[a]

Atom pair[b]	l_{ij}	r_{ij}[c]
O-C	0.048	1.431
C-C	0.052	1.526
C-H	0.079	1.112
O···C_3	0.066	2.440
O···C_4	0.067	2.360
C_2···C_5	0.063	2.432
C_2···C_6	0.087	3.641
C_2···C_7	0.161	3.156
C_3···C_4	0.070	2.539
C_3···C_6	0.215	4.142
C_3···C_7	0.250	4.186
C_4···C_6	0.092	4.686

[a] Calculated at 20°C. Only the mean amplitudes for relatively important atom pairs are listed. [b] See Figure 1 for atom numbering. [c] The r_a distances corresponding to the final molecular geometry given in Table 18.

TABLE 18

Observed structural parameter values for the most stable conformer of diisopropyl ether[a]

	Model 1[b]	Model 2[c]
r_g(C-H)	1.117(2)	1.117(2)
r_g(C-O)	1.433(3)	1.432(2)
r_g(C-C)	1.527(2)	1.527(2)
$\angle_\alpha$COC	116.9(16)	117.8(14)
$\angle_\alpha OCC_3$	111.5(7)	109.9(9)
$\angle_\alpha OCC_4$	106.5(4)	106.2(5)
$\angle_\alpha$CCC	112.9(7)	112.7(5)
$\angle_\alpha CCH_{i\text{-}Pr}$	109.7[d]	109.7[d]
$\angle_\alpha CCH_{Me}$	111.1(9)	110.7(8)
$\phi_1 (=\phi_2)$	38(3)[e]	41(3)[f]
l(C-H)	0.077(3)	0.078(3)
l(C-O)	0.049(3)	0.049(4)
l(C-C)	0.052[g]	0.052[g]
k_l[h]	0.94(2)	0.95(1)
k_s[h]	0.94(3)	0.95(3)
R	0.0582	0.0488

[a] Bond lengths and mean amplitudes in Å, and angles in degrees. Values in parentheses are the limits of error attached to the last digit of the parameter values. [b] The result obtained by assuming that only the conformer with C_2

symmetry exists in the vapour phase. The parameters listed in this column should be regarded as the final results. [c] The result obtained for the conformational composition of 73(8)% C_2 + 27(8)% C_s. [d] Fixed value (see text). [e] Observed values of the dihedral angles, $C_5OC_2C_3$ and $C_5OC_2C_4$, are -82° and 155° , respectively. [f] Observed values of the dihedral angles, $C_5OC_2C_3$ and $C_5OC_2C_4$, are -79° and 159° , respectively. [g] Calculated value. [h] k_1 and k_s are the indices of resolution for the long and short camera distances, respectively.

TABLE 19

Constrained model for conformational mixture of diisopropyl ether[a]

Symmetry	C_2	C_s
r(O-C)	r_1	r_1+0.004
r(O-C)	r_1	r_1-0.010
$r(C_2-C_3)$	r_2	r_2
$r(C_2-C_4)$	r_2	r_2
$r(C_5-C_6)$	r_2	r_2+0.005
$r(C_5-C_7)$	r_2	r_2+0.005
r(C-H)	r_3	r_3
$\angle C_2O_1C_5$	θ_1	θ_1+1.7
$\angle O_1C_2C_3$	θ_2	$(\theta_2+\theta_3)/2$
$\angle O_1C_2C_4$	θ_3	$(\theta_2+\theta_3)/2$
$\angle O_1C_5C_6$	θ_3	$(\theta_2+\theta_3)/2$+4.4
$\angle O_1C_5C_7$	θ_2	$(\theta_2+\theta_3)/2$+4.4
$\angle C_3C_2C_4$	θ_4	θ_4-0.1
$\angle C_6C_5C_7$	θ_4	θ_4+0.1
$\angle C_{3,4}C_2H_{i\text{-}Pr}$	θ_5	θ_5-0.3
$\angle C_{6,7}C_5H_{i\text{-}Pr}$	θ_5	θ_5-1.3
$\angle CCH_{Me}$	θ_6	θ_6
$\phi_1(C_5O_1C_2H_8)$	ϕ_1	0
$\phi_2(C_2O_1C_5H_{21})$	ϕ_1	180

[a] Adjustable parameters in the least-squares calculation are

r_1, r_2, r_3, θ_1, θ_2, θ_3, θ_4, θ_5, θ_6, and ϕ_1.

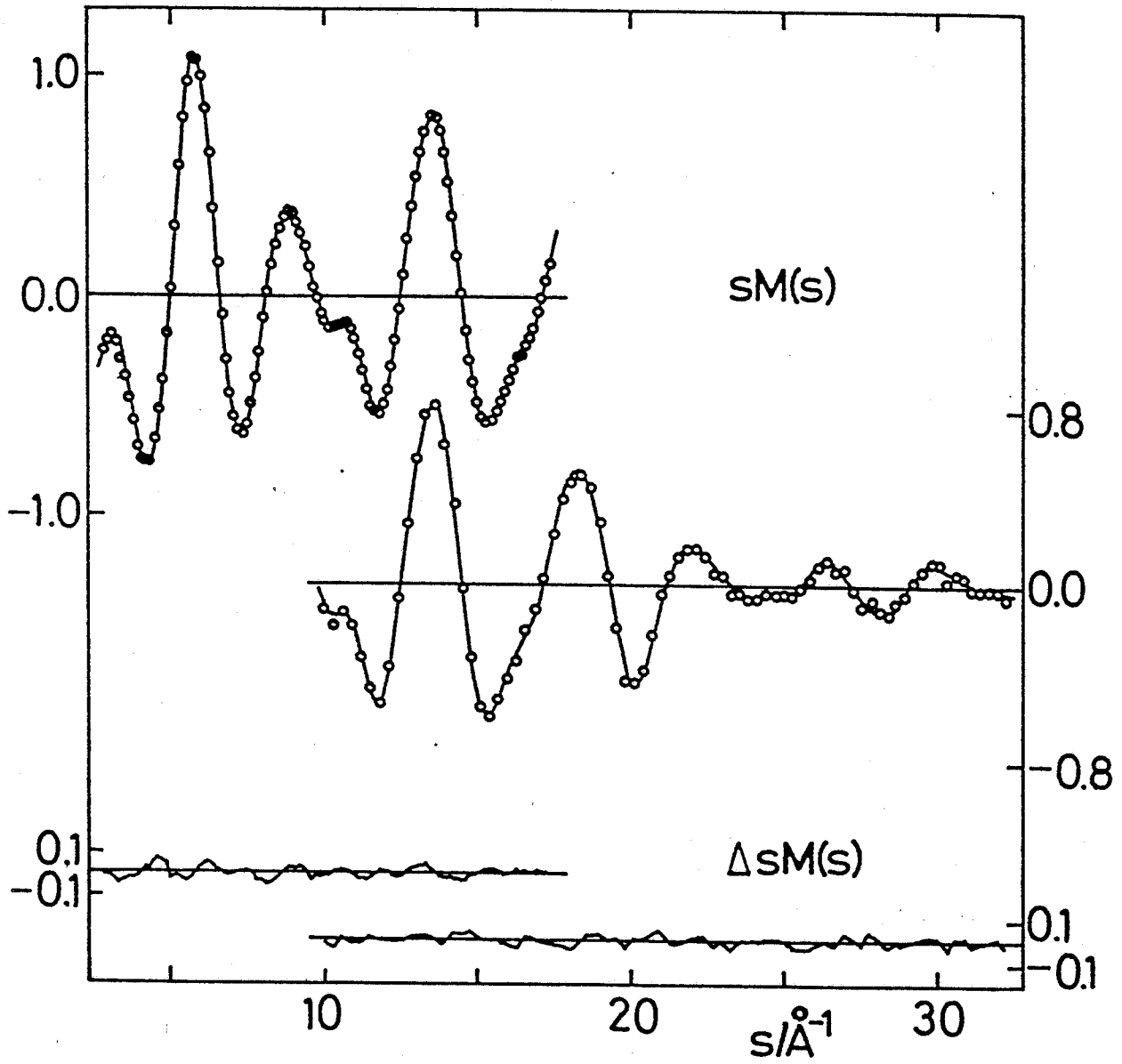

Figure 5 Experimental molecular scattering intensities (open circles) and the theoretical ones (solid curves) for the most stable conformer of diisopropyl ether; $\Delta sM(s) = sM(s)^{obs.} - sM(s)^{calc.}$.

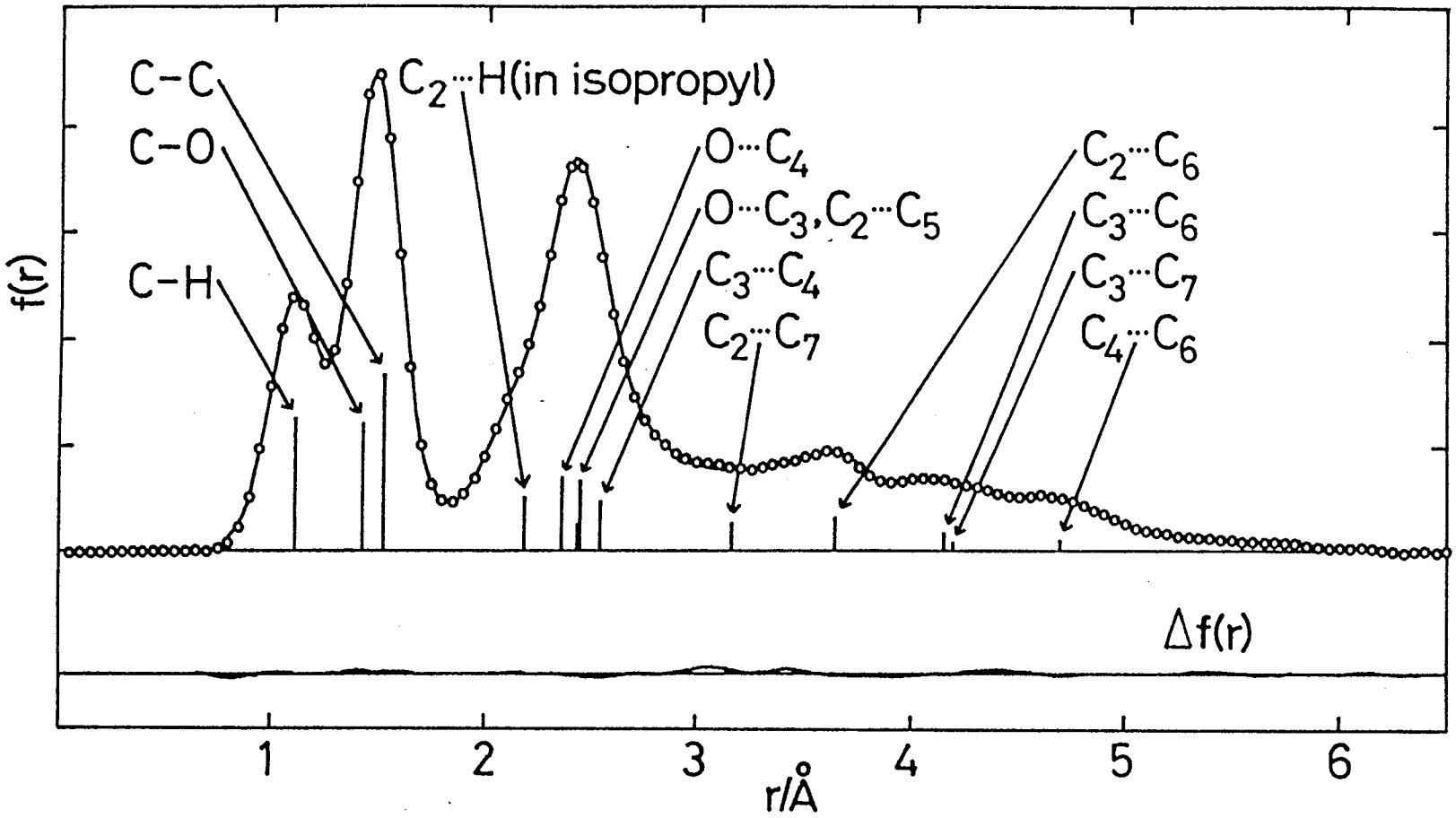

Figure 6 Experimental radial distribution curve (open circles) and the theoretical one (solid curve) for the most stable conformer of diisopropyl ether; $\Delta f(r) = f(r)^{obs.} - f(r)^{calc.}$.

5-4 Diisopropylamine

Table 20 shows the calculated mean amplitudes for relatively important atom pairs. Mean amplitudes except l(C-N) and l(C-H) were fixed at the calculated values. The position of the hydrogen atom attached to the nitrogen atom is quite difficult to be determined by GED. The values of ∠CNH were fixed at the average of the ∠CNH values calculated by using the MM2 force field. The average ∠CNH value of the 4-21G geometry was not adopted by the following two reasons. That is, the corresponding value of dimethylamine is inaccurate by about 3° compared with the r_s structure and the empirical $r_\alpha - r_e$ corrections have not been given for bond angles [51,52]. The value of r_g(N-H) was estimated by adding the empirical correction of 0.031 Å [52] to the r_e distance obtained by the 4-21G calculation. The $CCH_{i\text{-}Pr}$ bond angles were fixed at the values from the 4-21G geometry [27]. In the data analyses assuming the existence of only one conformer (single conformer model), it was found that $\phi_1(C_5NC_2H)$ and $\phi_2(C_2NC_5H)$ are nearly equal and impossible to be determined separately at sufficient precision. Therefore the structural parameters were determined by assuming $\phi_1 = \phi_2$. The differences between the ϕ_1 and ϕ_2 values of the MM2 and 4-21G geometries are 0.7° and 2.1° , respectively. Considering the experimental errors accompanied with the ϕ_1 and ϕ_2 values, the constraint, $\phi_1 = \phi_2$, does not contradict

the results of the MM2 and 4-21G calculations.

The NCC angles were constrained by referring to the MM2 and 4-21G geometries. One constraint is that the bond angles, $\angle NCC_3$ and $\angle NCC_4$, are equal to $\angle NCC_7$ and $\angle NCC_6$, respectively, referring to the MM2 geometry and another is that $\angle NCC_3 = \angle NCC_7 - 3.7°$ and $\angle NCC_4 = \angle NCC_6$ on the basis of the 4-21G geometry. The ϕ_1-values given by the least-squares analyses with the above two constraints converged to about 50° , which is similar to that given by the 4-21G calculation, but is different by 12° from the value obtained by the MM2 calculation. This suggests that the 4-21G geometry of the most stable conformer is more reliable than the MM2 geometry. Therefore, the analysis with the restriction based on the MM2 geometry was not adopted in the present study. The result using the constraints based on the 4-21G geometry is listed in Table 21. The molecular scattering intensities and RD curves are shown in Figs. 7 and 8, respectively.

Further investigation was performed employing the conformational mixture model on the basis of the MM2 results. According to the MM2 results, the next stable conformer is a $C_1(\phi_1 = -28.3°, \phi_2 = 59.8°)$ or $C_1(\phi_1 = 60.8°, \phi_2 = -26.6°)$ conformer. No large structural differences were found between these two conformers except for those related with the hydrogen atom attached to the nitrogen atom (see Table 8 in Chapter 3). Thus only the $C_1(\phi_1 = -28.3°,$

ϕ_2 = 59.8°) conformer was incorporated in the later analysis. The structure of the C_1 conformer was fixed at the calculated one. An additional constraint, $\angle NCC_4 = \angle NCC_3 - 1.9°$, was made for the most stable conformer on the basis of the 4-21G geometry.

The final result of the conformational analysis, which is listed in the third column in Table 21, shows that the next stable conformer has the 3^{+12}_{-3}% population. This result is consistent with the MM2 calculations and also with the results of the vibrational spectroscopy. The other stable conformers predicted by the MM2 calculations were not taken into the data analysis, since they were estimated to have smaller populations than the second conformer. The comparison of the geometry of the most stable conformer determined by GED with the corresponding MM2 geometry suggests that the geometry of the second conformer given by the MM2 calculation is not so reliable. The uncertainties in the dihedral angles, ϕ_1 and ϕ_2, of the second conformer are estimated to be about 10° referring to the experimental and MM2 geometries of the most stable conformer. The uncertainties in the dihedral angles are considered to be most serious among the errors in the structural parameters of the second conformer. However, the population of the next stable conformer is small and it is expected that the result is little influenced by the uncertainty in the geometry of the second conformer.

TABLE 20

Calculated mean amplitudes (l_{ij}) for the most stable conformer of diisopropylamine (in Å)[a]

Atom pair[b]	l_{ij}	r_{ij}[c]
N-C	0.050	1.470
C-C	0.052	1.528
N-H	0.074	1.030
C-H	0.079	1.114
$N \cdots C_3$	0.067	2.457
$N \cdots C_4$	0.067	2.426
$N \cdots C_6$	0.067	2.425
$N \cdots C_7$	0.067	2.510
$C_2 \cdots C_5$	0.063	2.522
$C_2 \cdots C_6$	0.073	3.778
$C_2 \cdots C_7$	0.178	3.146
$C_3 \cdots C_4$	0.070	2.528
$C_3 \cdots C_5$	0.167	3.100
$C_3 \cdots C_6$	0.186	4.304
$C_3 \cdots C_7$	0.353	4.891
$C_4 \cdots C_5$	0.073	3.778
$C_4 \cdots C_6$	0.095	4.799
$C_4 \cdots C_7$	0.198	4.372
$C_6 \cdots C_7$	0.070	2.529

[a] Calculated at 20°C. Only the mean amplitudes for

relatively important atom pairs are listed. [b] See Figure 3 for atom numbering. [c] The r_a distances corresponding to the final molecular geometry given in Table 21.

TABLE 21

Observed structural parameter values for the most stable conformer of diisopropylamine[a]

	Model 1[b]	Model 2[c]
r_g(N-H)	1.035[d]	1.035[d]
r_g(C-H)	1.120(2)	1.120(2)
r_g(C-C)	1.531(3)	1.530(4)
r_g(C-N)	1.471(4)	1.472(4)
$\angle_\alpha$CNC	119.3(11)	118.9(11)
$\angle_\alpha NCC_3$	109.7(9)	110.3(3)
$\angle_\alpha NCC_4$	108.7(5)	108.4[e]
$\angle_\alpha NCC_6$	108.7[e]	108.4[e]
$\angle_\alpha NCC_7$	113.4[e]	114.0[e]
$\angle_\alpha$CCC	111.8(7)	111.6(9)
$\angle_\alpha$CNH	108.7[d]	108.7[d]
$\angle_\alpha CCH_{i\text{-}Pr}$	108.5[d]	108.5[d]
$\angle_\alpha CCH_{Me}$	111.5(8)	111.6(8)
$\phi_1 (=\phi_2)$	50(4)[f]	51(4)[g]
l(N-H)	0.074[h]	0.074[h]
l(C-H)	0.079(3)	0.079(3)
l(C-C)	0.052[h]	0.052[h]
l(C-N)	0.048(5)	0.048(5)
k_l[i]	1.00(2)	1.00(2)
k_s[i]	0.91(3)	0.91(3)
R	0.0562	0.0566

[a] Bond lengths and mean amplitudes in Å, and angles in degrees. Values in parentheses are the limits of error attached to the last digit of the parameter values. [b] The result obtained by assuming that only the conformer exists in the vapour phase. The constraints, $\angle NCC_3 = \angle NCC_7 - 3.7°$ and $\angle NCC_4 = \angle NCC_6$, are used. [c] The result obtained for the conformational composition of $97^{+3}_{-12}\%$ C_1 ($\phi_1 = \phi_2$) + $5^{-3}_{+12}\%$ C_1 ($\phi_1 = -28°$, $\phi_2 = 60°$). Further constraint, $\angle NCC_4 = \angle NCC_3 - 1.9°$ is used. The parameters listed in this column should be regarded as the final results of the present study. [d] Fixed value (see text). [e] Obtained by the value of $\angle NCC_3$ or $\angle NCC_4$. [f] Observed values of the dihedral angles, $C_5NC_2C_3$ and $C_5NC_2C_4$, are -69° and 168°, respectively. [g] Observed values of the dihedral angles, $C_5NC_2C_3$ and $C_5NC_2C_4$, are -69° and 169°, respectively. [h] Calculated value. [i] k_l and k_s are the indices of resolution for the long and short camera distances, respectively.

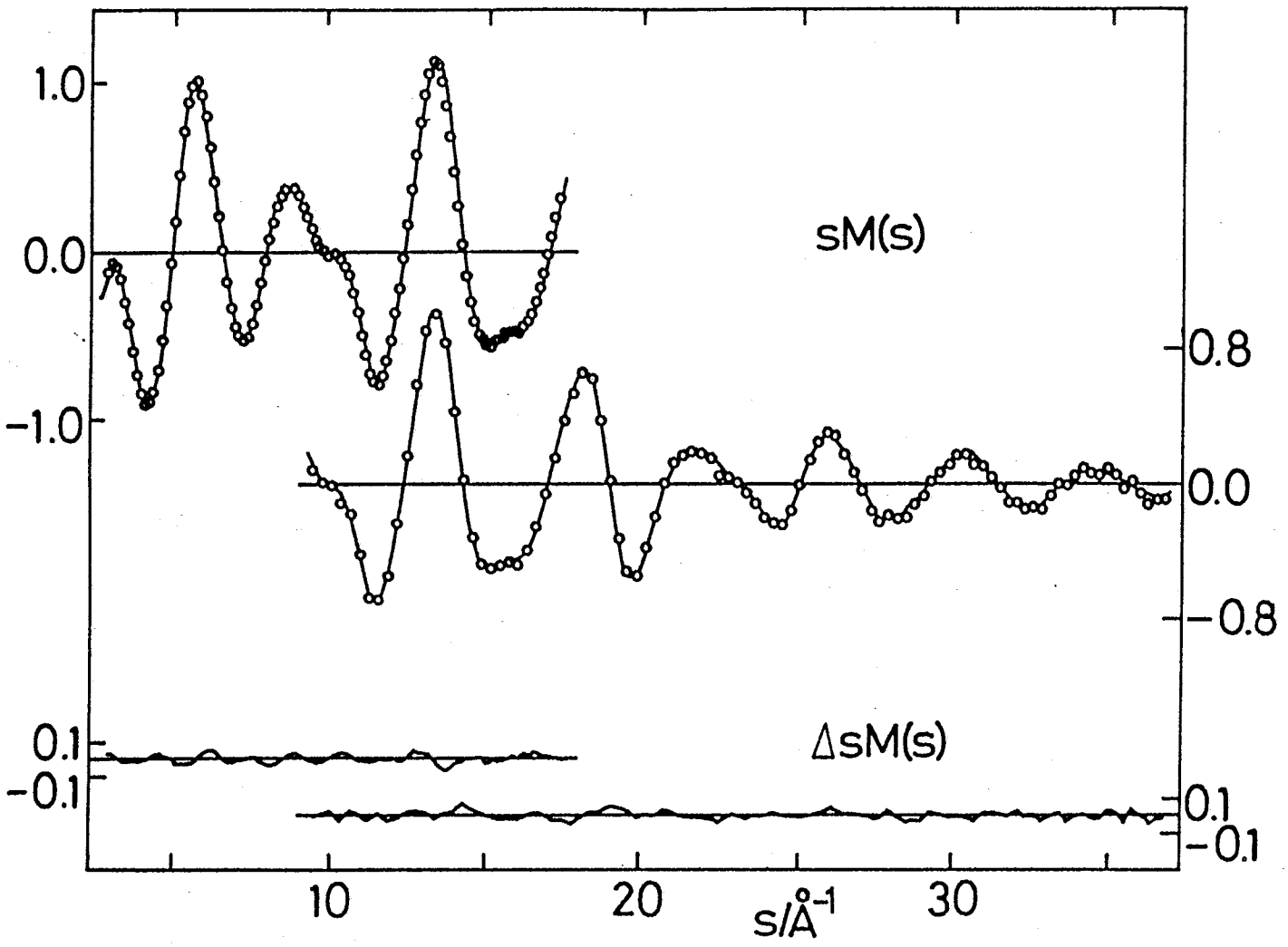

Figure 7 Experimental molecular scattering intensities (open circles) and the theoretical ones (solid curves) for the most stable conformer of diisopropylamine; $\Delta sM(s) = sM(s)^{obs.} - sM(s)^{calc.}$.

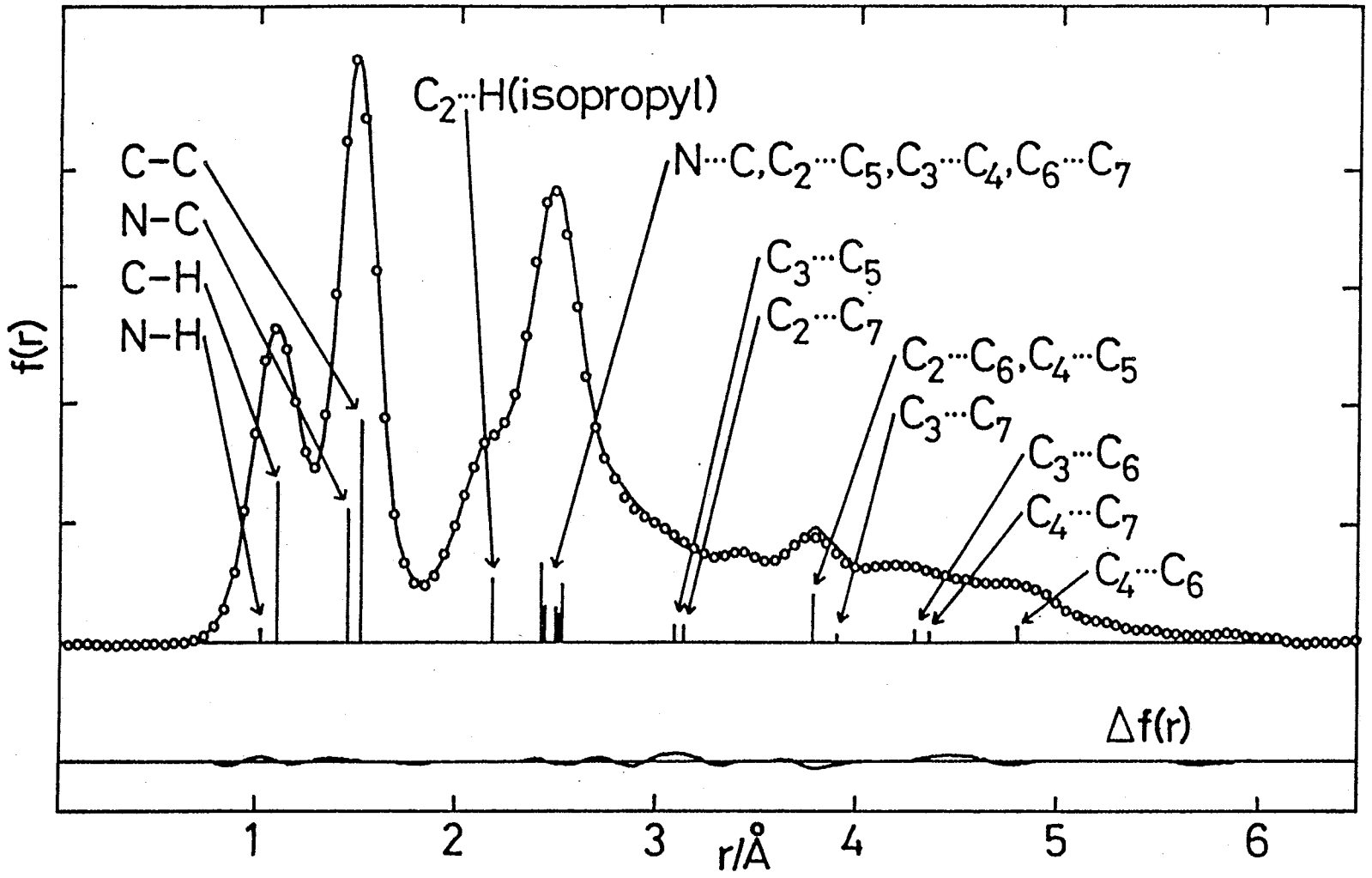

Figure 8 Experimental radial distribution curve (open circles) and the theoretical one (solid curve) for the most stable conformer of diisopropylamine; $\Delta f(r) = f(r)^{obs.} - f(r)^{calc.}$.

5-5 Diisopropyl Sulfide

The analyses were carried out by using a model constructed by employing the results of the MM2 calculations. The model included three stable conformers given by the MM2 calculations: the C_2 conformer with $\phi_1 = \phi_2 = 44°$, the C_1 conformer with $\phi_1 = 12°$ and $\phi_2 = -52°$, and the C_1 conformer with $\phi_1 = 17°$ and $\phi_2 = 175°$. Hereafter, the two C_1 conformers are expressed as $C_1(12,-52)$ and $C_1(17,175)$, respectively.

The RD curves for the three conformers are shown in Fig. 9. The value of ϕ_1 $(=\phi_2)$ of the C_2 conformer was determined to be 57(6)° by GED and the R-factor was 0.0757. For the $C_1(17,175)$ conformer the values of ϕ_1 and ϕ_2 could be refined in the analysis and the values of ϕ_1 and ϕ_2 and the R-factor were 32(16)°, 170(13)°, and 0.1250, respectively. The ϕ_1 and ϕ_2 of the $C_1(12,-52)$ conformer were not determined by GED. Therefore, these values were fixed at the MM2 values and the R-factor of 0.1604 was obtained. The RD curves and R-factor showed that the C_2 conformer reproduced the experimental data best. This is in good agreement with the results of the MM2 calculations and vibrational spectroscopy.

The conformational analysis was carried out by mixing the three conformers with the additional assumptions as follows: (1) The bond lengths are the same in these

conformers; (2) the SCC angles of the C_1 conformers are different from the values of $\angle SCC_3$ and $\angle SCC_4$ determined for the C_2 conformer and the difference values are taken from the MM2 geometries; and (3) the differences between the CCC and $CCH_{i\text{-}Pr}$ angles of the C_1 and C_2 conformers are equal to those calculated by the MM2 calculation.

The populations of the C_2 and $C_1(17,175)$ conformers were refined as the adjustable parameters in the least-squares calculations. The values of ϕ_1 and ϕ_2 in the C_1 conformers were fixed at the calculated values, since the concentrations of the two conformers were found to be small. The values of ϕ_1 and ϕ_2 in the $C_1(17,175)$ conformer were determined on the assumption that only this conformer exists in the vapour phase. The values were uncertain because of the inappropriate assumption. The resulting conformational composition was not physically acceptable, since the $C_1(-12, 52)$ conformer has a negative concentration (-13%). Therefore, the population of this conformer was set to be zero in the later analysis.

The final results are listed in Table 22. The mean amplitudes used for the C_2 and $C_1(17,175)$ conformers are listed in Table 23. The RD curves and molecular scattering intensities are shown in Figs. 10 and 11, respectively. The concentration of the $C_1(17,175)$ conformer is 17(11)%. The normal coordinate analysis predicted the existence of not the $C_1(12,-52)$ conformer but the $C_1(17,175)$ conformer.

Therefore, the results of GED and vibrational spectroscopy are consistent with each other.

TABLE 22

Structural parameter values observed for the most stable conformer of diisopropyl sulfide[a]

r_g(S-C)	1.829(2)	l(S-C)	0.059(3)
r_g(C-C)	1.530(2)	l(C-C)	0.049(3)
r_g(C-H)	1.118(3)	l(C-H)	0.080(4)
$\angle_\alpha CSC$	103.8(9)	k_l[c]	0.97(3)
$\angle_\alpha SCC_3$	113.1(4)	k_s[c]	0.96(5)
$\angle_\alpha SCC_4$	106.4(5)	R	0.0729
$\angle_\alpha CCC$	111.1(9)		
$\angle_\alpha CCH_{i\text{-}Pr}$	109.3(18)		
$\angle_\alpha CCH_{Me}$	111.1(12)		
ϕ_1 ($=\phi_2$)	60(8)[b]		

[a] Bond lengths and mean amplitudes in Å and angles in degrees. Values in parentheses are the limits of error attached to the last digit of the parameter values. The result obtained for the conformational composition of 83(11)% C_2 ($\phi_1 = \phi_2$) + 17(11)% C_1 ($\phi_1 = 17°$, $\phi_2 = 175°$).
[b] Observed values of the dihedral angles, $C_5SC_2C_3$ and $C_5SC_2C_4$, are -61° and 175°, respectively. [c] k_l and k_s are the indices of resolution for the long and short camera distances, respectively.

TABLE 23

Mean amplitudes (l_{ij}) calculated for diisopropyl sulfide (in Å)[a]

	$C_2(60,60)$		$C_1(17,-175)$	
Atom pair[b]	l_{ij}	r_{ij}[c]	l_{ij}	r_{ij}[c]
S-C	0.053	1.827	0.053	1.827
C-C	0.051	1.529	0.051	1.529
C-H	0.079	1.113	0.079	1.113
$S \cdots C_3$	0.071	2.801	0.074	2.746
$S \cdots C_4$	0.075	2.687	0.072	2.728
$S \cdots C_6$	0.075	2.687	0.073	2.770
$S \cdots C_7$	0.071	2.801	0.073	2.789
$C_2 \cdots C_5$	0.080	2.871	0.081	2.912
$C_2 \cdots C_6$	0.080	4.190	0.194	3.399
$C_2 \cdots C_7$	0.182	3.291	0.190	3.302
$C_3 \cdots C_4$	0.069	2.520	0.068	2.537
$C_3 \cdots C_5$	0.182	3.291	0.176	3.766
$C_3 \cdots C_6$	0.173	4.648	0.276	4.566
$C_3 \cdots C_7$	0.359	3.814	0.288	3.635
$C_4 \cdots C_5$	0.080	4.190	0.127	4.074
$C_4 \cdots C_6$	0.093	5.328	0.249	4.251
$C_4 \cdots C_7$	0.173	4.648	0.210	4.728
$C_6 \cdots C_7$	0.069	2.520	0.068	2.548

[a] Calculated at 20°C. Only the mean amplitudes for

relatively important atom pairs are listed. [b] See Figure 4 for atom numbering. [c] The r_a distances obtained from the final result.

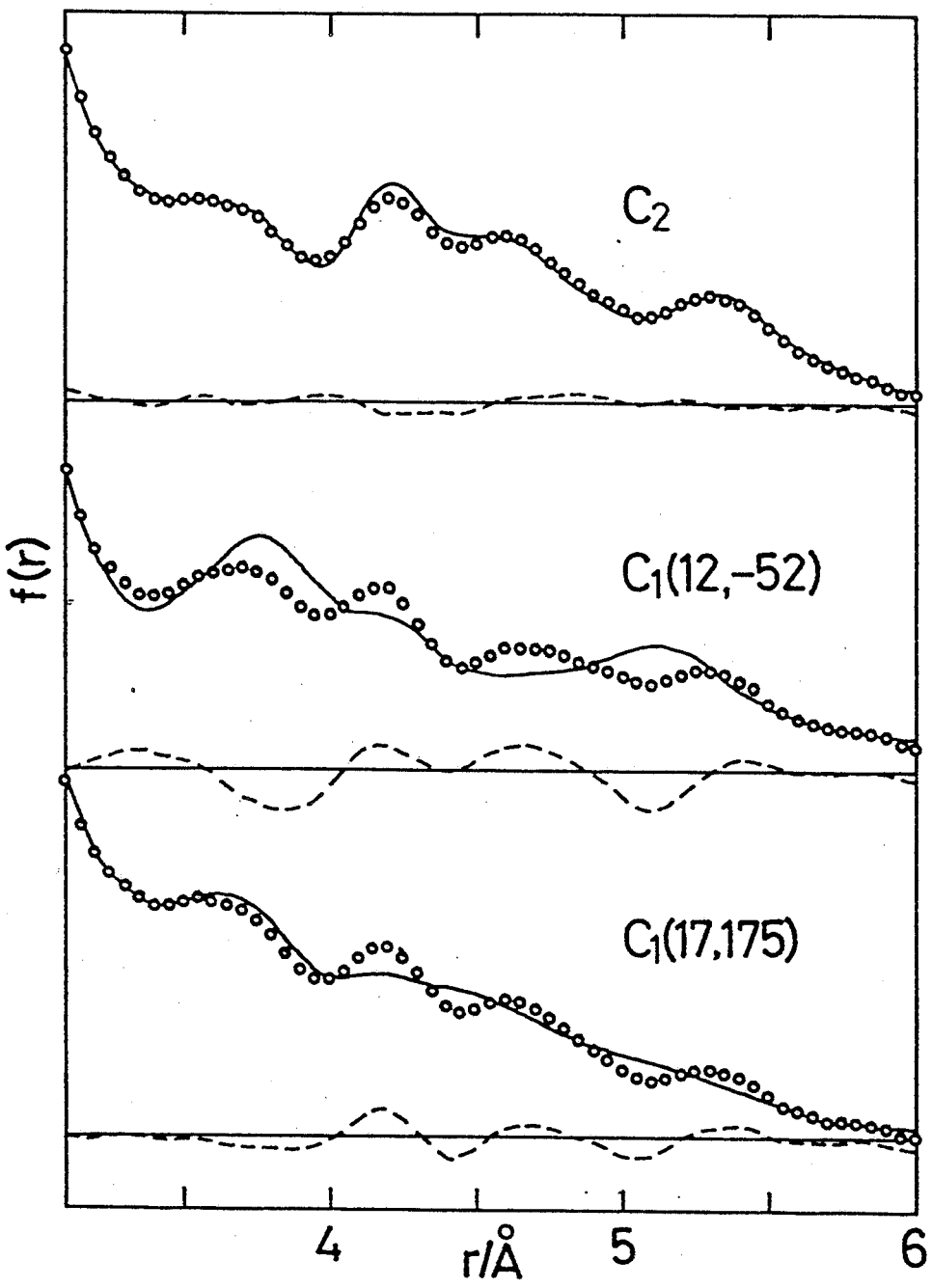

Figure 9 Experimental radial distribution curves (open circles) and the theoretical ones (solid lines) for the C_2, $C_1(12,-52)$, and $C_1(17,175)$ conformers. The residuals (broken lines) are shown in the same scale

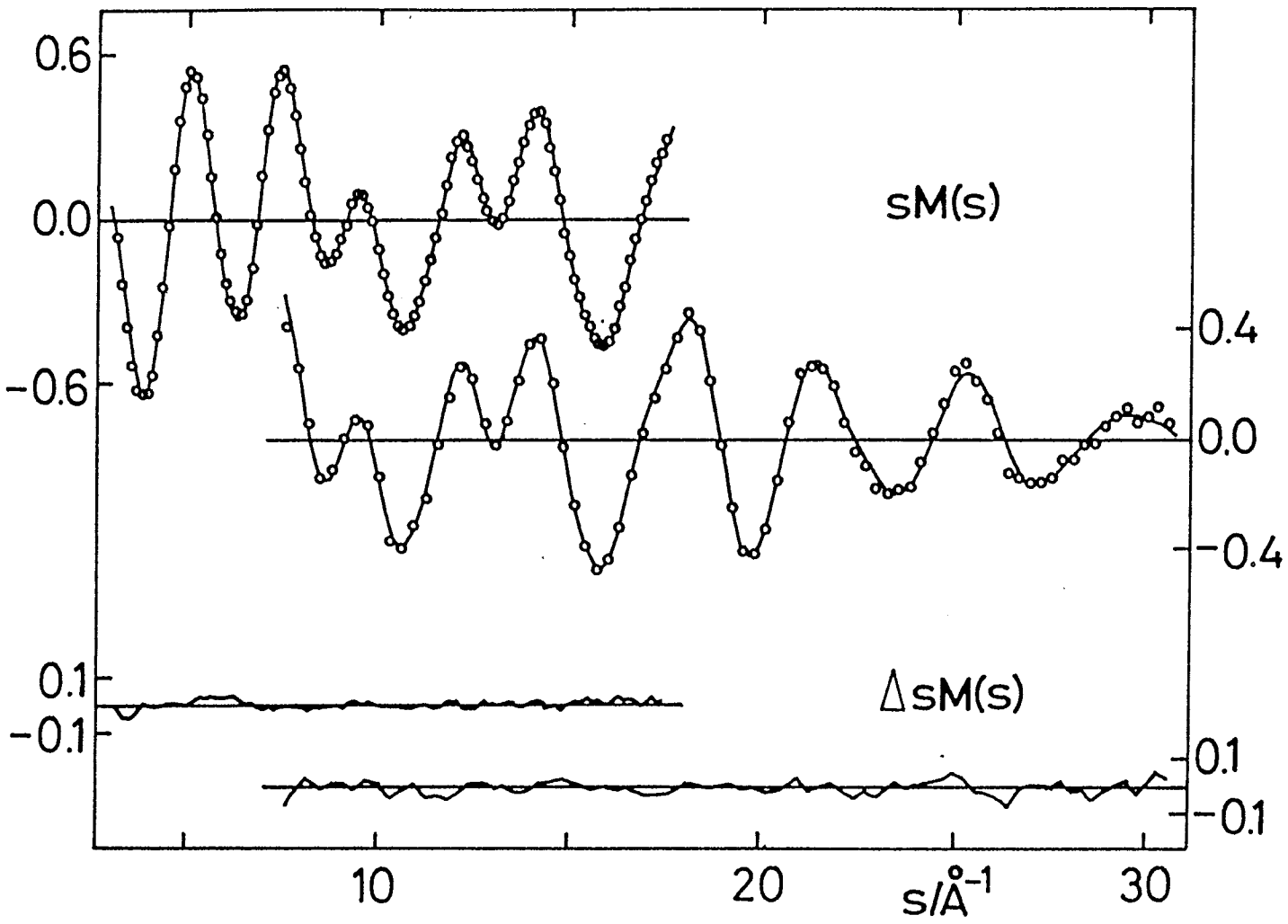

Figure 10 Experimental molecular scattering intensities (open circles) and the theoretical ones (solid curves) for the conformational composition of 83% C_2 + 17% C_1(17,175); $\Delta sM(s) = sM(s)^{obs.} - sM(s)^{calc.}$.

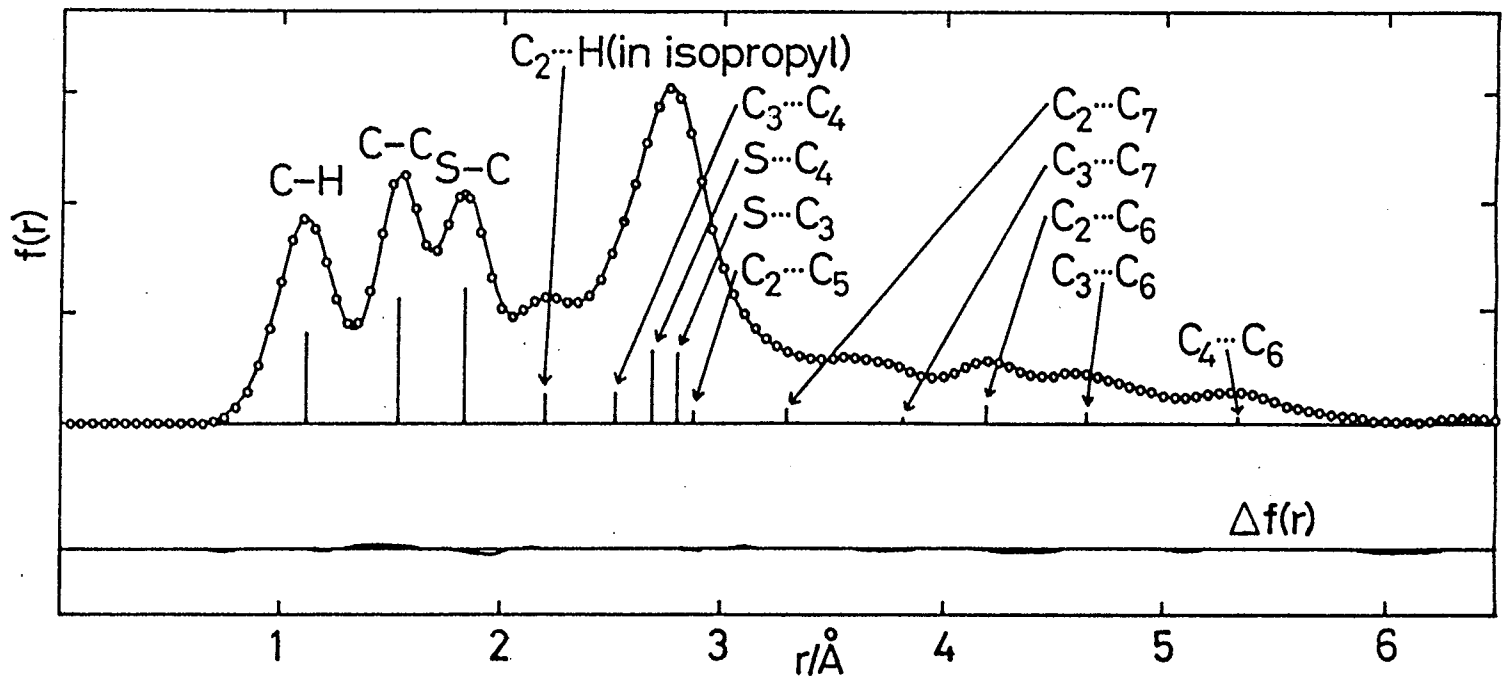

Figure 11 Experimental radial distribution curve (open circles) and the theoretical one (solid curve) for the conformational composition of 83% C_2 + 17% C_1(17,175); $\Delta f(r) = f(r)^{obs.} - f(r)^{calc.}$.

5-6 Diisopropyl Ketone

The following assumptions in data analyses were made by referring to the results of the ab initio calculations and considering that it is difficult to determine the coordinates of hydrogen atoms precisely by GED: (1) all C-H bond lengths are equal; (2) four methyl groups have the same local geometry with C_{3v} symmetry and have no tilt; (3) each methyl group takes staggered conformation against the C-C(=O) bond; (4) the geometry of the $OC_2C_3C_4$ group is planar; (5) $\angle C_5C_3H$ and $\angle C_7C_4H$ are equal to $\angle C_6C_3H$ and $\angle C_8C_4H$, respectively. Thus, r(C=O), $r(C_2-C_3)$, $r(C_2-C_4)$, $r(C_3-C_5)$, $r(C_3-C_6)$, $r(C_4-C_7)$, $r(C_4-C_8)$, r(C-H), $\angle C_3C_2C_4$, $\angle OC_2C_3$, $\angle C_2C_3C_5$, $\angle C_2C_3C_6$, $\angle C_2C_4C_7$, $\angle C_2C_4C_8$, $\angle C_5C_3C_6$, $\angle C_7C_4C_8$, $\angle C_{5,6}C_3H_{i\text{-}Pr}$, $\angle C_{7,8}C_4H_{i\text{-}Pr}$, $\angle CCH_{Me}$, $\phi_1(C_4C_2C_3H_{i\text{-}Pr})$ and $\phi_2(C_3C_2C_4H_{i\text{-}Pr})$ were selected as independent structural parameters. The restrictions given by these assumptions are looser than those made for $(i\text{-}Pr)_2O$, $(i\text{-}Pr)_2NH$, and $(i\text{-}Pr)_2S$, since isopropyl groups are not treated as equivalent.

The mean amplitudes and shrinkage corrections were fixed at the values calculated by using the harmonic force constants: the determination of the force constants except the torsional force constant of the isopropyl groups has been discussed in Chapter 4. The torsional force constant of the isopropyl groups was estimated by the same manner as for $(i\text{-}Pr)_2O$ and $(i\text{-}Pr)_2NH$ and the resulting value is 0.026

mdyn Å rad^{-2}. Table 24 shows the calculated mean amplitudes for relatively important atom pairs.

The conformational analysis was carried out by assuming the existence of the C_1 ,C_2 and C_s conformers which are suggested to be stable by the ab initio calculations. The molar fractions of the C_1 and C_2 conformers were refined as the least-squares parameters. The number of the independent structural parameters for the C_1 conformer is 21 whereas 12 and 14 independent structural parameters are required for defining the geometries of the C_2 and C_s conformers, respectively. It was difficult to determine all of them by GED alone. Therefore, the external constraints were needed to reduce the number of adjustable parameters. The differences among similar structural parameters of the C_1, C_2 and C_s conformers were fixed at the values given by the ab initio calculations as shown in Table 25. For this purpose, the calculated r_e distances had been converted to the r_g distances by making the empirical corrections [52]. Consequently, 13 structural parameters, r_1 - r_3, θ_1 - θ_4, τ_1 - τ_3, and the conformational composition were adjusted in the least-squares analysis. At first, the data analysis was performed by assuming the existence of only one conformer. The τ_1, τ_2 and τ_3 values were fixed at the calculated values. The R-factors obtained for the C_1, C_2 and C_s conformers were 0.0736, 0.1039 and 0.1191, respectively. The RD curves of the three conformers are shown in Fig. 12.

The R-factor and the agreement between the observed and calculated radial distribution curves show that the C_1 conformer is predominant. The agreement between the observed and calculated RD curves for the C_2 conformer only is poor.

In the later analyses the mixture of the three conformers was assumed. The ϕ_1 and ϕ_2 values in the C_1 and C_2 conformers were fixed at the values obtained by the ab initio calculations, since these values were not determined by GED. Final values of the adjustable parameters are listed in Table 26 together with the limits of error. The structures of the three conformers are specified by these values and the relation given in Table 25. The limits of error were estimated to be $\sqrt{(2.6\sigma)^2+\varepsilon^2}$, where σ presents the standard error and ε is the systematic error due to the uncertainties in scale factors. Other systematic errors were considered to be negligible.

The $r_g - r_e$(4-21G) values of r(C=O) and r(C-H) were obtained to be -0.001(3) and 0.036(3) Å by comparing the observed values with the values of the 4-21G geometries. These values are in good agreement with the values (0.000(4) and 0.034(10) Å) estimated by Schäfer [52]. The $r_g - r_e$ value of r(C-C) was not determined in the present study since the empirical corrections were made for the C-C bond lengths. The molar fractions of the C_1, C_2, and C_s conformers were determined to be 51(24), 20(18) and 29(10)%,

respectively. These values show that the energy differences among the three conformers are zero within experimental errors. The molecular scattering intensities and RD curves obtained by the best analysis are shown in Figs. 13 and 14, respectively.

The above conclusion is dependent on the results of the ab initio calculations, since the structural constraints needed for the analysis of GED data were taken from the 4-21G geometries. The accuracy of the calculated differences in the bond lengths and bond angles of the similar type is expected to be at the level of a few thousandths of angstrom and a few degrees, respectively [52]. The uncertainties in the differences in the C-C bond lengths are comparable to the experimental errors and little affect the results. However, the uncertainties in the constraints with respect to the CCC bond angles were found to be sensitive to the molecular intensities in the s-range of 6 $Å^{-1}$ to 7 $Å^{-1}$. The values of $\Delta sM(s)$ in this s-range could be removed by the refinement of some of the differences between the CCC bond angles except for ∠CC(=O)C. However, since the results depended on the selection of the differences to be refined, the definite conclusion could not be obtained.

The force constant about the isopropyl torsion is 0.026 mdyn Å rad^{-2}. The value implies that the small amplitude approximation employed in the GED analysis is not rigid (see the discussion for $(i\text{-}Pr)_2NH$ in Section 5-2). The treatment

of the large-amplitude motion in the analysis of GED data is impossible for lack of the knowledge on the potential energy function against ϕ_1 and ϕ_2. The result proposed in the present study is the best result we can obtain.

TABLE 24

Calculated mean amplitudes (l_{ij}) for diisopropyl ketone (in Å)[a]

atom pair[b]	C_1 conformer		C_2 conformer		C_s conformer	
	l_{ij}	r_{ij}[c]	l_{ij}	r_{ij}[c]	l_{ij}	r_{ij}[c]
O-C	0.040	1.214	0.040	1.214	0.040	1.215
C_2-C_3	0.052	1.532	0.052	1.532	0.052	1.526
C_2-C_4	0.052	1.529	0.052	1.532	0.052	1.531
C_3-C_5	0.052	1.531	0.053	1.540	0.053	1.536
C_3-C_6	0.053	1.541	0.052	1.528	0.053	1.536
C_4-C_7	0.052	1.527	0.052	1.528	0.053	1.536
C_4-C_8	0.052	1.538	0.053	1.540	0.053	1.536
C-H	0.079	1.112	0.079	1.112	0.079	1.112
O $\cdots$ C_3	0.061	2.391	0.061	2.399	0.061	2.398
O $\cdots$ C_4	0.061	2.406	0.061	2.399	0.061	2.387
O $\cdots$ C_5	0.178	2.866	0.167	3.445	0.170	3.408
O $\cdots$ C_6	0.214	3.064	0.108	2.760	0.170	3.408
O $\cdots$ C_7	0.108	2.772	0.108	2.740	0.204	2.944
O $\cdots$ C_8	0.161	3.465	0.167	3.445	0.204	2.944
C_2 $\cdots$ C_5	0.077	2.502	0.076	2.534	0.076	2.516
C_2 $\cdots$ C_6	0.078	2.483	0.076	2.506	0.076	2.516
C_2 $\cdots$ C_7	0.076	2.504	0.076	2.506	0.077	2.484
C_2 $\cdots$ C_8	0.076	2.530	0.076	2.534	0.077	2.484
C_3 $\cdots$ C_4	0.067	2.601	0.067	2.604	0.067	2.609
C_3 $\cdots$ C_7	0.078	3.876	0.078	3.878	0.204	3.598

$C_3 \cdots C_8$	0.230	3.073	0.235	3.101	0.204	3.598
$C_4 \cdots C_5$	0.165	3.730	0.235	3.101	0.243	3.127
$C_4 \cdots C_6$	0.237	3.448	0.078	3.878	0.243	3.127
$C_5 \cdots C_6$	0.074	2.535	0.073	2.528	0.073	2.557
$C_5 \cdots C_7$	0.186	4.829	0.239	4.410	0.304	4.403
$C_5 \cdots C_8$	0.247	4.450	0.542	3.602	0.419	3.688
$C_6 \cdots C_7$	0.245	4.636	0.104	4.943	0.419	3.688
$C_6 \cdots C_8$	0.445	3.394	0.239	4.410	0.304	4.403
$C_7 \cdots C_8$	0.073	2.539	0.073	2.528	0.073	2.557

[a] Only the mean amplitudes for relatively important atom pairs are listed. [b] See Figure 2 for atom numbering.
[c] The r_a distances obtained from the structural parameter values in Table 26 and the relations among the structural parameters (Table 25).

TABLE 25

Relations among structural parameters[a]

	C_1 symmetry	C_2 symmetry	C_s symmetry
r(C=O)	r_1	r_1	r_1+0.001
$r(C_2-C_3)$	r_2	r_2	r_2-0.006
$r(C_2-C_4)$	r_2-0.003	r_2	r_2-0.001
$r(C_3-C_5)$	r_2-0.001	r_2+0.008	r_2+0.004
$r(C_3-C_6)$	r_2+0.009	r_2-0.004	r_2+0.004
$r(C_4-C_7)$	r_2-0.005	r_2-0.004	r_2+0.004
$r(C_4-C_8)$	r_2+0.006	r_2+0.008	r_2+0.004
r(C-H)	r_3	r_3	r_3
$\angle C_3C_2C_4$	θ_1	θ_1+0.1	θ_1+0.9
$\angle O_1C_2C_3$	179.3-θ_1/2.0	179.95-θ_1/2.0	180.15-θ_1/2.0
$\angle O_1C_2C_4$	180.7-θ_1/2.0	179.95-θ_1/2.0	178.95-θ_1/2.0
$\angle C_2C_3C_5$	θ_2	θ_2+1.5	θ_2+1.1
$\angle C_2C_3C_6$	θ_2-1.6	θ_2+0.4	θ_2+1.1
$\angle C_2C_4C_7$	θ_2+0.3	θ_2+0.4	θ_2-1.0
$\angle C_2C_4C_8$	θ_2+1.7	θ_2+1.5	θ_2-1.0
$\angle C_5C_3C_6$	θ_2-0.2	θ_2+0.1	θ_2+1.3
$\angle C_7C_4C_8$	θ_2+0.9	θ_2+0.1	θ_2+0.3
$\angle C_{5,6}C_3H_{i\text{-}Pr}$	θ_3	θ_3-1.1	θ_3-0.65
$\angle C_{7,8}C_4H_{i\text{-}Pr}$	θ_3+1.1	θ_3-1.1	θ_3-0.25
$\angle CCH_{Me}$	θ_4	θ_4	θ_4
$\phi_1(C_4C_2C_3H)$	τ_1	τ_3	0[b]
$\phi_2(C_3C_2C_4H)$	τ_2	τ_3	180[b]

[a] Adjustable parameters in the least-squares calculation are r_1, r_2, r_3, θ_1, θ_2, θ_3, θ_4, τ_1, τ_2 and τ_3. [b] These values are determined by symmetry consideration.

TABLE 26

Observed geometrical parameters of diisopropyl ketone[a]

r_1	1.215(3)	τ_1	16[b]
r_2	1.534(1)	τ_2	-62[b]
r_3	1.118(3)	τ_3	59[b]
θ_1	117.0(7)	X_1[c]	0.51(24)
θ_2	110.4(3)	X_2[c]	0.20(18)
θ_3	109.0[b]	k_l[d]	1.01(2)
θ_4	111.1(8)	k_s[d]	0.89(2)
		R[e]	0.0651

[a] Bond lengths and angles are r_g and r_α structures, respectively. Limits of error are shown in parentheses. [b] Fixed values given by the ab initio calculations. [c] X_1 and X_2 denote the relative abundance of the C_1 and C_2 conformers, respectively. The relative abundance of the C_s conformer is 0.29(10). [d] k_l and k_s are the indices of resolution for the long and short camera distances, respectively. [e] R-factor.

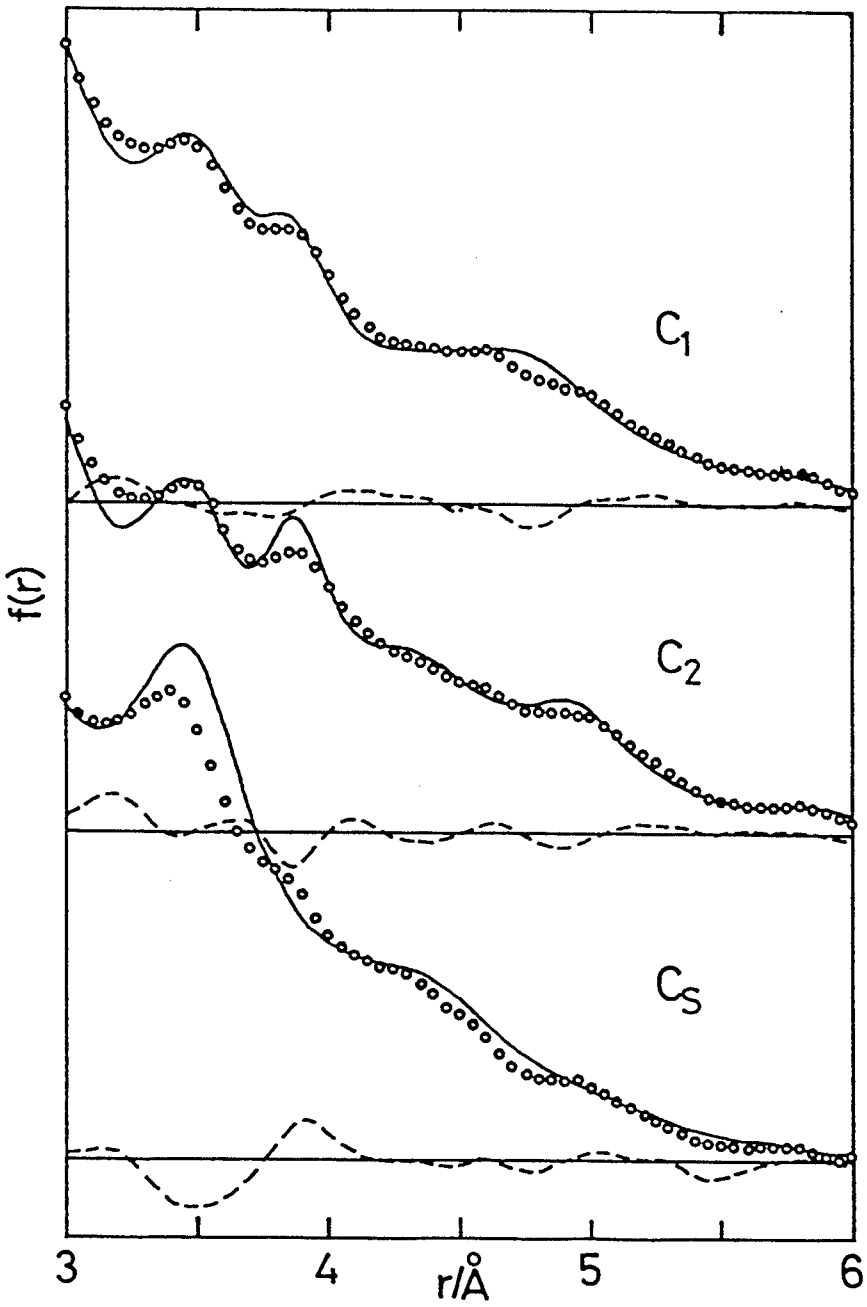

Figure 12 Experimental radial distribution curves (open circles) and the theoretical ones (solid lines) for the C_1, C_2 and C_s conformers of diisopropyl ketone. The residuals (broken lines) are shown in the same scale.

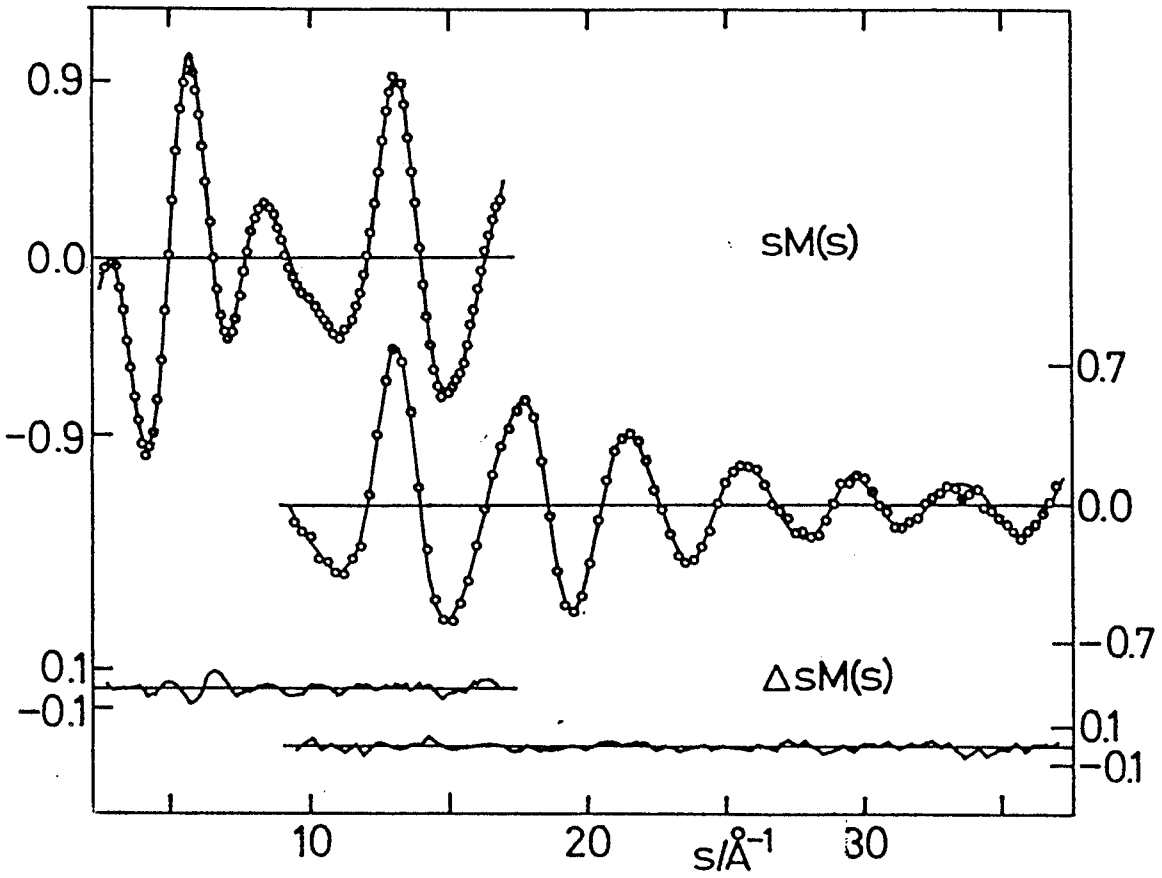

Figure 13 Experimental molecular scattering intensities (open circles) and the theoretical ones (solid curves) for the conformational composition of 51% C_1 + 20% C_2 + 29% C_s; $\Delta sM(s) = sM(s)^{obs.} - sM(s)^{calc.}$.

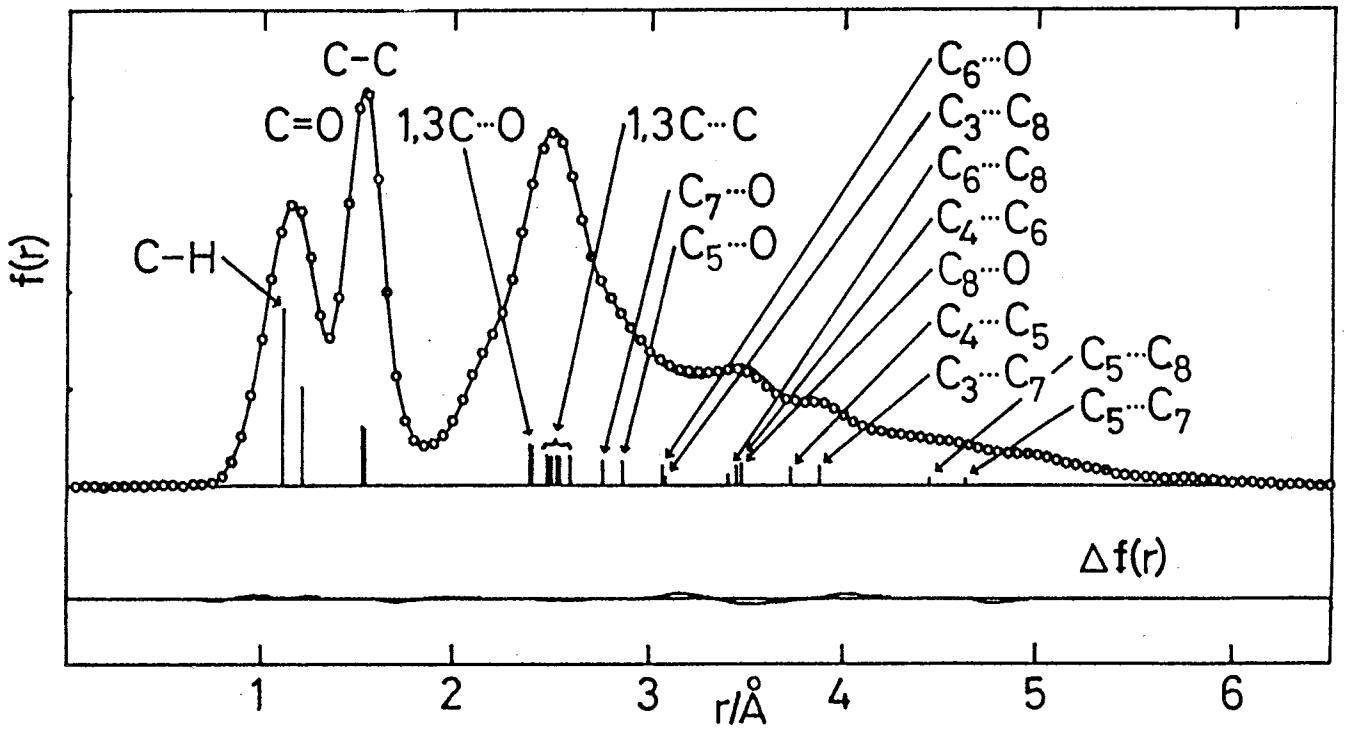

Figure 14 Experimental radial distribution curve (open circles) and the theoretical one (solid curves) for the conformational composition of 51% C_1 + 20% C_2 + 29% C_s; $\Delta f(r) = f(r)^{obs.} - f(r)^{calc.}$. Relatively important atom pairs of the C_1 conformer are shown by vertical bars.

Chapter 6

Discussion

6-1 Comparison of the Structure of Each Diisopropyl Compound with Those of Related Molecules

Diisopropyl Ether. The difference between $\angle OCC_3$ and $\angle OCC_4$ indicates that the C-O bonds are not in the symmetry planes of isopropyl groups as is the case with isopropyl methyl ether [74] and gauche-isopropyl alcohol [75]. The observed difference between two OCC angles in $(i\text{-}Pr)_2O$ (5.0(8)°) is nearly equal to the corresponding differences in isopropyl methyl ether (6.0°) and gauche-isopropyl alcohol (4.4°).

In isopropyl methyl ether the CH_3 group interacts with the gauche CH_3 group in the isopropyl group more strongly than with the trans CH_3 group. This difference in interaction causes the difference between the OCC angles for the isopropyl group. Similar interactions cause the difference between $\angle OCC_3$ and $\angle OCC_4$ in $(i\text{-}Pr)_2O$. The isopropyl group in $(i\text{-}Pr)_2O$ deviates by 22° from the staggered conformation (see Fig. 15). This deviation is 9° larger than that in isopropyl methyl ether [74] which has only one isopropyl group. These facts show that the CH_3-CH_3 interactions between the isopropyl groups play an important role in mutual arrangement of the two isopropyl groups.

Main structural parameters are compared with those of related ethers in Table 27. Molecules with bulkier substituents have larger r(C-O) except for dipropyl ether

[76]. The r(C-O) and ∠COC of $(i\text{-}Pr)_2O$ are about 0.018 Å and 5° larger than the corresponding values of dimethyl ether [77] and ethyl methyl ether [78]. The r(C-C) of diisopropyl ether is 0.007 Å longer than that of ethyl methyl ether. These results reflect steric interactions between the isopropyl groups. It is reasonable that the r(C-O) of ethyl methyl ether is slightly longer than that of dimethyl ether, but it seems unnatural that the r(C-O) of dipropyl ether is shorter than that of ethyl methyl ether. Moreover, the HCH bond angle of dipropyl ether is considered to be too small. It seems worthwhile to reinvestigate the structure of dipropyl ether.

Hayashi and Adachi [79] determined the r_s structures of trans-ethyl methyl ether, trans-trans-propyl methyl ether, and trans-trans-diethyl ether. Two common features can be seen in these structures. First, the C-C bond length adjacent to an oxygen atom is about 0.01 Å shorter than that of a normal hydrocarbon [80] (see Table 28). Second, alkyl groups R and R' in ROR' tilt towards the lone pair electrons on the oxygen atom. The isopropyl groups in $(i\text{-}Pr)_2O$ and isopropyl methyl ether [74] and the methyl groups in dimethyl ether [77] also tilt towards the lone pair electrons. The r_g(C-C) of ethyl methyl ether [78] is also shorter than that of a normal hydrocarbon although the tilt of ethyl and methyl groups has not been made clear. The C-C bond of $(i\text{-}Pr)_2O$ is lengthened by steric repulsion but its

length is still shorter than that of a normal hydrocarbon. This shortening of the C-C bond lengths adjacent to an oxygen atom can be related to the electronegativity of the oxygen atom [79,81]. It is considered that the tilt of R and R' groups is caused by the steric repulsion between R and R' groups.

Diisopropyl amine. The values of r_g(N-C) and ∠CNC (r_a) of dimethylamine were determined by Beagley and Hewitt [82] to be 1.456(2) Å and 111.8(6)° , respectively. These values are smaller than the corresponding values of $(i\text{-Pr})_2NH$ by 0.016 Å and 7.1° . These differences are considered to reflect differences in steric repulsion between the substituents attached to a nitrogen atom. Fjeldberg et al. [7] determined the molecular structure of $(t\text{-Bu})_2NH$ by GED. However, the structure of $(t\text{-Bu})_2NH$ was not included in discussion, since the reported geometry was considered to be unreliable*.

---

* Comparing the 4-21G geometry of $(t\text{-Bu})_2NH$ with the observed one, Siam et al. [83] suggested that the geometry obtained by GED is not reliable because of the incomplete data analysis. Recently Konaka and Yanagihara have compared their structural data of $t\text{-BuNH}_2$ with those of $(t\text{-Bu})_2NH$ [84]. According to them, the C-N distance (1.467(13) Å) of $(t\text{-Bu})_2NH$ is unnaturally shorter than that (1.492(6) Å) of $t\text{-BuNH}_2$, whereas the C-C distance (1.561(6) Å) of $(t\text{-Bu})_2NH$ is too long.

Diisopropyl sulfide. The main structural parameters of sulfides are shown in Table 29. The observed r_g(S-C) and ∠CSC values of $(i\text{-Pr})_2S$ are 0.02 Å and 6° larger than the corresponding values of Me_2S [85] and EtSMe [86], respectively. The difference between the r_g(C-C) values in $(i\text{-Pr})_2S$ and EtSMe could not be detected. On the other hand, the observed r_g(C-C) value of $(t\text{-Bu})_2S$ is 0.009 Å larger than that of $(i\text{-Pr})_2S$. The observed values of r_g(S-C) and ∠CSC in $(t\text{-Bu})_2S$ are about 0.03 Å and 9° larger than the corresponding values in $(i\text{-Pr})_2S$, respectively. Therefore, the effect of the steric repulsion between the substituents attached to a sulfur atom are clearly seen in r(S-C) and ∠CSC. The C-C bond lengths are less sensitive to the steric hindrance.

The difference of 6.7(6)° found between $\angle SCC_3$ and $\angle SCC_4$ indicates that two isopropyl groups tilt in the direction away from each other. The tilt angle of the isopropyl group was defined by using an axis placed in the SC_2C_4 plane by referring to the tilt angle of t-butyl groups of $(t\text{-Bu})_2S$. This axis was chosen so that the C_4 carbon atom can be moved to the position of the C_3 carbon atom by the rotation around this axis. Then the tilt angle is defined as the angle between the S-C_2 axis and this axis. The value is calculated to be 4.2° from the SCC_3, SCC_4, and $C_3C_2C_4$ bond angles. This value is smaller than the tilt angle, 7(2)°, of t-butyl groups in $(t\text{-Bu})_2S$ but larger than that of methyl

groups in dimethyl sulfide (2.4°). This is reasonable since the tilt angle is expected to reflect the magnitude of the steric hindrance. The SCC bond angles of trans and gauche EtSMe (r_s structure) [87,88] are 109.5(3)° and 114.7(1)° , respectively. The difference between ∠SCC of the two conformers and the difference between $\angle SCC_3$ and $\angle SCC_4$ of $(i\text{-}Pr)_2S$ have the same sign and nearly equal values.

Diisopropyl Ketone. Table 30 compares the principal structural parameter values of $(i\text{-}Pr)_2CO$ with those of acetone [89] and ethyl methyl ketone [90]. The observed $r_g((O=)C\text{-}C)_{av}$ value of $(i\text{-}Pr)_2CO$ is 0.01 Å larger than that of acetone. The observed value of $\angle CC(=O)C$ of $(i\text{-}Pr)_2CO$ is nearly equal to those of acetone and ethyl methyl ketone. The fact that the isopropyl/methyl substitution gives little change to the CC(=O)C angle of $(i\text{-}Pr)_2CO$ suggests that the non-bonded interactions between isopropyl groups and the oxygen atom are competitive with the interactions between isopropyl groups.

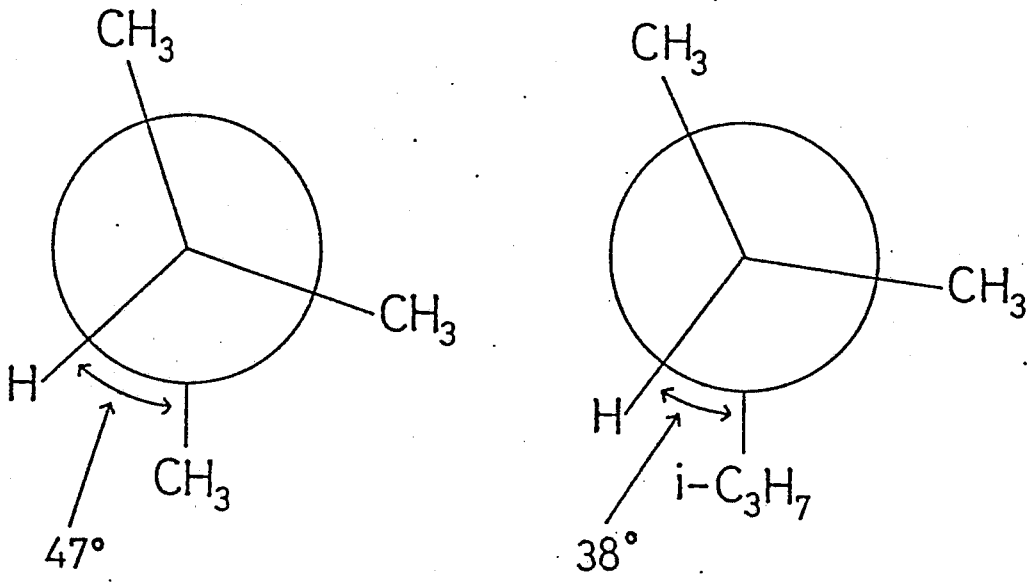

Figure 15 Newman projections: left, isopropyl methyl ether; right, diisopropyl ether.

TABLE 27

Comparison of the structures of related ethers[a]

	Me_2O[b]	EtOMe[c]	$(n\text{-}Pr)_2O$[d]	$(i\text{-}Pr)_2O$[e]
r_g(C-O)	1.415(1)	1.418(2)	1.405(6)	1.433(3)
r_g(C-C)		1.520(4)	1.526(8)	1.527(2)
r_g(C-H)	1.118(2)	1.118(4)	1.120(6)	1.117(2)
$\angle_\alpha$COC	111.8(2)	111.9(5)	116.1(36)	116.9(16)
$\angle_\alpha$HCH	109.2(2)	109.0(4)	103.8[f]	107.8(8)[g]

[a] Bond lengths in Å and angles in degrees. [b] Ref. 77. [c] Ref. 78. [d] This work. [e] Ref. 76. [f] Calculated from ∠CCH(methyl). [g] Calculated from $\angle CCH_{Me}$

TABLE 28

C-C bond lengths adjacent to an oxygen atom[a]

	t-EtOMe[b]	tt-(n-Pr)OMe[b]	tt-Et_2O[b]
r_s(C-C)	1.521(7)	1.516(15)	1.517(5)
Δ[c]	0.005	0.010	0.009
	EtOMe[d]	$(i\text{-Pr})_2O$[e]	
r_g(C-C)	1.520(4)	1.527(2)	
Δ[f]	0.012	0.005	

[a] In units of Å. Values in parentheses are the limits of error. [b] Ref. 79. [c] Difference between r_s(C-C) and that of propane [80], 1.526(2) Å. [d] Ref. 78. [e] This work. [f] Difference between r_g(C-C) and that of propane [80], 1.532(3) Å.

TABLE 29

Molecular structures of related sulfides[a]

	Me_2S[b]	EtSMe[c]	$(i\text{-}Pr)_2S$[d]	$(t\text{-}Bu)_2S$[e]
r_g(S-C)	1.807(2)	1.813(4)	1.829(2)	1.854(5)
r_g(C-C)		1.536(8)	1.530(2)	1.539(3)
r_g(C-H)	1.116(3)	1.111(8)	1.118(3)	1.127(4)
$\angle_\alpha$CSC	99.05(4)	97.1(11)	103.8(9)	113.2(12)

[a] Bond lengths in Å and angles in degrees. The limits of error are shown in parentheses. [b] Ref. 85. [c] Ref. 86. [d] This work. [e] Ref. 5.

TABLE 30

Comparison of the structures of related ketones[a]

	Me_2CO[b]	EtCOMe[c]	$(i\text{-}Pr)_2CO$[d]
r_g(C=O)	1.213(4)	1.219(3)	1.215(3)
r_g((O=)C-C)	1.520(3)	1.518[e]	1.533(1)[f]
r_g(C-C)		1.531[e]	1.536(1)[f]
∠CC(=O)C	116.0(3)	116.1(31)	117.0(7)
∠(O=)CCC		113.5(17)	110.4(3)[f]

[a] Bond lengths in Å and angles in degrees. The limits of error are shown in parentheses. [b] Ref. 89. [c] The r_α structure. Ref. 90. [d] This work. [e] Fixed values. [f] Average values.

6-2 Comparison between Experimental and Theoretical Structures

According to the results of the GED analysis, the most stable conformers of $(i\text{-}Pr)_2X$ (X = O, NH, S) have the C_2 or nearly C_2 symmetry. These results agree with the results of the MM2 calculations for $(i\text{-}Pr)_2X$ and the result of the 4-21G calculation for $(i\text{-}Pr)_2O$. In the case of $(i\text{-}Pr)_2CO$, the C_1 conformer is most abundant. The observed relative abundance of the C_1 conformer of $(i\text{-}Pr)_2CO$, 51(24)%, is consistent with the value, 67%, obtained by the 4-21G calculation. The results of the MM2 calculations by using the new parameter set for ketones show that two conformers are major constituents; one has the C_1 symmetry with ϕ_1 = 10° and ϕ_2 = -52° and the 65% population, the other has the C_2 symmetry with $\phi_1 = \phi_2$ = 63° and the 26% population. On the other hand, the most stable conformer has the C_2 symmetry and the 65% population according to the MM2 calculation with the original parameter set. Thus, the MM2 force field with the original parameter set fails to predict the most stable conformer.

The observed geometries of the most stable conformers of $(i\text{-}Pr)_2X$ (X = O, NH, S, and CO) are compared with the results of the MM2 calculations in Table 31. The results of $(i\text{-}Pr)_2CH_2$ [23] are also shown in this table. The observed values of ϕ_1 ($=\phi_2$) of $(i\text{-}Pr)_2NH$ and $(i\text{-}Pr)_2S$ are different

from the corresponding MM2 results by 12° and 15°, respectively. The steric repulsion between the isopropyl groups leads to the elongation of r(C-X) and opening of ∠CXC. For $(i\text{-}Pr)_2X$ (X = O, NH, and S), the ∠CXC values of the MM2 calculations are about 3° smaller than the corresponding r_α values. A similar trend was reported for $(t\text{-}Bu)_2S$ [5].

The structures of the most stable conformers of diisopropyl compounds $(i\text{-}Pr)_2X$ (X= O, NH, CO and CH_2) predicted by using the 4-21G basis set are compared with the experimental structures in Table 32. Calculated r_e bond lengths were converted to r_g values by making the empirical corrections proposed by Schäfer et al. [51,52]. The 4-21G geometries reproduced the observed geometries better than the MM2 geometries. It was found that the calculated ϕ_1 values are nearly equal to the observed values. It is noted that the deviation of the calculated COC and CNC bond angles of dimethyl ether and -amine from the experimental values (r_s structure) is 2.4° and 2.5°, respectively [52]. Therefore, the calculated COC and CNC angles of the diisopropyl compounds are expected to be about 2.5° larger than the observed values. However, such large discrepancies in ∠COC and ∠CNC were not recognized in $(i\text{-}Pr)_2O$ and $(i\text{-}Pr)_2NH$. The COC bond angle of t-butyl methyl ether given by the 4-21G calculation is 119.1° [27], which agrees with the value of 118.9(14)° determined by GED [91] within the

experimental error.

TABLE 31

Structural differences between the MM2 geometries and the geometries determined by GED[a]

	$(i\text{-Pr})_2O$ X=O	$(i\text{-Pr})_2NH$ X=N	$(i\text{-Pr})_2CH_2$ X=C	$(i\text{-Pr})_2S$ X=S	$(i\text{-Pr})_2CO$ X=C
r(C-X)	-0.007(3)	-0.005(4)	0.004(1)	-0.004(2)	-0.006(1)
r(C-C)	0.013(2)	0.009(4)	0.004(1)	0.007(2)	0.002(1)
r(C-H)	0.002(2)	-0.006(2)	-0.004(1)	-0.004(3)	-0.004(3)
∠CXC	-2.7(16)	-2.7(11)	-1.3(6)	-3.1(9)	1.5(7)
$\angle XCC_3$	-0.6(7)	2.7(3)[b]	1.0(8)	-3.3(4)	0.8(3)b
$\angle XCC_4$	1.7(4)	0.4(3)[b]	0.1(4)	1.5(5)	
∠CCC	-3.0(7)	-1.8(9)	-1.8(8)	-0.5(9)	-0.6(3)[b]
$\angle CCH_{Me}$	-0.2(9)	-1.6(8)	0.3(4)	0.4(12)	0.2(8)
ϕ_1	2(3)	11(4)[b]	4(2)	-16(8)	6,9

[a] Bond lengths in Å and angles in degrees. The MM2 structural parameter values minus the values obtained by GED are shown. The values in parentheses are the limits of experimental error. [b] Average value.

TABLE 32

Structural differences between the 4-21G geometries and the geometries determined by GED[a]

	$(i\text{-Pr})_2O$ X=O	$(i\text{-Pr})_2NH$ X=N	$(i\text{-Pr})_2CH_2$ X=C	$(i\text{-Pr})_2CO$ X=C
r(C-X)	-0.003(3)	-0.005(4)	0.001(1)	-0.001(1)
r(C-C)	-0.004(2)	-0.002(4)	0.001(1)	-0.001(1)
r(C-H)	-0.001(2)	-0.003(2)	-0.001(1)	-0.002(3)
∠CXC	0.5(16)	-0.2(11)	-1.3(6)	1.5(7)
$\angle XCC_3$	-1.8(7)	-0.5(3)[b]	0.6(8)	-0.4(3)b
$\angle XCC_4$	-0.8(4)	-0.5(3)[b]	0.4(4)	
∠CCC	-0.6(7)	-1.1(9)[b]	-1.6(8)	-0.4(3)[b]
$\angle CCH_{Me}$	-0.9(9)	-1.2(8)	-0.2(4)	-0.6(8)
ϕ_1	-3(3)	-3(4)	1(2)	0

[a] Bond lengths in Å and angles in degrees. The 4-21G structural parameter values minus the values obtained by GED are shown. The values in parentheses are the limits of experimental error. [b] Average value.

6-3 Discussion on the Conformations of Diisopropyl Compounds

In contrast with $(i\text{-}Pr)_2X$ (X = O, NH, CH_2, S), the population of the C_2 conformer is not predominant for $(i\text{-}Pr)_2C{=}O$. The energy differences between the C_2, C_1 and C_s conformers of $(i\text{-}Pr)_2C{=}O$ are found to be nearly equal to zero considering the multiplicity of the conformers. According to the 3-21G calculations for $(i\text{-}Pr)_2C{=}CH_2$, the two stable conformers with the C_2 ($\phi_1 = \phi_2 = 30°$) and C_s symmetry ($\phi_1 = 0°$ and $\phi_2 = 180°$) have nearly equal energies but the C_1 conformer corresponding to that of $(i\text{-}Pr)_2C{=}O$ is not stable. Therefore the difference in the conformational behaviour of $(i\text{-}Pr)_2C{=}O$ and $(i\text{-}Pr)_2X$ can not directly be related with the existence of the double bond.

Recently it has been found by GED that the most stable conformer of isopropyl methyl ketone [92] takes a molecular geometry in which one of the methyl groups in the isopropyl group is eclipsed with the carbonyl bond. Wiberg et al. [93,94] performed ab initio SCF calculations for some molecules with one carbonyl group by using the 3-21G and 6-31G* basis sets. The most stable conformer of isopropyl methyl ketone given by the theoretical calculations [94] is in good agreement with that determined by GED. According to Wiberg [94], the potential function of the isopropyl torsion in isopropyl methyl ketone can be decomposed into three

components; (1) a three-hold potential as found for acetone; (2) the attractive interaction of the dipole moment of the carbonyl group with the induced dipole moment of the isopropyl group; and (3) the repulsive interaction between the isopropyl group and the methyl group attached to the carbonyl group. We explain the conformation of $(i\text{-}Pr)_2C{=}O$ and the conformational differences between the diisopropyl compounds by developing the above idea. For the diisopropyl compounds the third component is the repulsive interaction between the isopropyl groups.

The methyl groups in acetone are known to take staggered conformations against C-C bonds [89]. Therefore, it is likely that the isopropyl groups of $(i\text{-}Pr)_2C{=}O$ prefer the staggered conformation against (O=)C-C bonds. The isopropyl groups of the C_2 conformer show no large displacement from the staggered form. In the case of the C_1 conformer, however, one isopropyl group is rotated by 44° from the staggered form. If we assume the potential function of the isopropyl torsion to consist of only the first component discussed by Wiberg [94], such a rotation introduces the energy increment of about 0.7 kcal/mol, since the height of the barrier for the isopropyl torsion is estimated to be about 0.8 kcal/mol from the barrier height of methyl torsion in acetone [93-95]. Applying the same consideration to the C_s conformer, we found that this conformer is less stable than the C_2 conformer by 0.8

kcal/mol.

Wiberg [94] showed that the interaction between the dipole moment of the carbonyl group and the induced dipole moment of an alkyl group stabilizes the eclipsed conformation of the alkyl group against the carbonyl group by about 1 kcal/mol and that the dipole-induced dipole interaction is proportional to $\cos^2\phi$, where ϕ is the dihedral angle of the $OCCC_{alkyl}$. Thus the isopropyl rotation of 44° in the C_1 conformer gives the energy increment of about 0.5 kcal/mol compared with the C_2 conformer. Similarly the energy of the C_s conformer is about 1.5 kcal/mol higher than that of the C_2 conformer. Then the combined effect of the first and second components is that the C_2 conformer is more stable than the C_1 and C_s conformers by about 1 and 2 kcal/mol, respectively. On the other hand, the GED analysis shows that the energy differences between the C_1, C_2 and C_s conformers are approximately zero. Thus the effect of the first two components must be canceled by the effect of the non-bonded interactions between the isopropyl groups. The energies due to the non-bonded interactions in the C_1 and C_s conformers are estimated to be about 1 and 2 kcal/mol smaller than that in the C_2 conformer, respectively.

The C_2 and C_s conformers of $(i\text{-}Pr)_2C{=}CH_2$ show large torsional displacement of one or two isopropyl groups from the staggered configuration. If we consider only the first

component, i.e., the increase in the energy by the isopropyl torsion, the energy increments of the two conformers are estimated to be equal to V_3 where V_3 is the potential barrier for isopropyl torsion. Therefore, the sum of the interactions between the $C=CH_2$ group and the isopropyl groups and the interaction between the isopropyl groups seem to have the nearly equal magnitudes in the C_2 and C_s conformers. Since the isopropyl groups of the C_2 conformer deviate from the staggered configuration by 30° , it is inferred that the interaction between the $C=CH_2$ group and the isopropyl groups is repulsive.

The V_3 values of $(i\text{-}Pr)_2X$ (X = O, NH, CH_2, S) are estimated to be three to four times as high as that of $(i\text{-}Pr)_2C=O$ referring to the barriers of Me_2X [95]. The energy increments due to the isopropyl rotations in the C_1 and C_s conformers of $(i\text{-}Pr)_2X$ (X = O, NH, CH_2, S) are estimated to be about 3 kcal/mol from the first component. No appreciable dipole-induced dipole interaction is expected for these diisopropyl compounds. Therefore, the C_1 and C_s conformers of $(i\text{-}Pr)_2X$ are considered to have very small populations.

6-4 Steric Effect on the Structures of Diisopropyl Compounds

The r(C-X) and ∠CXC are considerably affected by the steric repulsion between the two isopropyl groups. In the following discussion, Δr and $\Delta\theta$ stand for the increase in r(C-X) and ∠CXC of diisopropyl compounds compared with those of dimethyl compounds. The torsional displacement $\Delta\phi$ of the isopropyl group from the staggered configuration and the tilt angle t of the isopropyl group also reflect the structural deformations due to steric effect. The observed values of Δr, $\Delta\theta$, $\Delta\phi$ and t are listed in Table 32.

The Δr and $\Delta\theta$ of $(i\text{-}Pr)_2O$ are 0.018(3) Å and 5.1(16)°. The Δr of $(i\text{-}Pr)_2NH$ is nearly equal to that of $(i\text{-}Pr)_2O$. However, the $\Delta\theta$ of $(i\text{-}Pr)_2NH$ is 2° larger than that of $(i\text{-}Pr)_2O$. This indicates that the substitution of isopropyl groups for methyl groups increases the CNC angle to a greater extent than the COC angle. On the other hand, the values of t and $\Delta\phi$ of $(i\text{-}Pr)_2NH$ is 1° and 14° smaller than the corresponding values of $(i\text{-}Pr)_2O$, respectively. These results are difficult to explain in terms of the steric repulsion between isopropyl groups alone. According to the valence-shell electron-pair repulsion (VSEPR) theory [78], the valence shell of the oxygen atom of $(i\text{-}Pr)_2O$ is more crowded with electrons than that of the nitrogen atom of $(i\text{-}Pr)_2NH$. Thus the CNC angle may be increased easily by the

steric repulsion of the two isopropyl groups compared with the COC angle. As a result, the geminal C···C distance of $(i\text{-}Pr)_2NH$ is about 0.10 Å longer than that of $(i\text{-}Pr)_2O$. This weakens the steric hindrance between the two isopropyl groups in $(i\text{-}Pr)_2NH$ and allows the tilt angle and the CNCH dihedral angle to approach the less distorted configuration, i.e., $t = 0°$ and $\Delta\phi = 0°$.

The clearance between the isopropyl groups increases in the order: $(i\text{-}Pr)_2O < (i\text{-}Pr)_2NH < (i\text{-}Pr)_2CH_2$. Therefore, the effect of the steric hindrance decreases in the order: $(i\text{-}Pr)_2O > (i\text{-}Pr)_2NH > (i\text{-}Pr)_2CH_2$. This is consistent with the fact that the values of Δr, t and $\Delta\phi$ decrease in this order. Such a discussion may not be valid for the values of $\Delta\theta$ which are sensitive to the bonding interaction as described by the VSEPR theory.

The t-value of $(i\text{-}Pr)_2S$, 4.2°, is larger than the values of $(i\text{-}Pr)_2X$ (X = O, NH, CH_2). This is consistent with the fact that the value of the SCC bending force constant, 0.850 mdyn Å rad^{-2} [34], is smaller than the values of the YCC bending force constants (Y = O, N, C) by 0.2 - 0.4 mdyn Å rad^{-2}.

One of the $\Delta\phi$ values of $(i\text{-}Pr)_2C{=}O$ is larger than the $\Delta\phi$ values of $(i\text{-}Pr)_2X$ (X = O, NH, CH_2, S). This is explained by the barrier height of the isopropyl torsion. The values of Δr, $\Delta\theta$, $\Delta\phi$ and t indicate that $(i\text{-}Pr)_2O$ is the most sterically hindered among the five molecules listed in Table

32. The observed values of Δr, $\Delta \theta$, $\Delta \phi$ and t agree well with the values obtained by the 4-21G calculations with some exceptions but they are in a little worse agreement with the results of the MM2 calculations.

TABLE 33

Steric effects on the molecular structures[a]

	$(i\text{-}Pr)_2O$	$(i\text{-}Pr)_2NH$	$(i\text{-}Pr)_2CH_2$[b]	$(i\text{-}Pr)_2S$[c]	$(i\text{-}Pr)_2CO$
Δr					
GED	0.018	0.016	0.007	0.022	0.013
4-21G	0.014	0.009	0.007		0.012
MM2	0.007	0.009	0.009	0.010	0.010
$\Delta\theta$					
GED	5.1	7.1	5.4	4.9	1.0
4-21G	3.6	4.2	4.2		2.7
MM2	2.8	4.3	4.8	2.7	1.9
$\Delta\phi$					
GED	22	9	2	0	44, 2
4-21G	25	12[d]	1		44, 2
MM2	20	2[d]	2	16	50, 7
t					
GED	3.2	2.4	1.0	4.2	-0.1[d]
4-21G	2.6	2.4[d]	1.7		-0.1[d]
MM2	1.8	2.7[d]	1.6	1.3	-0.5[d]

[a] Δr and $\Delta\theta$ stand for the increase in r(C-X) and ∠CXC of the most stable conformers of diisopropyl compounds compared with those of dimethyl compounds. $\Delta\phi$ represents the deviations of the dihedral angles of the most stable conformers from 60° . t denotes the tilt angle of the

isopropyl groups. Lengths in Å and angles in degrees. [b] Ref. 23. [c] The 4-21G geometry was not obtained. [d] Average value.

Chapter 7

Summary

The molecular structures and conformations of $(i\text{-}Pr)_2O$, $(i\text{-}Pr)_2NH$, $(i\text{-}Pr)_2S$ and $(i\text{-}Pr)_2C{=}O$ have been determined by gas electron diffraction with the help of the normal coordinate analyses of the vibrational spectra and the MM2 and 4-21G calculations. The most stable conformers of $(i\text{-}Pr)_2O$ and $(i\text{-}Pr)_2S$ have the C_2 symmetry and the skeletal geometry of the most stable conformer of $(i\text{-}Pr)_2NH$ has nearly the C_2 symmetry. On the other hand, the energy differences between the C_2, C_1 and C_s conformers are quite small in $(i\text{-}Pr)_2C{=}O$. The determined molecular structures are listed in Tables 18, 21, 22, and 26 in Chapter 5. The difference in the conformation of diisopropyl compounds has been discussed in terms of non-bonded and dipole-induced dipole interactions, and the three-hold potential barriers of dimethyl compounds. The differences in the structural parameters of the most stable conformers have been explained by taking into account both non-bonded and bonding-electron interactions.

References

1 H. B. Burgi and L. S. Bartell, J. Am. Chem. Soc., 94, 5236(1972).

2 L. S. Bartell and W. F. Bradford, J. Mol. Struct., 37, 113(1977).

3 H. Oberhammer, R. Schmutzler and O. Stelzer, Inorg. Chem., 17, 1254(1978).

4 S. K. Doun and L. S. Bartell, J. Mol. Struct., 63, 249(1980).

5 A. Tsuboyama, S. Konaka, M. Kimura, J. Mol. Struct., 127, 77(1985).

6 D. W. H. Rankin, H. E. Robertson, R. Seip, H. Schmidbaur and G. Blaschke, J. Chem. Soc. Dalton Trans., 827(1985).

7 T. Fjeldberg, M. F. Lappert and S. J. Smith, J. Mol. Struct., 140, 209(1986).

8 L. S. Bartell, F. B. Clippard, Jr., and T. L. Boates, Inorg. Chem., 9, 2436(1970).

9 B. Beagley and R. G. Pritchard, J. Mol. Struct., 84, 129(1982).

10 T. Fjeldberg, R. Seip, M. F. Lappert and A. J. Thorne, J. Mol. Struct., 99, 295(1983).

11 A. Almenningen, T. Fjeldberg and E. Hengge, J. Mol. Struct., 112, 239(1984).

12 T. Fjeldberg, J. Mol. Struct., 112, 159(1984).

13 A. H. Cowley, J. E. Kilduff, E. A. V. Ebsworth, D. W. H.

Rankin, H. E. Robertson and R. Seip, J. Chem. Soc. Dalton Trans., 689(1984).

14 B. Csákvvári, Z. Wagner, P. Gömöry, F. C. Mijlhoff, B. Rozsondai and I. Hargittai, J. Organometal. Chem., 107, 287(1976).

15 B. Beagley, R. G. Pritchard and J. O. Titiloye, J. Mol. Struct., 176, 81(1988).

16 R. L. Hilderbrandt, J. D. Wieser and L. K. Montgomery, J. Am. Chem. Soc., 95, 8598(1973).

17 O. V. Dorofeeva, V. S. Mastryukov, N. L. Allinger and A. Almenningen, J. Phys. Chem., 89, 252(1985).

18 K. Siam, O. V. Dorofeeva, V. S. Mastryukov, J. D. Ewbank, N. L. Allinger and L. Schäfer, J. Mol. Struct.(Theochem), 164, 93(1988).

19 N. S. Chui, H. L. Sellers, L. Schäfer and K. Kohata, J. Am. Chem. Soc., 101, 5883(1979).

20 V. J. Klimkowski, J. D. Ewbank, C. V. Alsenoy, J. N. Scarsdale and L. Schäfer, J. Am. Chem. Soc., 104, 1476(1982).

21 P. Pulay, G. Fogarasi, F. Pang and J. E. Boggs, J. Am. Chem. Soc., 101, 2550(1979).

22 N. L. Allinger, J. Am. Chem. Soc., 99, 8127(1977).

23 M. Sugino, H. Takeuchi, T. Egawa and S. Konaka, to be submitted for publication.

24 J. S. Binkley, J. A. Pople and W. J. Hehre, J. Am. Chem. Soc., 102, 939(1980).

25 R. G. Snyder and G. Zerbi, Spectrochim. Acta, Part A, 23A, 391(1967).

26 A. D. H. Clague and A. Danti, Spectrochim. Acta, Part A, 24A, 439(1968).

27 L. Schäfer, private communication.

28 P. Pulay, Mol. Phys., 17, 197(1969).

29 P. Pulay, Theor. Chim. Acta, 50, 299(1979).

30 P. Pulay, in H. F. Schäfer III (Ed.), "Modern Theoretical Chemistry", Vol. 4, New York, Plenum Press, 1977, p. 153.

31 D. W. Scott and G. A. Crowder, J. Chem. Phys., 46, 1054(1967).

32 M. Ohsaku, H. Murata and Y. Shiro, Spectrochim. Acta, 33A, 467(1977).

33 M. Sakakibara, I. Harada, H. Matsuura and T. Shimanouchi, J. Mol. Struct., 49, 29(1978).

34 D. W. Scott and M. Z. El-Sabban, J. Mol. Spectrosc., 30, 317(1969).

35 M. Ohsaku, Bull. Chem. Soc. Jpn., 49, 2627(1976).

36 M. S. Gordon, J. S. Binkley, J. A. Pople, W. J. Pietro and W. J. Hehre, J. Am. Chem. Soc., 104, 2797(1982).

37 M. Aroney, D. Izsak and R. J. W. Le Fèvre, J. Chem. Soc., 4148(1961).

38 M. Hirota, T. Hagiwara and H. Satonaka, Bull. Chem. Soc. Jpn., 40, 2439(1967).

39 U. W. Suter, J. Am. Chem. Soc., 101, 6481(1979).

40 N. Fuson, M. L. Josien and E. M. Shelton, J. Am. Chem.

Soc., 76, 2526(1954).

41 G. J. Karabatsos, J. Org. Chem., 25, 315(1960).

42 J. E. Katon and F. F. Bentley, Spectrochim. Acta, 19, 639(1963).

43 T. Ohba, S. Ikawa and S. Konaka, unpublished results.

44 Y. Murata, K. Kuchitsu and M. Kimura, Jpn. J. Appl. Phys., 9, 591(1970).

45 A. Tsuboyama, A. Murayama, S. Konaka and M. Kimura, J. Mol. Struct., 118, 351(1984).

46 S. Konaka and M. Kimura, Bull. Chem. Soc. Jpn., 43, 1693(1970).

47 M. Kimura, S. Konaka and M. Ogasawara, J. Chem. Phys., 46, 2599(1967).

48 C. Tavard, D. Nicolas and M. Rouault, J. Chim. Phys., 64, 540(1967).

49 L. V. Vilkov, V. S. Mastryukov and N. I. Sadova, "Determination of the Geometrical Structure of Free Molecules", Mir Publishers, Moscow, 1983.

50 L. C. Snyder and H. Basch, "Molecular Wave Functions and Properties", Wiley, New York, 1972.

51 L. Schäfer, C. V. Alsenoy and J. N. Scarsdale, J. Mol. Struct.(Theochem), 86, 349(1982).

52 L. Schäfer, J. Mol. Struct., 100, 51(1983).

53 K. Kuchitsu and S. J. Cyvin, "Molecular Structures and Vibrations", S. J. Cyvin (Ed.), Elsevier, Amsterdam, 1972, Chapter 12.

54 J. P. Bowen, A. Pathiaseril, S. Profeta, Jr. and N. L. Allinger, J. Org. Chem., 52, 5162(1987).

55 S. Mizushima and T. Shimanouchi, "Sekigaisen-Kyushu to Raman-koka", Kyoritsu, Tokyo, 1958.

56 R. L. Hilderbrandt, J. Mol. Spectrosc., 44, 599(1972).

57 M. Iwasaki and K. Hedberg, J. Chem. Phys., 36, 2961(1962).

58 J. R. Durig, G. A. Guirgis and D. A. C. Compton, J. Phys. Chem., 83, 1313(1979).

59 T. Kitagawa, K. Ohno, H. Sugeta and T. Miyazawa, Bull. Chem. Soc. Jpn., 45, 969(1972).

60 G. Gamer and H. Wolff, Spectrochim. Acta, part A, 29A, 129(1973).

61 G. Dellepiane and G. Zerbi, J. Chem. Phys., 48, 3573(1968).

62 D. W. Scott and G. A. Crowder, J. Mol. Spectrosc., 26, 477(1968).

63 P. Cossee and J. H. Schachtschneider, J. Chem. Phys., 44, 97(1966).

64 Z. Buric and P. J. Krueger, Spectrochim. Acta, 30A, 2069(1974).

65 R. G. Snyder and J. H. Schachtschneider, Spectrochim. Acta, 21, 169(1965).

66 K. Kuchitsu and L. S. Bartell, J. Chem. Phys., 35, 1945(1961).

67 H. Takeuchi, M. Fujii, S. Konaka and M. Kimura, J. Phys.

Chem., 91, 1015(1987).

68 H. Takeuchi, S. Konaka and M. Kimura, J. Mol. Struct., 146, 361(1986).

69 H. Kondo, H. Takeuchi, S. Konaka and M. Kimura, Nippon Kagaku Kaishi, 1458(1986).

70 J. H. M. ter Brake and F. C. Mijlhoff, J. Mol. Struct., 77, 109(1981).

71 J. H. M. ter Brake, J. Mol. Struct, 118, 63(1984); 118, 73(1984).

72 D. Van Hemelrijk, B. Van den Enden, H. J. Geise, H. L. Sellers and L. Schäfer, J. Am. Chem. Soc., 102, 2189(1980).

73 W. Pyckhout, C. Van Alsenoy, H. J. Geise, B. Van der Veken, P. Coppens and M. Traetteberg, J. Mol. Struct., 147, 85(1986).

74 J. Nakagawa, M. Imachi and M. Hayashi, J. Mol. Struct., 112, 201(1984).

75 A. A. Abdurakhmanov, M. N. Elchiev and L. M. Imanov, Zh. Strukt. Khim., 15, 42(1974).

76 E. E. Astrup, Acta Chim. Scand., A31, 125(1977).

77 K. Tamagawa, M. Takemura, S. Konaka and M. Kimura, J. Mol. Struct., 125, 131(1984).

78 K. Oyanagi and K. Kuchitsu, Bull. Chem. Soc. Jpn., 51, 2237(1978).

79 M. Hayashi and M. Adachi, J. Mol. Struct., 78, 53(1982).

80 For convenience the r(C-C) value of propane was used as

the standard C-C bond length. J. H. Callomon, E. Hirota, K. Kuchitsu, W. J. Lafferty, A. G. Maki and C. S. Pote, "Structure Data of Free Polyatomic Molecules", Landolt-Börnstein, New Series, K. -H. Hellewege Ed., Springer-Verlag, West Berlin, 1976, Vol. II/7.

81 R. J. Gillespie, J. Chem. Educ., 40, 295(1963); 47, 18(1970).

82 B. Beagley and T. G. Hewitt, Trans. Fadad. Soc., 64, 2561(1968).

83 K. Siam, J. D. Ewbank, L. Schäfer and C. Van Alsenoy, J. Mol. Struct.(Theochem), 153, 165(1987).

84 S. Konaka and N. Yanagihara, J. Mol. Struct., in press.

85 T. Iijima, S. Tsuchiya and M. Kimura, Bull. Chem. Soc. Jpn., 50, 2564(1977).

86 K. Oyanagi and K. Kuchitsu, Bull. Chem. Soc. Jpn., 51, 2243(1978).

87 M. Hayashi, M. Adachi and J. Nakagawa, J. Mol. Spectrosc., 86, 129(1981).

88 M. Adachi, J. Nakagawa and M. Hayashi, J. Mol. Spectrosc., 91, 381(1982).

89 T. Iijima, Bull. Chem. Soc. Jpn., 45, 3526(1972).

90 M. Abe, K. Kuchitsu and T. Shimanouchi, J. Mol. Struct., 4, 245(1969).

91 A. Suwa, H. Ohta and S. Konaka, J. Mol. Struct., 172, 275(1988).

92 T. Sakurai, M. Ishiyama, H. Takeuchi, K. Takeshita, K.

Fukushi and S. Konaka, J. Mol. Struct., in press.

93 K. B. Wiberg and E. Martin, J. Am. Chem. Soc., 107, 5035(1985).

94 K. B. Wiberg, J. Am. Chem. Soc., 108, 5817(1986).

95 J. R. Durig, S. M. Craven and W. C. Harris, "Vibrational Spectra and Structure", J. R. Durig (Ed.), Marcel Dekker, New York, 1972, Vol. 1, Chapter 4.